Modeling Water Flow and Phosphorus Fate and Transport in a Tile-Drained Clay Loam Soil Using HYDRUS (2D/3D)

by

Shuang Ye (Lucia) Qiao

Department of Bioresource Engineering
McGill University, Montreal
Quebec, Canada

March 2014

A thesis submitted to McGill University in partial fulfillment of the requirements of the degree of Master of Science

Abstract

Phosphorus (P) is an important agricultural non-point source pollutant that could contribute to eutrophication of surface waters. In this study, the HYDRUS (2D/3D) model was evaluated for simulation of water flow and P transport in a clay loam soil in southern Ontario. The model was calibrated and validated using field data from two 0.1 ha test plots between 2008-2011. These plots have controlled tile drainage and a corn-soybean crop rotation. The surface and sub-surface water flows in test plots were monitored and samples collected continuously year round using an auto-sampling system. The model simulated water flow and P relatively well, with weekly modeling efficiency of 0.513 to 0.738 for validation of water flow, and weekly modeling efficiency of 0.587 to 0.768 for validation of dissolved P loss in tile drainage. Most of the deviation of simulated water flow occurred between November to February, which suggests the model would greatly benefit from optimization of snow dynamics and frozen soil conditions. Some of the simulation errors may also be attributed to soil cracking in the summer which consequently enhanced macropore flow. The model predicted daily water flow poorly, suggesting presence of time lag between simulation and measurements. Limitations of the model include lack of simulation of particulate P loss and surface runoff P loss. This model should be tested further for other soils in southern Ontario as well as other parts of Canada before its validity can be established.

Résumé

Le phosphore (P) est un important polluant de sources diffuses qui pourrait contribuer à l'eutrophication des eaux de surface. Dans cette étude, la capacité à simuler le débit de l'eau et le transport de P dans les sols argileux ou limon argileux du Sud de l'Ontario du modèle HYDRUS (2D/3D) a été évalué. Le modèle a été calibré et validé utilisant des données de terrain de deux parcelles d'essai de 0.1 ha entre 2008 et 2011. Ces parcelles ont contrôlées le drainage et la rotation des cultures de maïs et de soya. Les écoulements des eaux de surface et dans le sol inclus dans les parcelles d'essai ont été contrôlés et les échantillons collectés continuellement toute l'année à l'aide d'un système d'échantillonnage automatisé. Le modèle a relativement bien simulé le débit de l'eau et le P, avec des efficacités de modélisation sur une base hebdomadaire de 0.513 à 0.738 pour la validation du débit de l'eau, et une efficacité de modélisation sur une base hebdomadaire de 0.587 à 0.768 pour la validation de la perte du P dissous dans le réseau de drainage. Une déviation du débit de l'eau simulé est survenue davantage entre les mois de novembre et février, ce qui suggère que le modèle aurait avantage à s'attarder à l'optimisation de la dynamique de la glace et de la neige sur les conditions du sol. Certaines des erreurs de simulation peuvent être attribuées aux fissures dans le sol qui surviennent en été, qui conséquemment, favorisent la circulation des micropores. Le modèle prédit mal le débit de l'eau journalier, démontré par la présence de décalage temporel entre la simulation et les prises de mesure. Les limites du modèle incluent un manque de simulation de la perte de la matière particulaire P et de la perte P en écoulement de surface. Ce modèle devra être testé davantage sur d'autres sols dans le Sud de l'Ontario ainsi que sur d'autres régions du Canada avant sa validité puisse être reconnue.

Acknowledgements

I would like to thank my supervisor Dr. Prasher for his constant guidance, his financial support, and his understanding and encouragement throughout my research. I would like to thank Dr. Chin Tan and Dr. Tiequan Zhang of Agriculture and Agri-Food Canada in Harrow, Ontario for generously providing valuable field data and answering many of my questions, thus making this project possible. I would like to thank Dr. Jirka Simunek for technical support with the HYDRUS (2D/3D) software. I would like to thank Ms. Lylia Khennache for helping me with the French translation of my abstract. I would like to thank Dr. Zhiming Qi for his critique and insights during thesis examination.

I would like to thank all my friends and my fellow graduate students for their friendship and support, especially Akaram, Ashutosh, Azhar, Eman, Golmar, Hui, Kirupa, Lylia, Luan, Sanaz, and Yashi. Your make graduate life wonderful and give me strength. Finally I thank my mother and father for their unconditional support of my studies and for bearing with all the ups and downs of my life but always believing in me. Thank you.

Table of Contents

Abstract **2**

Résumé **3**

Acknowledgements **4**

Table of Contents **5**

List of Tables **7**

List of Figures **8**

List of Abbreviations and Symbols **9**

Chapter 1 Introduction **12**

1.1 Background on Phosphorus Fertilizer Use and Pollution 12

1.2 Introducing the Project 14

1.3 Objective 16

1.4 Scope 16

1.5 Thesis Outline 17

Chapter 2 Literature Review **18**

2.1 Phosphorus Chemistry in Soil 18

2.1.1 Chemical forms of P 18

2.1.2 Phosphorus measurement methods 23

2.2 Subsurface Hydrology and P Movement 25

2.3 Review of Field Studies on Phosphorus Losses 28

2.4 Review of Phosphorus Modeling 32

2.5 Overview of Models 36

Chapter 3 Methods **41**

3.1 Field Site and Experiment Description 41

3.2 Scope of Model 45

3.3 Model Equations, Settings, and Inputs 48

3.3.1 Soil profile in 2D 48

3.3.2 Tile drain representation 49

3.3.3 Soil hydraulic property and water flow equations 49
3.3.4 Leaf area index 52
3.3.5 Precipitation 53
3.3.6 Potential evapotranspiration 53
3.3.7 Heat transport and snow 55
3.3.8 Initial pressure head 56
3.3.9 Initial soil phosphorus concentration 57
3.3.10 Phosphorus fertilization 58
3.3.11 Boundary conditions 59
3.3.12 Phosphorus transport 60
3.3.13 Phosphorus adsorption 61
3.3.14 Crop phosphorus uptake 61
3.3.15 Special settings during model validation 63
3.3.16 Statistics 64
3.3.17 Sensitivity analyses 65
Chapter 4 Results and Discussion 67
4.1 Water Flow Calibration 67
4.2 Water Flow Validation 72
4.3 Phosphorus Calibration and Validation 75
4.4 Sensitivity Analyses I: Water Flow 78
4.5 Sensitivity Analyses II: P loss 82
4.6 Difficulties and Limitations of HYDRUS (2D/3D) modeling 87
Chapter 5 Summary and Conclusions 92
5.1 Summary and Conclusions 92
5.2 Recommendations for Future Studies 93
References 96

List of Tables

Table 3.1 Water quality sampling periods for the field experiment. 46
Table 3.2 Field measurements of soil properties 50
Table 3.3 van Genuchten soil parameters estimated using the Rosetta module 51
Table 3.4 Multipliers of potential evapotranspiration (PET) during model calibration and validation periods 54
Table 3.5 Water balance of plots 5 and 9 for 365 days from June 4th, 2008 to June 3rd, 2009 excluding soil water storage 55
Table 3.6 Initial pressure head simulation settings for calibration and validation 57
Table 3.7 Summary of boundary conditions for water flow, solute, and heat transport 60
Table 3.8 Active root uptake threshold and simulated root P uptake by crops 62
Table 3.9 Sensitivity analyses of parameters affecting water flow 66
Table 3.10 Sensitivity analyses of parameters affecting P simulation 66
Table 4.1 Statistics of water flow calibration for plots 5 and 9 69
Table 4.2 Simulation errors of subsurface tile drainage during model calibration period 70
Table 4.3 Simulation errors of surface runoff during model calibration period 70
Table 4.4 Statistics of water flow validation for plots 5 and 9 74
Table 4.5 Simulation errors of subsurface tile drainage during model validation period 74
Table 4.6 Simulation errors of surface runoff during model validation period 75
Table 4.7 Statistics of phosphorus calibration and validation for plots 5 and 9 76
Table 4.8 Simulation errors in plot 5 P loss and tile drainage flow by sampling periods 77
Table 4.9 Simulation errors in plot 9 P loss and tile drainage flow by sampling periods 77

List of Figures

Figure 2.1 Simplified P chemistry in agricultural soil 18

Figure 2.2 Phosphorus analysis of water samples..... 24

Figure 3.1 Site plan of the AAFC-Harrow research site 43

Figure 4.1(a) Daily precipitation and temperature during model calibration period 68

Figure 4.1(b) Water flow calibration for plot 5 from June 4th, 2008 to Oct 23rd, 2009 68

Figure 4.1(c) Water flow calibration for plot 9 from June 4th, 2008 to Oct 23rd, 2009 68

Figure 4.2(a) Daily precipitation and temperature during model validation period. 73

Figure 4.2(b) Water flow validation for plot 5 from June 11th, 2010 to Aug 5th, 2011..... 73

Figure 4.2(c) Water flow validation for plot 9 from June 11th, 2010 to Aug 5th, 2011 73

Figure 4.3 P loss in tile drainage, simulated from June 17th, 2008 to Feb 11th, 2009..... 75

Figure 4.4(a) Tile drainage simulation in plot 9 as affected by saturated hydraulic conductivity (K_s) in surface soil layer 79

Figure 4.4(b) Surface runoff simulation in plot 9 as affected by saturated hydraulic conductivity (Ks) in surface soil layer 79

Figure 4.5 Water flow simulation in plot 9 as affected by PET multiplier 80

Figure 4.6 Water flow simulation in plot 9 as affected by crop canopy interception..... 81

Figure 4.7 Water flow simulation in plot 9 as affected by heat transport and snow accumulation functions ..... .82

Figure 4.8 Simulated tile drainage P loss in plot 9 as affected by adsorption coefficient K_d in all soil layers 83

Figure 4.9 Simulated tile drainage P loss in plot 9 as affected by 1-site or 2-site adsorption..... 84

Figure 4.10 Simulated tile drainage P loss in plot 9 as affected by longitudinal dispersivity of all soil layers 84

Figure 4.11 Simulated tile drainage P loss in plot 9 as affected by aqueous diffusion rate of P..... 85

Figure 4.12 Simulated tile drainage P loss in plot 9 as affected by various fertilization rates 86

Figure 4.13 Simulated tile drainage P loss in plot 9 as affected varying concentrations of initial soil P at the start of the experiment 87

List of Abbreviations and Symbols

Units are listed in brackets where applicable, and unit-less parameters are indicated by (-)

AAFC	Agriculture and Agri-Food Canada
APEX	Agricultural Policy / Environmental eXtender model
C	carbon
CHEMFLO-2000	software for simulating water movement and chemical fate and transport in vadose zones
DNA	deoxyribonucleic acid
DRAINMOD	software for simulating hydrology of poorly drained, high water table soils
DRP	dissolved reactive phosphorus
DSSAT	Decision Support System for Agrotechnology Transfer software
Eqn	equation
FE-mesh	finite element mesh
GDD	growth degree-days (^{o}C)
GDD_{cum}	cumulative growth degree-days (^{o}C) (Eqn 3.6-3.8)
$H_2PO_4^-$, HPO_4^{2-}	solution P, orthophosphate ions
Hydrus-1D	software package for simulating water flow, heat, and solute transport in variably saturated porous media
HYDRUS (2D/3D)	software package for simulating water, heat, and solute movement in two- and three-dimensional variably saturated media
K	potassium
LAI	leaf area index (-) (Eqn 3.6-3.7, 3.9, 3.11-12)
LEACHM	Leaching Estimation and Chemistry Model
N	nitrogen
NSE	Nash-Sutcliffe model efficiency (-)
OH	hydroxyl ion
P	phosphorus
PET	potential evapotranspiration (cm)
PO_4	phosphate
ppm	parts per million
R^2	coefficient of determination (-)
RZWQM2	Root Zone Water Quality Model 2

A	amplitude of sine wave (^{o}C) (Eqn 3.13 temperature function)
A	cross-section area (m^2) (Eqn 2.6 Ficks's law, and Eqn 2.8-2.9 Darcy's Law)
a, b, c	integers for balancing chemical equations (-) (Eqn 2.1 and 2.4)
b	soil buffer capacity (-) (diffusion equation, Eqn 2.7)
b	Y-intercept of linear regression (Eqn 3.16)
b1	non-linearity exponent in Freundlich isotherm (-) (Eqn 2.2)
$b \leq 3$	degree of protonation of phosphate ion, ranging from 0-3 (Eqn 2.1)
c	concentration of P in solution (mg/L) (Eqn 2.2-2.3)
c_k	concentration of P in solution (mg /cm^3) (Eqn 3.14)
dc/dt	net rate of diffusion (mg/m^2/s) (Eqn 2.6)
dc/dx	concentration gradient along axis of diffusion (mg/m^3/m) (Eqn 2.6)
De	effective diffusion coefficient (m^2/s) (Eqn 2.6-2.7)
Dw	diffusion coefficient in water (m^2/s) (Eqn 2.7)
dh	difference in hydraulic head (m) (Eqn 2.8-2.10)
dl	difference in distance (m) (Eqn 2.8-2.9)
dx	difference in distance in x direction (m) (Eqn 2.10)
h	hydraulic head (cm) (Eqn 3.1-3.2, 3.4-3.5)
l	pore connectivity, usually 0.5 is the average value for soils (-) (Eqn 3.2)
l, m	ionic charges (-) (Eqn 2.4 precipitation and dissolution)
m	coefficient related to n, the pore size distribution index (-) (Eqn 3.1-3.3)
m	slope of linear regression (Eqn 3.16)
n	pore size distribution index (-) (Eqn 3.1-3.3)
n	total number of observations (-) (Eqn 3.15, 3.17)
K	hydraulic conductivity (m/s) (Eqn 2.8-2.10)
K_d	general adsorption coefficient (Eqn 3.14)
K_{ij}^{A}	anisotropy tensor used for anisotropic medium (-) (Eqn 3.4)
K_r	relative hydraulic conductivity (cm/day) (Eqn 3.5)
K_s	saturated hydraulic conductivity (cm/day) (Eqn 3.1-3.2, 3.5)
k	coefficient governing radiation extinction by canopy (-) (Eqn 3.11-3.12)
k_F	Freundlich adsorption coefficient (Eqn 2.2)
k_L	Langmuir adsorption coefficient (Eqn 2.3)
$\bar{O}$	mean of observed data (Eqn 3.15, 3.17)
O_i	observed data (Eqn 3.15, 3.17)
Q	discharge (m^3/s) (Eqn 2.8-2.9)
q	quantity of P adsorbed (mg P/kg soil) (Eqn 2.2-2.3)

q_{max}	maximum P adsorption in soil in Langmuir isotherm (mg P/kg soil) (Eqn 2.3)
S	metal ion in hydroxylated mineral (Eqn 2.1 ligand exchange reaction)
S	sink term (Eqn 3.4 Richard's equation)
$\bar{S}$	mean of simulated data (Eqn 3.17)
S_e	effective water content (-) (Eqn 3.2)
S_i	simulated data (Eqn 3.15, 3.17)
s_k	adsorbed P (mg P/cm^3) (Eqn 3.14)
T	tortuosity factor (-) (Eqn 2.7)
T_{base}	base temperature above which crop can grow productively (^{o}C) (Eqn 3.8)
T_{max}	maximum temperature of the day (^{o}C) (Eqn 3.8)
T_{min}	minimum temperature of the day (^{o}C) (Eqn 3.8)
T_0	temperature at time zero (^{o}C) (Eqn 3.13)
$\overline{T}$	average temperature at soil surface during period t_p (^{o}C) (Eqn 3.13)
t	time (day) (Eqn 3.4, 3.13)
t_p	time period for one cycle of sine wave (day) (Eqn 3.13)
v	specific discharge (m^2/s) (Eqn 2.8-2.10)
x	observed field data (Eqn 3.16)
x_i	spatial coordinates (-) (Eqn 3.4)
y	prediction of simulated data (Eqn 3.16)
α	inverse of air entry value or bubbling pressure (1/cm) (Eqn 3.1)
β_k	empirical coefficient for adsorption equation (-) (Eqn 3.14)
η_k	empirical coefficient for adsorption equation (-) (Eqn 3.14)
θ	volumetric water content (-) (Eqn 2.7, 3.1, 3.4)
θ_r	residual water content (-) (Eqn 3.1)
θ_s	saturated water content (-) (Eqn 3.1)
ψ	pressure head (m) (Eqn 2.10)

Chapter 1 Introduction

1.1 Background on Phosphorus Fertilizer Use and Pollution

In modern agriculture, phosphorus (P) is one of the most essential crop nutrients. It is required in large quantities by crops, and usually every ton of crop dry biomass contains 0.8 to 7 kilograms of P (Wild and Jones, 1988). P is necessary for important plant functions such as deoxyribonucleic acid (DNA), cell membrane, etc. (Raghothama, 2005), and its role is irreplaceable by any other element in the periodic table.

Despite its importance, P is naturally scarce in soil in plant-available form. While the total P content in the soil may appear sufficient for plant demand, most of it forms bonds with soil particles by adsorption or precipitation processes, and becomes largely unavailable to plants (McGechan and Lewis, 2002). A very small fraction that remains in the soil solution are the orthophosphate ions (PO_4^{3-}); these are readily available to plants but are usually present at concentrations far below ideal plant demand (Raghothama, 2005). Since deficiency of P may cause delayed crop growth (Wild and Jones, 1988) and result in reduced yield and profit, P fertilizers are commonly used in agriculture to guarantee crop yield.

There are two main types of P fertilizers, inorganic and organic. The inorganic fertilizers are produced from mined phosphate rocks such as apatite (Stewart et al., 2005), transformed into phosphoric acid, and then made into final fertilizer products with various chemical formulas such as calcium phosphates, ammonium phosphates, ammonium polyphosphates, potassium phosphates, etc. (Havlin et al., 2005; Leikam and Achorn, 2005). Inorganic fertilizers constitute the majority of P fertilizer usage. It is estimated that, in 2012, global production of phosphate rocks reached 210 million tons (U.S. Geological Survey, 2013b) and the majority of these were intended for fertilizer usage. The other type of fertilizer is organic, which is often the manures of poultry, cattle, and hogs, generated by animal production farms as waste products. The production and usage levels of manures are more difficult to estimate than that of inorganic fertilizers. Furthermore, because of

their animal origin, P content in organic fertilizers would vary depending on animal and feed type, and can only be quantified using laboratory tests. Utilizing manures with unknown P content would increase the risk of excess fertilization beyond crop needs.

While the use of P fertilizers is strongly encouraged in agriculture, excess fertilization of P can lead to P pollution and eutrophication in surface water bodies. Eutrophication is the condition where inorganic nutrients such as nitrogen (N) and P become enriched in water bodies and lead to degradation of water quality by promoting excess growth of algae (U.S. Geological Survey, 2013a). Eutrophication may occur naturally but human activities are now a major contributing factor.

There is a strong link between agriculture and eutrophication. The agriculture sector is estimated to contribute to 82% of total P pollution in Canada (Canada Gazette, 2009). Normally, the soil can act as a sink trapping P by the chemical adsorption process (McGechan and Lewis, 2002), but if the amount of P (i.e. added by fertilization) exceeds capacity of the sink, the excess P may be lost from agricultural fields by means of surface runoff and subsurface tile drainage. Past studies have shown correlation between soil P concentrations and the amount of P lost via tile drainage (Heckrath et al., 1995) and surface runoff (Sharpley, 1995). When P enters water bodies, it becomes one of the nutrients that limit the growth of algae in rivers, lakes and ponds (Guildford and Hecky, 2000). Excess P can create algal blooms in water, which in turn block out sunlight necessary for the survival of aquatic plants, deplete oxygen levels in water, and ultimately lead to death of aquatic plant and fish species (Art, 1993). This can also lead to adverse health effects for humans and livestock that come in contact with the water (Dawson, 1998).

Remediation of eutrophication is difficult at the level of rivers and lakes. While P removal from water bodies is possible using chemical (Surampalli et al., 1995) or biological approaches (Oehmen et al., 2007), it is usually complex, costly and time consuming to do so on a large scale. The removal of P by wastewater treatment of drainage water is also impractical, due to the non-point-source nature of agricultural pollution. The only remaining strategy is the prevention of

P pollution, primarily by means of controlling fertilization. Considering that excess fertilization of P occurs in 71% of the world's cropland areas (MacDonald et al., 2011), this is likely the most effective approach although it remains a challenge.

To minimize P pollution, it is recommended that the quantity of fertilizer application be strictly controlled. For example, soils with high P concentration should receive little or no fertilizer, and soils insufficient in P should be given fertilizers based on existing soil P concentration. Enforcing this environment-friendly practice requires many efforts: soil tests must be performed periodically to quantify the existing P content; fertilizers (especially manures) need to be analyzed for P content; government regulations of fertilization need to be derived for proper implementation. To support such regulations, there needs to be sufficient knowledge regarding the movement and loss of P from agricultural soil, and mathematical relationships need be developed to make predictions of future P loss based on existing data.

1.2 Introducing the Project

In this study, computer modeling will be used to quantify the tile drainage loss of dissolved P from agricultural fields. Computer modeling is an excellent method to study P losses. Previous studies have shown success of computer modeling in predicting N and pesticides losses in soil-crop systems with reasonable accuracy (Carsel et al., 1985; Salazar et al., 2009). Compared to field agricultural experiments that may take decades and vast resources to complete, the modeling approach is significantly faster, more cost effective, and can provide insights of mathematical relationships of complex soil and P interactions.

While N and P are both important contributors to fresh water eutrophication, N has been extensively studied by modeling (Benbi and Richter, 2002; Manzoni and Porporato, 2009), while the numbers of studies focused on P have been more limited. The fact that P undergoes adsorption also causes P modeling to be more difficult than that of N. There have been modeling equations developed for various P processes in soil (Goldberg and Sposito, 1984a, b; Jones et al., 1984);

studies have modelled P in soil column leaching and laboratory experiments (Abou Nohra et al., 2007; Ben-Gal and Dudley, 2003; Elmi et al., 2012; Tim and Mostaghimi, 1989); and a limited number of studies have modelled P in entire agricultural fields (Goulet et al., 2006; Larsson et al., 2007; Morrison et al., 2013; Sedorovich et al., 2007; van der Salm et al., 2011) although the number of studies in the last category is rather limited.

While the laboratory and soil column studies offer great insight into P chemistry and transport processes, ultimately the field scale models are most useful for predicting P fate and transport in real agricultural landscapes. Field scale modeling is complex due to unpredictability of field conditions as well as interactions of many factors such as weather, fertilizers, soil type, crops, and subsurface tile drainage. Tile drainage is commonly utilized in provinces of Ontario and Quebec, and other regions of wet climate to remove excess water from the field. It can drastically increase the amount of water leaving an agricultural field, and may consequently increase P loss. Some tile drainage installations also employ water table control, using riser structure to control drainage and conserve more water in dry periods. Compared with regular tile drainage, controlled tile drainage can reduce the amount of water leaving the fields, consequently reducing P loss (Tan and Zhang, 2011). Currently, among the field scale P simulations, one of the most under-studied aspects is P loss via subsurface tile drainage in heavy clay soils. Previous modeling work have either reported simulation errors in this area due to difficulty of simulating macropores flow (Larsson et al., 2007; Morrison et al., 2013; van der Salm et al., 2011) or lack tile drainage simulation completely (Sedorovich et al., 2007).

We selected the experimental site, an Agriculture and Agri-Food Canada (AAFC) research field located at Woodslee, near Harrow, Ontario, for the study of P loss. The site located on the north shore of Lake Erie is desirable and strategic, as Lake Erie has had a long history of eutrophication problems. In 1972, Canada and the United States signed the Great Lakes Water Quality Agreement (Anon., 1972) to control and reduce the loading of P as well as other nutrients and harmful substances into the Great Lakes. This agreement has been resigned in 1978 then

supplemented again in 1983 to further reduce P loads. In the recent years, the most severe case of phosphorus pollution occurred in the western basin of Lake Erie, where this study site eventually contributes drainage water to. In the spring of 2009, the average total P concentration measured in western Lake Erie was 58 μg P /L, well above the target level of 15 μg P /L (Environment Canada, 2012) despite declining P concentrations since the 1970s. It is hoped that, by studying the P loss in the region, a model will be developed to predict future levels of P pollution, and reveal insights of better management practices suitable for agriculture in this region.

1.3 Objective

The main goal of the project was to simulate phosphorus fate and transport in a subsurface drained clay loam soil. The specific objectives of the project were to:

1. simulate surface and subsurface water flow in a tile-drained clay loam soil.
2. simulate fate and transport of P in soil, and loss of dissolved P via tile drainage.

These objectives were met by using the HYDRUS (2D/3D) model to simulate observed data from the AAFC experimental field near Harrow, Ontario. Field measurements of water flow and P loss data from 2008 to 2011 were used to evaluate the model.

1.4 Scope

In this study, the HYDRUS (2D/3D) model was evaluated for water flow and P movement in a clay loam soil in southern Ontario. The model was calibrated with observed field data from 2008-2009, and validated with field data from 2010-2011. While the model simulated water flow and tile drainage loss of dissolved P relatively well, it should be tested for other soils in southern Ontario as well as other parts of Canada before any concrete conclusions can be drawn about its validity. The model did not simulate P transport in surface runoff, nor did it consider the loss of particulate P.

1.5 Thesis Outline

Chapter 1 is the introduction of this project. Chapter 2 is a review of literature on P chemistry, previous field studies and modeling work, and compares different computer models for their suitability for P simulation. Chapter 3 is the methods section, which explains site description, field experimental design, data collection, the HYDRUS (2D/3D) model, model input parameters, and the statistical methods used to for model evaluation. Chapter 4 presents and discusses the results of model calibration and validation for water flow and P losses, and results of model sensitivity analyses. Chapter 5 is the summary and conclusion of the thesis and provides recommendations for future studies.

Chapter 2 Literature Review

2.1 Phosphorus Chemistry in Soil

Soil may contain significant amounts of phosphorus, ranging from 0.2-3 g of P per kg of soil, but generally less than 1% of the total P is immediately available for plants (Richardson et al., 2005). This is because soil P exists in many different chemical and biological forms, and only selected forms are available for plant use. A simplified representation of P cycle is shown in Figure 2.1, grouping different forms of P into four pools. The following section will describe these forms of P and explain the chemical and biological processes involved.

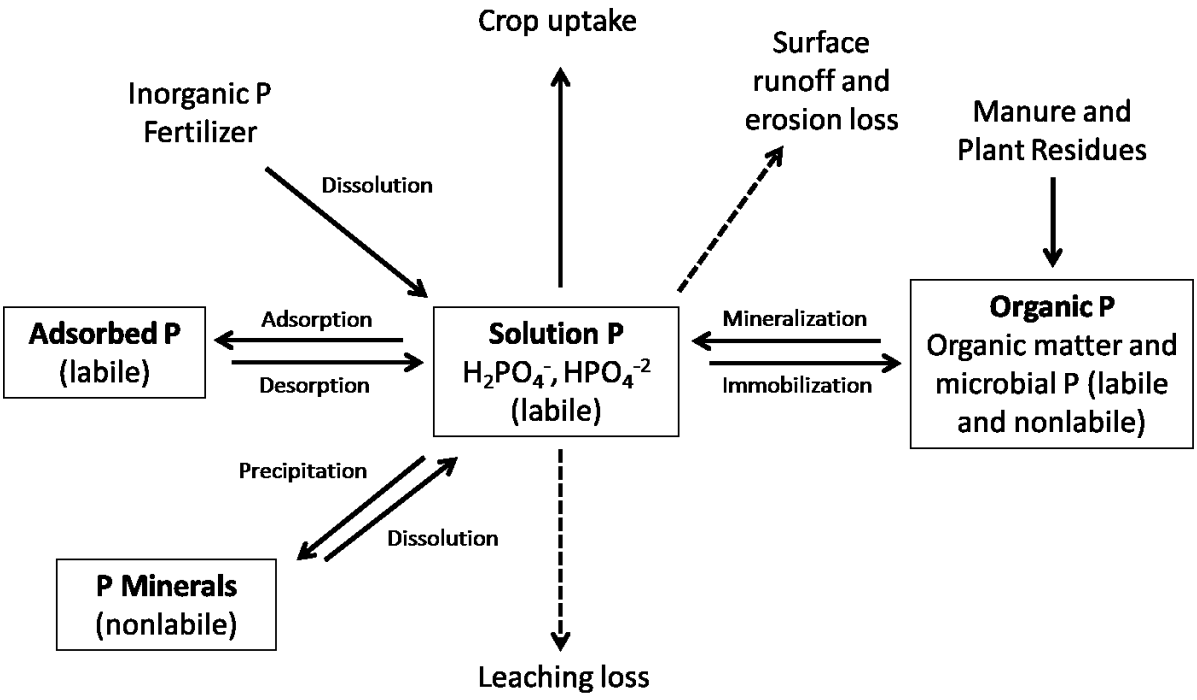

Figure 2.1 Simplified P chemistry in agricultural soil, adapted from Havlin et al. (2005).

2.1.1 Chemical forms of P

Solution P

Solution P refers to dissolved inorganic P, mainly orthophosphate ions $H_2PO_4^-$ and HPO_4^{-2}

which are present at very low concentrations (generally < 5 μM) in soil solution at equilibrium (Condron et al., 2005). The two forms of orthophosphate ions exist at similar concentrations at pH 7.2; below this pH $H_2PO_4^-$ is the more abundant form, whereas above this pH HPO_4^{-2} is more abundant (Havlin et al., 2005).

Despite its low concentration, solution P is the most important form of P for agricultural purposes because it determines the amount of crop P uptake. Generally the concentration of solution P needs to exceed 0.025 ppm to expect 95% maximum yield of corn, and needs to exceed 0.200 ppm to expect 95% maximum yield of soybeans (Havlin et al., 2005).

Plant roots can specifically take up and transport phosphate ions via membrane-associated proteins (Richardson et al., 2005). The natural concentration of P in plant-available form is often about 2 μM in soil solution, far below the P concentration in plant tissues which are generally 5-20 μM (Raghothama, 2005). Plants can passively uptake P as roots extract water from the soil; however this passive process is not enough to satisfy P demand. Active root uptake of P, a process which uses energy to transport P across cell membranes, is the crucial process of crop P uptake (Raghothama and Karthikeyan, 2005). In addition, symbiosis of plants with mycorrhizal fungi can also assist P uptake, as these fungi provide a mycorrhizal hyphae "extension" to the plant roots and increase surface area of P absorption (Bolan, 1991).

To supplement the pool of solution P for crops, inorganic fertilizers such as calcium phosphates, ammonium phosphates, ammonium polyphosphates, potassium phosphates, etc. are commonly used in modern agriculture (Havlin et al., 2005). Inorganic fertilizers in solid state are immobile in soil and inaccessible to plant uptake until they dissolve to solution P.

P availability in soil is highest at pH 6.5. At lower pH, P may attach to Fe or Al minerals by adsorption or precipitation; whereas at higher pH, P may attach to Ca and Mg minerals (Havlin et al., 2005). This brings the topic to adsorbed P.

Adsorbed P

Adsorbed P is attached to soil particle surfaces by a chemical bond (McGechan and Lewis, 2002). The process of adsorption is the attachment of P to soil mineral by forming one chemical bond, and the process of desorption is the detachment of P back into solution P form. The adsorbed P is considered "labile" because it can be desorbed and thus become accessible for plant uptake (Havlin et al., 2005). P adsorption is pH-dependent. In acidic soils, the Fe, Al minerals of clay are the preferred surfaces of P adsorption, whereas in neutral or basic soils, Ca and Mg become the preferred surfaces (Havlin et al., 2005). Goldberg and Sposito (1985) used the following equation to describe the generalized ligand exchange reaction of the adsorption/desorption process:

$$aSOH_{(s)} + H_bPO_4{}^{b\leq 3}{}_{(aq)} + cH^+{}_{(aq)} \leftrightarrow S_aH_cPO_{4\,(s)} + bH_2O_{\,(l)} + (a-b)OH^-{}_{(aq)} \qquad (2.1)$$

where
a, b, c = integers for balancing chemical equation
S = metal ion in hydroxylated mineral
OH = reactive surface hydroxyl
$b \leq 3$ is the degree of protonation of phosphate ion, ranging from 0-3

The adsorption of P has been mathematically described and tested using many different sorption isotherms. The two most popular isotherms are the Freundlich and Langmuir equations. The Freundlich equation shown below in Equation 2.2 (McGechan and Lewis, 2002) may be quite reliable at low concentrations of solution P but does not account for a maximum sorption capacity of the soil (Havlin et al., 2005).

$$q = k_F c^{b1} \qquad (2.2)$$

where
q = quantity of P adsorbed (mg P/kg soil)
c = concentration of P in solution (mg/L)
k_F = Freundlich adsorption coefficient
b1 = exponent generating non-linearity

The Langmuir isotherm in Equation 2.3 (McGechan and Lewis, 2002) accounts for maximum

P sorption capacity in soil and therefore is more accurate than the Freundlich isotherm at high concentrations of solution P.

$$q = q_{max}\left(\frac{k_L c}{1 + k_L c}\right) \tag{2.3}$$

where
q = quantity of P adsorbed (mg P/kg soil)
q_{max} = maximum P adsorption in soil (mg P/kg soil)
k_L= Langmuir adsorption coefficient
c = concentration of P in solution (mg/L)

Freundlich and Langmuir isotherms are not perfect and both have both been reported to be inaccurate for simulating P data (Ben-Gal and Dudley, 2003; Elmi et al., 2012). Other equations have also been developed to describe adsorption. Examples include the Tempkin and Elovich equations, and modified versions of the Freundlich and Langmuir equations (McGechan and Lewis, 2002). There is also the two site non-equilibrium adsorption concept, which allows some adsorption sites to have kinetic adsorption rate and others sites to have instantaneous adsorption rate (van Genuchten and Wagenet, 1989). In addition, a non-ideal competitive adsorption model, originally intended for metal adsorption onto organic matter (Koopal et al., 1994) has been applied to P adsorption (Abou Nohra et al., 2007) for selected soils with high accuracy.

The sorption of P is also affected by other chemical species present in soil, as well as soil characteristics. The abiotic anions (i.e. OH^-, $H_3SiO_4^-$, SO_4^{-2}) in soil solution may compete with P ions for adsorption sites, leading to a decrease in P adsorption. High Al and Fe content (i.e. clay) and smaller size of soil particles provide a greater number of adsorption sites in soil. Finally, organic matter in soil tends to increase P availability by releasing anions that compete with P for adsorption sites (Havlin et al., 2005).

P minerals

P minerals include naturally occurring soil minerals and P precipitated from soil solution. Precipitated P is distinctly different from adsorbed P because the former has more than one

covalent bond with the soil mineral surface, whereas the latter only has one bond. Precipitated P is considered "non-labile", not very accessible to plants at least in the short term (Havlin et al., 2005). Precipitation and dissolution can be illustrated using a generalized equilibrium equation shown below (Pierzynski et al., 2005). This process converts labile solution P into non-labile precipitated form.

$$aM^{m+}{}_{(aq)} + bL^{l-}{}_{(aq)} \leftrightarrow M_aL_{b(s)} \quad (2.4)$$

where
a, b = integers for balancing chemical equation
$M_aL_{b(s)}$ = P mineral
m, l = ionic charges

Havlin et al. (2005) illustrated precipitation using an example of orthophosphate precipitation onto Al in acidic soil:

$$Al(OH)_2^+ + H_2PO_4^- \leftrightarrow Al(OH)_2H_2PO_4 \quad (2.5)$$

where
$Al(OH)_2^+$ = example of soil mineral surface
$H_2PO_4^-$ = solution P (orthophosphate ion)
$Al(OH)_2H_2PO_4$ = example of precipitated P on soil mineral surface

Organic P

Organic P refers to P in organic compounds which generally represents 30-65% of total soil P (Condron et al., 2005). These mainly exist in solid or semi-solid form, such as inositol phosphates in humus, organophosphate pesticides, decaying plant residues, animal manures, bacterial P, etc.; but these also include a few soluble molecules such as deoxyribonucleic acid (DNA) and ribonucleic acid (McKelvie, 2005). Among all the organic P molecules, phytate, a cation derivative of inositol hexakisphosphate, may account for 16-50% of all soil organic P (Richardson et al., 2005).

Organic P turnover rate in soil is determined by mineralization and immobilization processes, both of which occur concurrently in soil and are mediated by soil microorganisms (Bolan, 1991;

Oberson and Joner, 2005; Richardson et al., 2005). Mineralization is the release of inorganic P ions (i.e. orthophosphates) from organic matter, whereas immobilization is the biological conversion of inorganic P into organic P, such as P being incorporated into bacterial biomass (Condron et al., 2005). Mineralization is also assisted by extracellular phosphatase activities of plants (Richardson et al., 2005). The rate of mineralization is closely associated with soil fertility and phosphatase enzyme activity (Condron et al., 2005). This rate generally increases with warm temperature and abundant precipitation which encourage microbial activities (Havlin et al., 2005). The C:P (carbon to phosphorus) residual ratio may play an important role, as a low residual ratio of C:P < 200 promotes mineralization whereas a high ratio of C:P > 300 tends to promote immobilization process (Havlin et al., 2005). Nitrogen in soil also stimulates plant P uptake by increasing plant root growth and increasing P availability in soil (Havlin et al., 2005).

2.1.2 Phosphorus measurement methods

The P measurement methods are reviewed here because experimental measurements of P do not necessarily correspond with the theoretical speciation of P. These measurements are usually defined based on chemical extractants or the extraction methods.

Soil Samples

There are several methods of soil P measurement. Total soil P is obtained by digesting a soil sample with strong acid (i.e. H_2SO_4, $HClO_4$) or Na_2CO_3. This method attempts to measure the sum of all the P forms in soil (Bender and Wood, 2000), however it is not a useful measurement for evaluating soil fertility in agriculture, as most of the total soil P is not available to crops. More useful methods test for available P using various extractants, and these measurements are commonly used as guidelines for fertilization requirements (Beegle, 2005). A few common extractants are listed below: Olsen P test uses extractant of 0.500 M $NaHCO_3$ at pH 8.5 (Olsen et al., 1954); Bray P 1 and P 2 tests use 0.030 M NH_4F and 0.025 M or 0.100 M HCl (Bray and

Kurtz, 1945); Mehlich-3 test uses 0.015 M NH_4F, 0.2 M CH_3COOH, 0.250 M NH_4NO_3, 0.013 M HNO_3, 0.001 M EDTA (Mehlich, 1984) .

Water Samples

P in water samples are analyzed differently than soil samples. Figure 2.2 shows the procedure and results of water sample analysis. The entire water sample can be analyzed to obtain total P measurement. Total P can be separated using 0.45 μm pore filter to obtain 2 fractions: the total dissolved P (Pote and Daniel, 2000b), and particulate P which does not pass through filter. The total dissolved P can be further divided into two sub-fractions by hydrolysis or oxidative digestion. The sub-fraction of dissolved organic P (also called soluble unreactive P) requires a digestion reaction to be detected by molybdate colorimetric test. The other sub-fraction, dissolved reactive P (DRP, also called soluble reactive P), may be detected without digestion reaction. The DRP is approximately a measurement of dissolved orthophosphates in solution (Pote and Daniel, 2000a).

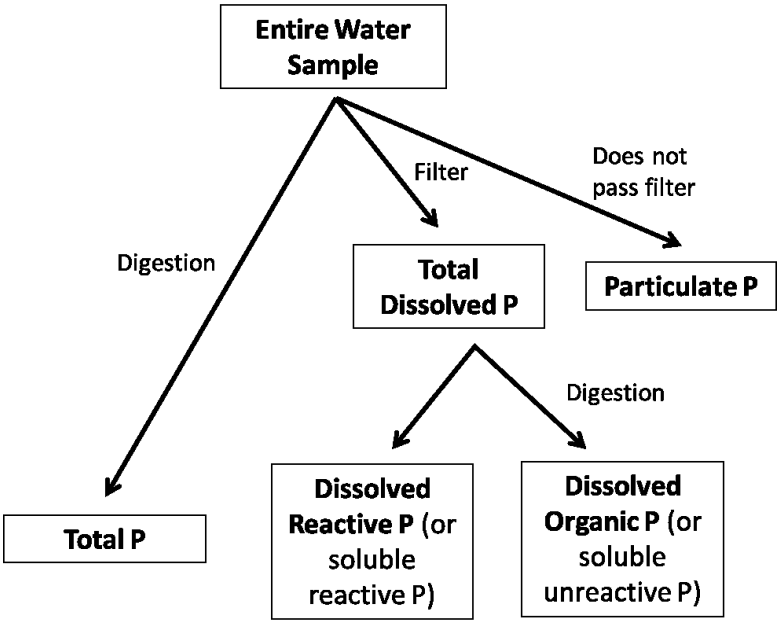

Figure 2.2 Phosphorus analysis of water samples, adapted from Pote and Daniel (2000a) and Pote and Daniel (2000b).

2.2 Subsurface Hydrology and P Movement

This section shall discuss the water movements in soil which heavily influence P mobility.

Infiltration

Infiltration is the process by which rainfall or irrigation water enters the soil at the soil surface, and moves downward in the unsaturated zone. The rate of infiltration depends on rainfall intensity, the initial soil moisture, slope gradient, and the characteristics of the soil itself (Freeze and Cherry, 1979). This process has the ability to move soluble and particulate P downward in soil.

Evaporation and evapotranspiration

Evaporation is the physical process by which water molecules in liquid state absorb heat, and leave the soil profile as water vapour. Transpiration is the biological process by which plants uptake water using roots, and evaporate the water via above-ground leaves and stems. Both processes remove water from the soil, and the rates of removal are usually higher in warmer temperatures. These processes create upward water movement, which may assist in plant uptake of nutrients such as P.

Diffusion and mass flow

As plant root tissues remove orthophosphate ions from the soil solution, diffusion and mass flow processes deliver more P to the root zone. Diffusion is the movement of ions from an area of high concentration to an area of low concentration, whereas mass flow is the ion transport to the plant root as a result of plant water uptake in evapotranspiration (Havlin et al., 2005). Of these two processes, diffusion contributes more than 80% of the P delivery and therefore is considered the primary mechanisms of P transport, especially in soils of low P content (Havlin et al., 2005). Diffusion can be described by Fick's law (Havlin et al., 2005):

$$\frac{dc}{dt} = De \times A \times \frac{dc}{dx} \quad (2.6)$$

where

dc/dt = net rate of diffusion (mg/m^2/s)
De = effective diffusion coefficient (m^2/s)
A = cross-section area through which the ions diffuse (m^2)
dc/dx = concentration gradient along axis of diffusion (mg/m^3/m)

The effective diffusion coefficient is calculated using the following equation (Havlin et al., 2005).

$$De = Dw \times \theta \times \frac{1}{T} \times \frac{1}{b} \quad (2.7)$$

where
De = effective diffusion coefficient (m^2/s)
Dw = diffusion coefficient in water (m^2/s)
θ = volumetric soil water content (-)
T = tortuosity factor (-)
b = soil buffer capacity (-)

Saturated flow

The flow of water in the saturated soil (below water table) may be described using Darcy's law in two equations (Freeze and Cherry, 1979) for discharge (Q) and specific discharge (v).

$$Q = -KA\frac{dh}{dl} \quad (2.8)$$

$$v = -K\frac{dh}{dl} = \frac{Q}{A} \quad (2.9)$$

where
Q = discharge (m^3/s)
v = specific discharge (m^2/s)
K = hydraulic conductivity (m/s)
A = cross-sectional area of flow path (m^2)
dh = difference in hydraulic head (m)
dl = difference in distance (m)

Unsaturated flow

The flow of water in an unsaturated, isotropic soil in direction of x can be described using the following equation (Freeze and Cherry, 1979).

$$v_x = -K(\psi)\frac{dh}{dx} \tag{2.10}$$

where
v = specific discharge (m^2/s)
K = hydraulic conductivity (m/s)
ψ = pressure head (m)
dh = difference in hydraulic head (m)
dx= difference in distance in x direction (m)

Preferential flow

Preferential flow occurs in macropores, which can be root channels or soil cracks that occur in dry soil conditions. Water flows quickly in these large-diameter channels, at rates much faster than soil matrix flow. The flow rate and flow volume of macropores are both difficult to measure and predict. The concentration of solutes in preferential flow can also be unpredictable because this flow does not necessarily pass through the soil matrix.

Factors that affect subsurface flow

A wide range of factors affect subsurface flow. Soil characteristics such as grain size and porosity have a significant impact on flow rates in both saturated and unsaturated flow (Freeze and Cherry, 1979). As for environmental factors, precipitation amounts and intensity affect infiltration; warm temperatures may increase evaporation and transpiration rates, and may even lead to soil cracks which become preferential flow channels. In addition, sub-zero winter temperatures cause snow accumulation, which delays infiltration and surface runoff until temperature rises above 0^oC.

2.3 Review of Field Studies on Phosphorus Losses

There is much evidence that correlation exists between the amount of P in soil and the quantity of P pollution. Heckrath et al. (1995) showed that, in a field with subsurface tile drainage, P may be retained well in plow layers when P concentration was below a critical limit. However when P concentration exceeded this limit, P loss in drainage water was proportional to the concentration of Olsen-P in soil. Sharpley (1995) demonstrated that P concentration in runoff water may be highly correlated (R^2>0.90) with the Mehlich-3 P content of surface soils.

A selected number of studies are reviewed below, concerning patterns of P loss in subsurface drainage mainly at the field scale, but these also include a few studies conducted at lysimeters or catchment scale. Factors affecting P loss will be discussed, as well as the timing and speciation of P loss.

Natural factors affecting P loss

P loss is strongly affected by soil characteristics. Beauchemin et al. (1998) highlighted the link between soil texture and P loss risks in subsurface drainage. The experiment was conducted at 27 flat terrain experiment sites in Quebec that contained nine soil types, five of which were clayey soils, two were medium textured soils, and two were coarse textured soils. In 1994, 14 of the 27 sites exhibited total P loss that exceeded the water quality guideline of 0.03 mg/L; ten of these 14 sites were clayey soils, three were coarse textured soils, and only one was medium textured soil. This demonstrated that flat, clayey soil with medium to high P content (i.e. from long term fertilization) may have the greatest risk of P loss in subsurface flow than other soil types; meanwhile medium textured soil exhibited the lowest risk. The experiment also found high variation in P speciation in subsurface drainage. For example, particulate P fraction ranged from 2-96% of total P, dissolved reactive P ranged from 0-59%, and dissolved organic P ranged from 0-79%. These variations were attributed to differences in soil management, crop type, and preferential flow.

Macropore flow has been proven to be an important pathway of P loss in subsurface drainage,

as reported by various field studies (Djodjic et al., 2000; Eastman et al., 2010; Laubel et al., 1999; Turtola and Jaakkola, 1995).

The elevation gradient is also an important factor. Melland et al. (2008) studied 4 hill slope pasture plots in southern Australia by measuring surface runoff and estimating subsurface flux from soil moisture. It was found that while N was mainly lost via subsurface flow, P was mainly lost via surface runoff. Similarly, the Heathwaite and Dils (2000) study conducted on a hill slope in UK also reported that surface runoff was an important pathway for P loss. In contrast, the main pathway of P loss on a flat terrain field in southern Ontario was found to be subsurface tile drainage (Tan and Zhang, 2011).

Management factors affecting P loss

Agricultural management practices are also important influences of P loss. Bengtson et al. (1988) investigated how subsurface tile drainage affected P loss in the field. This experiment was conducted at four test plots in Mississippi which had alluvial clay loam soil. Two of the plots had tile drainage installed, while the other two were control plots without tile drainage. All four test plots had surface drainage. The presence of tile drainage had increased total drainage volume by 35%, while reducing P loss by 36%. P speciation was not studied in this experiment.

Water table control of tile drainage also has significant impact on P loss. Tan and Zhang (2011) investigated the effects of regular free tile drainage versus controlled drainage with sub-irrigation at two 0.33 ha sites in the Great Lakes area. With regular free drainage, 95-97% of total P loss occurred in the tile drains, and the remaining 3-5% was lost by surface runoff. The pattern was very different from the controlled drainage system with sub-irrigation, where tile drainage contributed 65-71% of total P loss, and surface runoff contributed 29-35%. As for P speciation, particulate P was the main form of P in both drainage systems, accounting for more than 80% of total P loss. In comparison with regular tile drainage, controlled drainage with sub-irrigation produced similar levels of total dissolved P while reducing particulate P by 15%. Therefore

controlled drainage with sub-irrigation may be a beneficial management option for reducing P loss under similar climate and soil conditions.

Turtola and Paajanen (1995) tested the effects of improved subsurface tile drainage on erosion, N loss, and P loss in heavy clay soil. A 29-year old tile drainage system was fitted with new drains to improve flow, and backfilled with either top soil or wood chips. The improved subsurface tile drain had increased subsurface flow volume while reducing P loss when top soil was used as backfill. At the same time, improved drainage had increased N loss, highlighting a difficulty to reduce N and P pollution simultaneously.

The combined effects of soil type and drainage were investigated by Eastman et al. (2010). Four experimental sites were setup to test sandy loam versus clay loam soil, and to test natural drainage versus artificial subsurface drainage. It was found that the presence of artificial subsurface drainage minimized P loss in sandy loam soil, but increased P loss in clay loam soil.

Gaynor and Findlay (1995) studied the effect of tillage on P loss in Brookston clay loam soil in the Great Lakes area. Here experimental plots of 0.1 ha size were fitted with tile drains and treated with three tillage treatments: conventional, ridges, and no-till. It was found that conservation tillage caused more P loss than conventional tillage, in terms of total P, total dissolved P, and orthophosphates. As for P speciation, dissolved P consisted of 84-93% of total P loss. Tile drainage had accounted for 55-68% of orthophosphate loss, while sediment P was mainly lost through surface runoff rather than tile drainage.

Timing of P loss

P loss from agricultural fields was generally found to be episodic, triggered by rainfall events of medium to high intensities. This pattern was reported for both surface runoff and subsurface drainage by numerous studies. Grant et al. (1996) studied four catchments with loamy soil during a 1-year study, where P loss was found to be episodic and occurred during storm events. Ulen and Persson (1999) studied six years of tile drainage P loss at a 4.43 ha drainage system in central

Sweden. The pattern of P loss was reported as episodic, as half of the yearly P transport occurred within 140 hours. Heathwaite and Dils (2000) found that surface runoff P loss on a hills lope catchment mainly occurred during high intensity rainfall events, but was an important pathway of P loss. Gelbrecht et al. (2005) found that P loss from a catchment site in northeastern Germany was strongly influenced by infrequent storm water events. Here the main P loss pathway was subsurface flow due to tile drainage presence. Tiemeyer et al. (2009) studied a small tile drained catchment in northeastern Germany. P loss was event based, as more than half of P loss occurred via fast flows that only made up of 18-23% of total water discharge volume.

P loss is also influenced by season. Tiemeyer et al. (2009) found that P loss was low during winter, but increased at snowmelt times likely due to P remobilization processes under anaerobic conditions. Turner and Haygarth (2000) found that total P concentration peaked in late spring season in leachate water from large scale monolith lysimeters.

Speciation of P loss

It is also important to examine the speciation of P loss. In a water sample, P may be measured as total P, total dissolved P, particulate P, dissolved reactive P, and dissolved organic P (Pote and Daniel, 2000a, b). Some studies have found that particulate P was the dominating form of P loss. Ulen and Persson (1999) found that particulate P accounted for 63% of total P loss at a 4.43 ha drainage system in central Sweden. Uusitalo et al. (2001) found that particulate P consisted of 92% of total P loss from two artificially drained clayey soils. Tan and Zhang (2011) reported that particulate P contributed more than 80% of total P loss in tile-drained Perth clay soil in southern Ontario.

Other studies have found that dissolved P dominated P loss. Gaynor and Findlay (1995) reported that dissolved P contributed to 84-93% of total P loss from tile-drained Brookston clay loam soil in southwestern Ontario. Turner and Haygarth (2000) found that P speciation in leachate from large-scale monolith lysimeters was mostly dissolved P. For clay loam soil, the speciation of

P loss was: 79% total dissolved P, 21% particulate P, 63% dissolved reactive P, and 16% dissolved unreactive P.

A number of factors contribute to the speciation of P loss, these include soil texture, vegetation cover, fertilization methods and flow pathways. Eastman et al. (2010) found that speciation in P loss was strongly dependent on soil texture rather than hydrology. The amount of particulate P may be linearly correlated with particulate matter in soil, as discovered by Laubel et al. (1999) in a controlled plot experiment with rain simulator. Sometimes the speciation of P varies even in a single study. Grant et al. (1996) studied four catchments with loamy soil during a one year study. Total dissolved P accounted for most of P loss in a grazing catchment, but particulate P accounted for most of P loss in other non-grazing catchments. Turtola and Jaakkola (1995) studied 16 field plots in Finland with heavy clay soil, with two crops of barley and grass ley. The grass ley crop had used higher fertilization rate with broadcast application, whereas barley crop had used less fertilizer with placement fertilizer application. Particulate P consisted of 69% of total P loss for barley crop, but only 35% of total P loss in grass ley crop, due to difference in fertilization amount and method. Heathwaite and Dils (2000) studied P loss at a hill slope catchment and found dissolved P to be the dominant species of matrix flow P loss. However particulate P dominated macropore flow, indicating that the pathway for loss also has significant impact on speciation.

2.4 Review of Phosphorus Modeling

Computer modeling is an effective method to study the effects of fertilization and other agricultural practices on P pollution. Advantages of modeling include its fast speed and cost-effectiveness compared with field or laboratory research. Disadvantages include unrealistic assumptions and oversimplifications of processes and concepts. Also models need to be validated with observed data, and model validity may not stretch across different soil, climate, drainage and management settings.

In the past, a number of studies have modelled P dynamics for laboratory, lysimeters and field-scale experiments. Various methods have been developed, ranging from index calculation to regression analysis, to numeric mechanistic models. Selected studies are reviewed here to provide an overview of recent and current modeling methods and scope.

Laboratory and lysimeter scale

Tim and Mostaghimi (1989) developed a 2-dimensional model to describe P movement and transformation in vadose zone. The model was able to simulate soil column data well with only 7% deviation. The simulation focused on P movement but not P loss pathways of tile drainage and surface runoff.

Ben-Gal and Dudley (2003) used the Hydrus-2D model to predict soil P distribution in greenhouse lysimeters under continuous point-source irrigation, with and without corn crop in sandy loam soil. Fertigation was applied continuously using buried point source dripper every 2 hours. This study offered insights of P distribution under real soil conditions as well as simulated conditions of an ideal soil. Although the modelled P distribution cannot be directly compared with measured distribution due to differences in P speciation (soluble P versus bicarbonate extractable P); the study highlighted an issue that the Langmuir adsorption isotherm, with an assumption of instantaneous adsorption, was perhaps inaccurate for modeling P. It was recommended that a two-site kinetic adsorption model be used to better describe adsorption kinetics. The drawback of this study was the short experimental duration of 13 days, which could not address long-term questions of P distribution and losses. Also the results may not apply to outdoor field conditions due to the lysimeter setting and continuous point source fertigation.

Abou Nohra et al. (2007) modified the Hydrus-1D model to include a non-ideal competition adsorption model for P. This modification provided excellent adsorption results (R^2 = 0.96) for selected soils in batch adsorption tests. This study provided a valuable modification of an existing model, although the new adsorption model still needs to be evaluated using field data.

Elmi et al. (2012) used the Hydrus-1D model to estimate PO_4 leaching and adsorption in reconstructed soil columns. The model could not correspond well with measured data, likely because it over-predicted adsorption using the Freundlich isotherm. In this particular study, Hydrus-1D could not account accurately the soil structures and preferential flow found in undisturbed soil.

Field scale

Goulet et al. (2006) evaluated the P index method using measured P loss from nine experimental plots near Quebec City. The P index was able to predict total P loss by r=0.63 at 0.10 probability. However this was not a mechanistic model, and therefore the P index method developed may not apply to other soil and climate types.

Sedorovich et al. (2007) used a process-based Integrated Farm Systems Model to evaluate P loss in sediment and dissolved form, for a corn production system in Texas. The model was able to simulate both inorganic and organic P, and was able to account for surface runoff, erosion losses, leaching, plus management options such as manure fertilization rates, conventional and conservation tillage. The model predicted total P loss accurately when annual P application was less than 250 kg/ha, however the speciation of soluble P versus sediment P was not predicted accurately. This model did not consider tile drainage.

Larsson et al. (2007) used a dual porosity ICECREAM model for simulating tile drainage P loss in a clayey soil. This was a mechanistic model with considerations of tile drainage P loss, macropore flow and loss of particulate P. The chemistry of P was described by six solute pools, three organic and three inorganic. Macropore flow was found to be a major pathway of P loss, accounting for 40% of tile drainage P loss in the simulation. The model was able to capture certain episodic events of P loss, however some short term fluctuations were captured less well, with model efficiency of 0.44 for water flow, 0.43 for dissolved reactive P, and -2.1 for particulate P in the validation period. Poor prediction of particulate P indicated the difficulty of simulating

particulate P loss through macropores in clay soil.

van der Salm et al. (2011) used the PLEASE model to simulate P loss at field scale. Thirty-one lowland sites in Denmark and Netherlands provided field data of P concentrations in tile drains, suction cups, and groundwater. The PLEASE model predicted P leaching based on the amount of adsorbed P and the P concentration in soil water plus the lateral groundwater flow, with good results. Modeling efficiency ranged from 0.36 for groundwater to 0.92 for total P fluxes. However the model strongly underestimated flow and P concentrations in heavy clay soils and peat soil types. The simulation error in heavy clay soil was attributed to macropore transport of P to tile drain pipes and an underestimation of overland flow.

Morrison et al. (2013) used the DRAINMOD model to simulate water flow in the field, and then used linear regression analysis based on water flow to predict P loss. This method provided a good estimation of water flow, with modeling efficiency of 0.70 to 0.83 for water flow validation. The subsequent regression analysis was able to predict P loss sufficiently well, with root mean square error of 0.97 to 3.41 for tile drainage P loss, and 0.85 to 9.75 for surface drainage P loss. Among the two experimental sites A and B, the regression analysis was more accurate for site A which had uniform soil conditions, and less accurate for site B which had soil cracking, preferential flow and higher P levels. This method of predicting P loss using flow-based regression analysis addressed a common problem that existing models often lack the ability to simulate P. However since this was not a mechanistic model, its validity for other soils and different climate patterns needs to be tested further.

After examining previous research, it is evident that there is a lack of modeling work in the area of P loss prediction in tile drainage (especially controlled tile drainage) using mechanistic modeling approach. Existing modeling work have highlighted difficulties of simulating P loss in macropore-prone heavy clay soils. This project will try to address these issues, but first a suitable model needs to be selected for the simulation of field data.

2.5 Overview of Models

Several field scale models are reviewed here for their ability to simulate key aspects of field conditions, including controlled tile drainage, surface runoff, and the ability to simulate P adsorption and transport processes.

DRAINMOD

DRAINMOD (Skaggs, 2012) is a 1-dimensional model for simulating hydrology, salinity and nitrogen dynamics of poorly drained, high water table soils. This model can simulate a wide range of water flow scenarios such as climatological inputs, evapotranspiration, surface runoff, conventional tile drainage, controlled tile drainage, sub-irrigation, freeze/thaw soil conditions, crop yield, etc. In addition it can also simulate wetland and wastewater. The latest version 6.1 includes salinity and nitrogen modules (Skaggs, 1980; Skaggs et al., 2012). DRAINMOD lacks a general solute module, which prohibits the simulation of any other solutes such as pesticides, ions, and P.

RZWQM2

The Root Zone Water Quality Model 2 (RZWQM2) (USDA Agricultural Systems Research Unit, 2013) is a 1-dimensional process-based model that simulates water flow, solute transport and biological processes in an agricultural crop system. Water flow is described by Brooks-Corey equation, and this model is able to simulate surface runoff, tile drainage, water table control, macropore flow, snow accumulation and melting. Heat transport can be simulated but not frozen soil conditions. RZWQM2 accounts for many agricultural management practices such as crop planting, harvest, tillage, manure and inorganic fertilizers, various irrigation methods, residual decomposition, etc. The model can simulate 23 crop species and their respective variety characteristics, a feature provided by the incorporated DSSAT 4.0 module; it can also simulate turf and tree growth. RZWQM2 has good modeling capabilities for C, N, and pesticides. However its

lack of general solute module means P cannot be simulated using this model. Attempting to use the pesticide feature to simulate P will be challenging.

CHEMFLO-2000

CHEMFLO-2000 (Nofziger and Wu, 2003) is a 1-dimensional model for simulating water flow and solute transport in soil. Richard's equation is used to describe water flow. Its major limitation is the lack of source and sink terms, which means it is unable to simulate tile drainage and root uptake. It also does not simulate macropore flow and hysteresis effects. Due to these limitations, this model is more suitable for soil column studies rather than field conditions.

APEX

The Agricultural Policy / Environmental eXtender (APEX) model (Williams et al., 2008) is a management tool for simulating field scale, farm scale, or small watershed scale landscapes. It is a multi-field extension version of the older Environmental Policy Integrated Climate (EPIC) model. APEX focuses on farm management, as it evaluates factors such as sustainability, wind and water erosion, economics, water and soil quality, plant competition, weather, and pests on a farm. In terms of hydrology, surface runoff is estimated based on SCS curve number method. The model can simulate major nutrients C, N, and P as well as sediments and pesticides. Advantages of its P module are the functions of simulating P in manure fertilizer, mineralization, crop yield, P runoff loss, as well as sediment P loss. APEX does account for subsurface drainage but it treats the underground drainage system as a modification of the natural lateral subsurface flow of the area. This likely would not permit simulation of controlled tile drainage.

LEACHM

The Leaching Estimation and Chemistry Model (LEACHM) (Hutson, 2003; Hutson and Wagenet, 1987) is a process-based model for simulating water flow, solute transport and reactions,

and plant uptake in the unsaturated zone. Water flow can be simulated using Richard's equation or the Addiscott mobile-immobile capacity model. Surface runoff and erosion are included in the model, and runoff is estimated using soil profile hydrology and SCS curve number method. The model includes pesticide transformations and transport functions, and sub-models of LEACHC, LEACHN, and LEACHP are designed to simulate C, N, and P nutrients with their respective reactions and transport pathways. This model is able to consider manure fertilizer, organic matter decomposition as well as interactions between C, N, and P pools, all of which mimic realistic field conditions. The main limitation of LEACHM is that it does not simulate subsurface tile drainage, which limits its usage to non-tile drained agricultural areas (Hutson, 2003).

Hydrus-1D

Hydrus-1D (Simunek et al., 2009) is a 1-dimensional numeric model for simulating water flow and solute transport in variably saturated porous media. Water flow can be simulated using a wide range of governing equations including van Genuchten-Mualem, Brooks-Corey, and Kosugi equations. It can account for macropore flow using mobile-immobile dual porosity equations, and it can simulate subsurface tile drainage by using either the Hooghoudt equation or the Ernest equation (Simunek et al., 2009). Hydrus-1D has a versatile solute transport module, as it can simulate a general solute with its adsorption, transport and reactions, as well as simulate major ions such as CO_2, Ca, Mg, Na, K, SO_4, Cl, NO_3, H_4SiO_4. Other functions of the Hydrus-1D model include heat transport, bacterial transport, 2-site adsorption, and inverse solution of problems. This model requires a large number of inputs parameters such as climatological data, soil properties, solute transport and reaction parameters, root depth, and crop properties. Limitations of the model include its inability to address uneven tile drainage spacing, controlled tile drainage, sub-irrigation, solid and manure fertilizers, as well as agricultural practices such as cropping and tillage. In the meantime, one major advantage of this model is that both the model and its source code are both freely available, which enables model modifications/coupling work, such as the HYDRUS-NICA

model (Abou Nohra et al., 2007) and the HYDRUS1D-PHREEQC model (Jacques and Simunek, 2005).

HYDRUS (2D/3D)

HYDRUS (2D/3D) (Sejna et al., 2011; Simunek et al., 2011) is a two- and three-dimensional model for simulating water flow and solute transport in variably saturated porous media. It is a commercial version of the Hydrus-1D model described previously, although HYDRUS (2D/3D) no longer retains the function of 1-dimensional modeling. Note that HYDRUS (2D/3D) should not be confused with an older Hydrus-2D model. Most of the water flow and solute transport functions remain the same as in Hydrus-1D model, but there are a number of improvements. The simulation of macropores can now be performed using an add-on dual permeability module to permit water and solute movement in both soil matrix and macropores. This is more realistic than the mobile-immobile equation for macropore flow, which assumes that flow only occurs in macropores but not in soil matrix. The soil profile can be simulated in two or three dimensions, allowing irregular shapes to be defined. Tile drainage representation is different from the Hydrus-1D model. In a regular finite element mesh (defined by triangular grid), a tile drain is represented by a hollow opening in the soil profile with seepage boundary condition; whereas in a rectangular finite element mesh (defined by rectangular grid), a tile drain is represented by a single node, using an approach developed based on electrical analog experiment by Vimoke and Taylor (1962). Controlled tile drainage can be simulated using the regular finite element mesh, by assigning a special seepage boundary condition with user-specified pressure head value. Sub-irrigation and triggered irrigation are also available functions. The limitations of HYDRUS (2D/3D) include a lack of agricultural management options such as fertilization, crops and tillage, plus incompatibility of several key functions. For example, the multiple solutes function is not compatible with active root uptake of solute, and this becomes an issue when crop nutrients N, P, K are simulated as solutes. The physical nonequilibrium setting for macropores is not compatible

with chemical nonequilibrium setting for 2-site adsorption. Also the general solute module can be rather simplistic when modeling complex solutes such as P, because the multiple solute representations only supports solutes arranged in a unidirectional reaction chain, it is not possible to setup bi-directional reactions/equilibriums between two solutes pools.

Despite these limitations, HYDRUS (2D/3D) is still the most suitable model for simulating P loss in tile drainage due to its capability of simulating controlled tile drainage and its general solute module. The other models described previously lack either tile drainage function, water table control, or lack the ability to simulate P reaction and transport. Therefore it was decided to use HYDRUS (2D/3D) model in this project to simulate water flow and P fate and transport in soil.

Chapter 3 Methods

3.1 Field Site and Experiment Description

All field data used in this study have been provided by Dr. Chin Tan and Dr. Tiequan Zhang of Agricultural and Agri-Food Canada (AAFC) at Harrow, Ontario, Canada.

Field site

The AAFC study site is located at Woodslee (latitude 42.1723 N, longitude 82.8173 W) near the town of Harrow, Ontario, Canada, which is between Lake St. Clair and the western basin of Lake Erie. The local soil is Brookston clay loam; it is 28% sand, 37% silt and 35% clay on average, with minor spatial variations across the site and across different soil depths. Average soil bulk density is 1.34 g/cm^3, and average porosity is 52.4%, both measured in 2010. The soil hydraulic conductivity (K_s) ranges from 1.7 to 11.9 cm/day, measured in 2008 across the site, and average K_s is 5.0 cm/day.

This site hosts 16 identical experimental plots, each plot measures 67.1 m long and 15.2 m wide, which is approximately 0.1 ha in area. The plots are hydraulically separated from each other by impermeable barriers that were installed vertically underground, which prevents subsurface water from flowing across plots. There are buffer strips between plots that are about 5 m wide, and the buffer zones have their own subsurface tile drainage to prevent water movement from buffer strips into plots.

Subsurface tile drainage has been installed on site to allow excess water to quickly drain out of the soil profile in wet seasons. Each plot currently has three tile drains at 0.85 m depth, installed parallel to the length of the plot. The tile drain pipes are 4-inch (10.16 cm) corrugated and perforated big "O" type. The spacing of tile drains is 3.8 m between adjacent drains, and 3.8 m between the tile drain and edge of the plot. There are water table control structures (risers) installed, which allow each plot to have individualized water table management, such as regular tile

drainage, controlled drainage and sub-irrigation. Water flow from tile drainage can be collected for flow volume monitoring and water quality sampling.

This site is also setup to monitor surface runoff. The soil surface on site has been leveled using laser equipment to achieve approximately 0.1% elevation gradient, and catch basins are set up at the end of each plot to collect surface runoff.

The tile drainage and runoff collected from the plots would then be delivered through underground pipes to a centralized instrumentation building, where 32 automatic gauges continuously monitor and record the flow rates of surface runoff and tile drainage of the 16 plots. Auto-samplers perform periodic sampling of water, and the water samples can then be analyzed in the laboratory for water quality such as N and P.

After water passes through the instrumentation building, it can be stored in a nearby reservoir pond for sub-irrigation purposes. There are currently four separate reservoir ponds that correspond to four different fertilization treatments in the 2008 experiment, explained in more details in the next section. The four ponds are also hydraulically separate from each other by vertical impermeable barriers.

Prior to 2004, the site was used for former experimentation with liquid manure and compost-cover crop phase. From 2005 to 2007, corn and soybean crops were planted. Before 2007, each plot only had two tile drains, and the third tile drain was installed in the centre of every plot between two existing tile drains during October and November of 2007. The installation process disturbed the soil directly above the new tile drain, although there was less soil disturbed than the trencher method. This soil disturbance will be taken into account by the model for the P simulation.

Field experiment description

The AAFC field experiment was initiated in the spring of 2008, and it is an ongoing project as of 2014. This experiment investigates the effects of P fertilizer type and water table

management on crop yield, tile drainage and surface runoff flow rates, and water quality. A general description of the experiment will be given below. More details of the experiment and preliminary results can be found in Tan et al. (2011).

For this experiment, the 16 experimental plots on site were assigned as eight pairs of duplicate plots to investigate eight combinations of treatments, which consist of two treatments of controlled tile drainage and four treatments of fertilization. Figure 3.1 is a schematic site plan which shows the layout of the site as well as the treatments assigned to each plot.

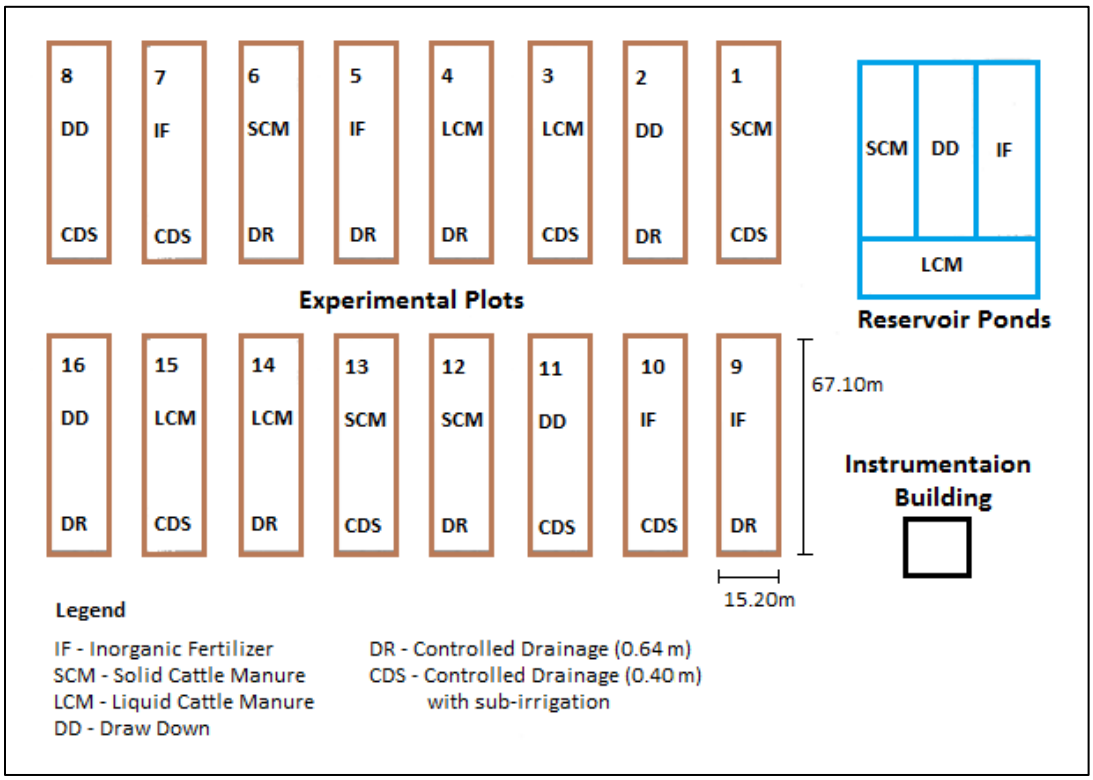

Figure 3.1 Site plan of the AAFC-Harrow research site (not drawn to scale).

The two treatments of controlled tile drainage differ in the depth of water table control and differ in sub-irrigation. The first treatment used risers to set the water table control at 0.64 m depth. The second treatment set the water table control at a shallower depth of 0.40 m, and in addition used water from reservoir ponds to sub-irrigate the field via tile drains.

The fertilization was performed every two years, during June 4th-17th, 2008 and June

11^{th}-25^{th}, 2010. Four fertilizer treatments were being tested for this experiment: inorganic fertilizer, liquid dairy cattle manure, solid dairy cattle manure, and P "draw down". They provided the same rates of nitrogen (N), phosphorus (P), and potassium (K) to every plot (the exception being the "draw down" treatment) but differed in the nature of P fertilizer. The Inorganic fertilizer treatment used only inorganic fertilizers, which were 100 kg P_2O_5/ha of Triple Superphosphate [$Ca(H_2PO_4)_2$•H2O], 200kg N/ha of NH_4NO_3, and 100 kg K/ha of KCl. The liquid and solid cattle manure treatments used manure disced to 7.6 cm (3-inch) depth to fulfill the P fertilization requirement of 100 kg P_2O_5/ha. Then the fields were supplemented with inorganic N and K fertilizers to reach 200kg N/ha and 100 kg K/ha, respectively. Finally, the plots that were fertilized for N and K using inorganic fertilizer, but not fertilized with P, were called the P "draw down" treatment. This was designed to observe patterns of crop yield and water quality under absence of P fertilization over time.

Prior to the start of the experiment, soil properties such as sand/silt/clay composition, saturated hydraulic conductivity (K_s), bulk density, field capacity, and permanent wilting point were measured for every plot. Some degree of spatial variability was observed across plots and over different depths. Initial soil P concentration was measured for each pair of duplicate plots as total soil P and Olsen P.

The field experiment aimed to replicate real cropping conditions. Corn and soybean crops were planted, with crop rotation occurring every 2 years similar to agricultural practices in the surrounding area. In 2008, corn variety NK-N23F-GT/CB/LL was planted at a density of 79,800 seeds/ha on June 18^{th} and harvested on Nov 5^{th}. In 2009, soybean variety Pioneer 92Y53RR was planted at 486,700 seeds/ha on May 22^{nd} and harvested on Oct 20^{th}. In 2010, corn variety NK-N23F-GT/CB/LL was planted at 79,700 seeds/ha on June 26^{th} and harvested on Nov 8^{th}. In 2011, soybean variety Pioneer 92Y53RR was planted at 486,700 seeds/ha on June 15^{th} and harvested on December 13^{th}.

Tillage and herbicide applications were used for all the experimental plots. Soil was tilled

using chisel plow, usually during the fall after crop harvest. If wet weather in fall did not permit tillage, it would be postponed until the following spring. Herbicides were applied for corn at a rate of 1.4 kg/ha of Roundup, 1.4 kg/ha of Dual II, and 1.0 kg/ha of Atrazine. Herbicides for soybean were applied at a rate of 1.4 kg/ha of Roundup, 1.4 kg/ha of Dual II, and 0.5 kg/ha of Sencor.

Field measurements and observations included crop yield, tile drainage flow rate, surface runoff flow rate, as well as the water quality of N and P in tile drainage and surface runoff water. The flow rates of tile drainage and surface runoff have been measured automatically on an hourly or half-hourly basis. Water samples were collected periodically during sampling periods of varying lengths, and only the average water quality data has been reported for each sampling period. The water quality tests concerning P include particulate P, total dissolved P, dissolved organic P, and dissolved reactive P (DRP).

3.2 Scope of Model

This modeling study will use the HYDRUS (2D/3D) software to simulate water flow and tile drain P loss from duplicate plots #5 and #9, which had the inorganic P fertilizer treatment and controlled drainage treatment with water table control at 0.64 m, with no sub-irrigation. The remaining plots were not simulated because they featured sub-irrigation and/or treatments of manure fertilizers. Sub-irrigation was not compatible with controlled tile drainage setting, while manure fertilizers could not be handled by HYDRUS (2D/3D).

For water flow simulation, the model considered precipitation, snow accumulation and melting, evaporation, crop transpiration, surface runoff, subsurface tile drainage flow, and crop water uptake. It did not consider hysteresis effects and macropore flow. The version of the software used (2.02.0680, without the Dual Permeability add-on module) did not permit simulation of macropore flow and matrix flow concurrently. The model used 507 days of water flow data from June 4th, 2008 to Oct 23rd, 2009 for calibration. The calibration period included the 2008 corn crop and the 2009 soybean crop. Model validation used 463 days of water flow data

from June 11th, 2010 to Aug 5th, 2011. The validation period included the 2010 corn crop, but only half of the 2011 soybean crop season due to lack of data after Aug 5th, 2011. Water flow rates were originally measured on hourly or half-hourly basis, and these have been compiled into daily flow rates for the purpose of this modeling study.

For P simulation, the model considered P fertilization, initial P concentration in soil profile before the experiment, P transport in soil by dispersivity and diffusion, P adsorption, crop uptake of P by passive and active means, and P loss in tile drainage. It did not consider P loss in surface runoff or particulate P. The model calibration and validation time periods for P simulation differ from those of water flow, due to P data being more limited than water flow data. P simulation was calibrated for 239 days from June 17th, 2008 to Feb 11th, 2009; and it was validated for 254 days from Feb 11th, 2009 to Oct 23rd, 2009. The calibration and validation periods of P simulation both occurred within the calibration period of water flow.

Measured P data was available for seven sampling periods (Table 3.1) from June 17th, 2008 to Oct 23rd, 2009. Each period ranged from 30 to 112 days, mainly decided by occurrence of rainfall events. Since water samples were collected and measured as composite samples, only one measured value of P concentration was available during each sampling period. That means a total of seven measurements of tile drainage P concentration were available for each experimental plot. In order to evaluate model performance, the model simulated P loss in daily time units but compiled results into sampling periods to compare with measured data.

Table 3.1 Water quality sampling periods for the field experiment.

Purpose	Sampling period #	Start date	End date	Number of days
Model calibration	122	17/06/2008	17/07/2008	30
	123	17/07/2008	22/10/2008	97
	124	22/10/2008	11/02/2009	112
Model validation	125	11/02/2009	27/03/2009	45
	126	27/03/2009	26/05/2009	61
	127	27/05/2009	16/07/2009	51
	128	17/07/2009	23/10/2009	99

The model used a simplified representation of P chemistry in soil. In reality, P exists in many different chemical forms. However due to limitations of the HYDRUS (2D/3D) software, representation of multiple solutes was not compatible with the function of active root nutrient uptake. Since the latter function was highly important for the P mass balance, multiple solutes of P could not be simulated. The model focused instead on solution P, also called orthophosphate ions ($H_2PO_4^-$, HPO_4^{2-}). It had been chosen for simulation due to its water soluble nature, its presence in neutral soil pH, its major role in soil adsorption and crop uptake, and its importance in tile drainage P loss. The P measurement of water quality that corresponds with solution P has been assumed to be dissolved reactive P (DRP) (Pote and Daniel, 2000a). As for the initial soil concentration of P, the model used soil Olsen P measurement and treated this as the sum of soluble orthophosphates and labile adsorbed P. The remaining P was assumed to be present in soil but not reactive during the duration of the P simulation, which was 495 days including calibration and validation. A further consequence of the single solute simulation was the model's inability to simulate organic processes involving P. In addition, HYDRUS (2D/3D) was not able to simulate P loss in surface runoff or by erosion.

The assumptions regarding the P chemistry are listed below, most of which will be explained in greater detail in the next section.

1. Equations and parameters regarding P transport, P adsorption, and P loss were assumed to be the same in duplicate plots 5 and 9.
2. The inorganic P fertilizer, Triple Superphosphate, dissolved in four days of rainwater at fixed concentration after fertilization.
3. P adsorption followed linear adsorption isotherm.
4. P adsorption assumed that instantaneous adsorption occurs at all the adsorption sites (1-site adsorption).
5. Crop uptake of P was assumed to be identical in duplicate plots 5 and 9.

3.3 Model Equations, Settings, and Inputs

The software package used by this modeling project was HYDRUS (2D/3D), version 2.02.0680 by pcprogress.com (Sejna et al., 2011; Simunek et al., 2011).

3.3.1 Soil profile in 2D

HYDRUS (2D/3D) offers both two- and three-dimensional modeling of the soil profile. For this field experiment, the rectangular shape of experimental plots permitted either 2D or 3D modeling (but not 1D modeling due to irregular spacing of its tile drains). The 2D mode was chosen for this model due to practical considerations of computer memory capacity and simulation run times.

Each experimental plot was rectangular in shape, 15.2 m wide by 67.1 m long, and the simulation depth was chosen to be 1.5 m. This model simulated a 2D cross-section (15.2 m wide by 1.5 m deep) of the experimental plot, and any output results had to be multiplied by the field length of 67.1 m to produce results for the entire plot. The cross-section was further divided vertically into three sections to achieve better convergence of simulation results. The divisions were based on mid-distance points between adjacent tile drains, and these sections were named "left edge", "center", and "right edge" sections for convenience. Each of these sections contained one tile drain. Due to uneven spacing of tile drains, the center section of the field was 3.8 m wide while the left edge and right edge sections were each 5.7 m wide. The edge and center sections were simulated separately, and after simulation, their outputs were combined to provide results for an entire field plot. Only one simulation was performed for the left and right edge sections as these were mirror images of each other.

Based on the defined dimensions of the soil profile, a triangular finite element mesh (FE-mesh) of nodes was created to serve as a basis for calculations. The FE-mesh was created with a stretch factor of 0.50 in the vertical direction, so that nodes were twice as dense in the vertical direction as in the horizontal direction. FE-mesh in the edge section of the field had 1947

nodes and FE-mesh in the center section had 1347 nodes.

3.3.2 Tile drain representation

Defining the tile drains was a key component of the soil profile design. As part of the triangular FE-mesh, each tile drain was defined as a hollow hole centered at the depth of 0.85 m. In the field, the actual tile drain pipes were standard 10.16 cm (4-inch) diameter corrugated pipes with partial permeability along the pipe walls. In this model, an effective diameter approach was used to overcome the difficulty of representing partial permeability. The actual pipe diameter of 10.16 cm was translated into 1.02 cm of effective diameter with full permeability through the pipe walls (Skaggs, 1980) in the model representation. The boundary condition used at the tile drains was seepage face, with a special option of seepage occurring at pressure head of +21 cm, which referred to the height of the water table control relative to tile drain location, calculated as the difference between the riser height of 0.64 m and the tile drain depth of 0.85 m.

3.3.3 Soil hydraulic property and water flow equations

Field measurements of soil properties have been conducted at four soil depths, shown in Table 3.2. Corresponding to these four depths, the soil profile in the model has been divided into four layers of soil, as shown in Table 3.3, with the assumption that soil at any depth would have the same properties as the nearest measurement depth.

Table 3.2 Field measurements of soil properties.

Plot #	Soil depth (cm)	Particle size analysis			Permanent wilting point[1] ($\%H_2O$)	Field capacity[2] ($\%H_2O$)	Hydraulic conductivity K_s (cm/day)	Bulk density (g/cm^3)
		% sand	% silt	% clay				
5	25	28.02	37.28	34.70	20.34	43.45	7.40	1.33
	45	27.57	32.34	40.09	19.40	38.50	n/a	n/a
	80	28.09	32.83	39.80	n/a	n/a	n/a	n/a
	120	25.01	36.20	38.79	n/a	n/a	n/a	n/a
9	25	29.94	36.33	33.73	19.80	39.60	3.10	1.37
	45	23.85	34.85	41.30	19.50	39.60	n/a	n/a
	80	25.94	33.00	41.06	n/a	n/a	n/a	n/a
	120	24.26	35.95	39.79	n/a	n/a	n/a	n/a

[1] Permanent wilting point was obtained via the pressure plate extraction method (Reynolds and Topp, 2007).

[2] Field capacity was determined using field collected soil cores incrementally saturated from bottom up over 4-day period under tension table (Reynolds and Topp, 2007).

The van Genuchten soil hydraulic functions (Equations 3.1 to 3.3) have been used to describe the soil hydraulic parameters (van Genuchten, 1980) in correspondence with Mualem pore size distribution (Mualem, 1976). Table 3.3 shows the van Genuchten soil parameters estimated using the built-in Rosetta module in HYDRUS (2D/3D).

$$\theta(h) = \begin{cases} \theta_r + \dfrac{\theta_s - \theta_r}{[1 + |\alpha h|^n]^m} & h < 0 \\ \theta_s & h \geq 0 \end{cases} \tag{3.1}$$

$$K(h) = K_s S_e^l \left[1 - \left(1 - S_e^{1/m}\right)^m\right]^2 \tag{3.2}$$

$$m = 1 - 1/n, \quad n > 1 \tag{3.3}$$

where

θ = water content (-)

h = hydraulic head (cm)

θ_r = residual water content (-)

θ_s = saturated water content (-)

α = inverse of air entry value or bubbling pressure (1/cm)

m = coefficient related to n, the pore size distribution index (-)

n = pore size distribution index(-)

K_s = saturated hydraulic conductivity (cm/day)
S_e = effective water content (-)
l = pore connectivity, usually 0.5 is the average value for soils (-)

Table 3.3 van Genuchten soil parameters estimated using the Rosetta module.

Plot #	Soil depth (cm)	θ_r	θ_s	α (1/cm)	n	K_s (cm/day)	l
5	0–35	0.0848	0.4853	0.0019	1.6964	8.05	0.5
	35–62.5	0.0741	0.4762	0.0043	1.4654	12.62	0.5
	62.5–100	0.0917	0.4727	0.0136	1.4029	16.03	0.5
	100–150	0.0915	0.4727	0.0126	1.4135	15.08	0.5
9	0–35	0.0741	0.4633	0.0032	1.5180	7.41	0.5
	35–62.5	0.0760	0.4702	0.0031	1.5260	8.35	0.5
	62.5–100	0.0917	0.4630	0.0138	1.3797	12.32	0.5
	100–150	0.0909	0.4615	0.0128	1.3989	11.61	0.5

Water flow in variably saturated porous media was solved by Richard's equation (Equation 3.4). The K term is the hydraulic conductivity, given by Equation 3.5.

$$\frac{\partial \theta}{\partial t} = \frac{\partial}{\partial x_i}\left[K\left(K_{ij}^{A}\frac{\partial h}{\partial x_j} + K_{iz}^{A}\right)\right] - S \tag{3.4}$$

$$K(h, x, y, z) = K_s(x, y, z)\, K_r(h, x, y, z) \tag{3.5}$$

where
θ = volumetric water content (-)
h = hydraulic head (cm)
S = sink term
x_i = spatial coordinates (-)
t = time (day)
K_{ij}^{A} = anisotropy tensor used for anisotropic medium (-)
K_r = relative hydraulic conductivity (cm/day)
K_s = saturated hydraulic conductivity (cm/day)

Macropore flow was not considered in the simulation because of the high variability of macropore formation and lack of macropore data. Hysteresis effects on the soil water retention curve were also not considered.

3.3.4 Leaf area index

The leaf area index (LAI) of crop canopy was not a required model input in HYDRUS (2D/3D). However since LAI determined several key inputs such as plant transpiration and nutrient uptake, it became an essential part of the model for both water flow and P transport simulations. Crop LAI was estimated for corn and soybean crops, based on maximum crop LAI as reported in literature as well as the cumulative growth degree-days (GDD) concept.

Maximum LAI for corn was set to 4.3, estimated from Loecke et al. (2004) which reported maximum corn LAI between 4.1 and 5.2. Maximum LAI for soybean was set to 6.4, estimated from Setiyono et al. (2008) which reported maximum soybean LAI between 5.0 and 7.8. LAI during each day of the growing season (Equations 3.6 and 3.7) was derived by curve fitting, based on maximum LAI estimates and cumulative growth degree-days (GDD_{cum}).

$$LAI_{corn} = -0.000006(GDD_{cum})^2 + 0.0102(GDD_{cum}) \quad (3.6)$$

$$LAI_{soybean} = -0.000006(GDD_{cum})^2 + 0.0124(GDD_{cum}) \quad (3.7)$$

Growth degree-days is a temperature index used for crop growth, with the assumption that crops only grow when temperature is warm enough, for example above 10°C. GDD_{cum} is the cumulative growth degree-days (°C) defined in Equation 3.8 (Loecke et al., 2004). For example, if the daily average temperature has been 13°C for three days, and the base temperature for the crop is 10°C, then the cumulative GDD would be (13°C - 10°C) x 3 days = 9°C.

$$GDD_{cum} = \sum_{i=1}^{n} \left[\left(\frac{T_{max} - T_{min}}{2} \right) - T_{base} \right] \quad (3.8)$$

where

T_{max} = maximum temperature of the day (°C)

T_{min} = minimum temperature of the day(°C)

T_{base} = base temperature above which crop can grow productively, T_{base} = 10°C

3.3.5 Precipitation

Daily precipitation rather than hourly precipitation was used as model input. Precipitation data was mostly measured at Whelan weather station, an AAFC weather station located less than 0.5 km from the experimental field. However during the winter period from Oct 1st, 2008 to Apr 30th, 2009, rain gauge problems at the Whelan station caused inaccurate measurements. Precipitation data from Harrow weather station (station ID 6133362, latitude 42.03 N, longitude 82.9 W) located 16.6 km away was used instead for this period (Environment Canada, 2008).

Not all of measured precipitation can reach soil. During crop growing season, the crop canopy may intercept a significant proportion of precipitation, which will never reach the soil profile. Baver (1938) and Lull (1964) reported that corn crop may intercept 16-22% of precipitation, whereas soybean crop may intercept 15-35% of precipitation. For this model, precipitation volumes during growing season were reduced to account for rain interception by crop canopy. It has been assumed that, on a daily basis, corn crops may intercept up to a maximum 20% of precipitation, while soybean crop may intercept a maximum 30% of precipitation. The "actual daily interception rate" was calculated based on the maximum interception by multiplying it with a ratio of current crop LAI to maximum LAI (Equation 3.9). The intercepted fraction of precipitation is assumed to never reach the soil profile, while the remaining precipitation became the precipitation input used by the model (Equation 3.10).

$$Actual\ interception\ rate = Max\ interception\ rate \times \frac{LAI}{max\ LAI} \tag{3.9}$$

$$Actual\ precipitation\ entering\ soil = Measured\ precipitation\ \times (1\ - Actual\ interception\ rate) \tag{3.10}$$

3.3.6 Potential evapotranspiration

Potential evapotranspiration (PET) values were originally estimated using a modified Priestley-Taylor method (Tan and Layne, 1981). However these values significantly overestimated PET, and multipliers with values between 0 to 0.6 were used to reduce the PET to realistic values during model calibration (see Table 3.4).

The justification of utilizing PET multiplier was obtained from the annual water balance of the soil profile. Tan et al. (2002) investigated a 3-year water balance of the local soil and found that that evapotranspiration used 55% of the total annual water input (i.e. precipitation), tile drain loss accounted for 30%, 8% was lost by surface runoff, and about 7% was the change in soil water storage. For this model, the water balances of plots 5 and 9 from June 2008 to June 2009 have been calculated in Table 3.5, using PET with and without the multipliers for comparison. It is evident that the Priestley-Taylor estimated PET (without multipliers) would have accounted for 95% of annual precipitation input, which was impossible because tile drainage and runoff during the same time period together accounted for 63-64% of precipitation. PET multipliers were necessary to maintain a realistic water balance. After applying the multipliers, PET values accounted for only 41% of precipitation input. Note that the water balance calculation here had used the precipitation value after crop interception, which was 980 mm of water; the original measured precipitation would have been 1030 mm.

Table 3.4 Multipliers of potential evapotranspiration (PET) during model calibration and validation periods.

PET multiplier	Model calibration period	Model validation period
0.6	June 1st–Aug 31st, 2008	June 1st–Aug 31st, 2010
0.2	Sept 1st–Oct 31st, 2008	Sept 1st–Oct 31st, 2010
0	Nov 1st, 2008–Mar.31st, 2009	Nov 1st, 2010–Mar.31st, 2011
0.6	Apr 1st–May 31st, 2009	Apr 1st–May 31st, 2011
0.4	June 1st–31st, 2009	June 1st–31st, 2011
0.6	July 1st–Aug 31st, 2009	July 1st–Aug 31st, 2011
0.2	Sept 1st–Oct 31st, 2009	Sept 1st–Oct 31st, 2011

Table 3.5 Water balance of plots 5 and 9 for 365 days from June 4th, 2008 to June 3rd, 2009 excluding soil water storage.

	Volume of water (mm)	% of precipitation
Precipitation after interception	980*	100%
PET estimated by modified Priestley-Taylor method	940	95%
PET reduced with multiplier	400	41%
Plot 5 tile drainage loss	480	48%
Plot 9 tile drainage loss	440	45%
Plot 5 surface runoff loss	140	14%
Plot 9 surface runoff loss	180	18%
Water balance error of plot 5 with PET multiplier **	-40	-4%
Water balance error of plot 9 with PET multiplier **	-40	-4%

* Precipitation without accounting for interception loss was 1030 mm for the specified time period.

** Water balance error = precipitation – PET with multiplier – tile drain – runoff

HYDRUS (2D/3D) requires that potential evaporation and potential transpiration values be entered as separate model inputs. LAI was used as a coefficient to divide PET into potential evaporation and potential transpiration, using Equations 3.11 and 3.12. The parameter k is a coefficient governing radiation extinction by canopy, usually ranging between 0.5 and 0.75 (Simunek et al., 2009). Here k has been calibrated to be 0.55.

$$Potential\ evaporation = PET \times e^{(-\mathrm{k} \times LAI)} \tag{3.11}$$

$$Potential\ transpiration = PET \times \left[1 - e^{(-\mathrm{k} \times LAI)}\right] \tag{3.12}$$

HYDRUS (2D/3D) computes the actual ET directly based on soil moisture and root water uptake; there is no need to use crop coefficient to calculate actual ET in the model.

3.3.7 Heat transport and snow

HYDRUS (2D/3D) considers heat transport in soil by both conduction and convection mechanisms. Atmospheric heat inputs were determined by Equation 3.13, a sine function which estimates daily temperature by the time of the day, and maximum temperature was set to occur at

1 pm every day by the 7π/12 term (Kirkham and Powers, 1972).

$$T_0 = \overline{T} + A\sin\left(\frac{2\pi t}{t_p} - \frac{7\pi}{12}\right) \quad (3.13)$$

where

T_0 = temperature at time zero (^oC)

$\overline{T}$ = average temperature at soil surface during period t_p (^oC)

t_p = time period for one cycle of sine wave, here t_p = 1 day

A = amplitude of sine wave (^oC)

t = local time within time period t_p, for example the hour of the day (day)

Heat transport was calculated throughout the soil profile, and the most important heat related function was the accumulation and melting of snow layer. In HYDRUS (2D/3D), precipitation is treated as rain when atmospheric temperature is above 2^{o}C, or treated as snow when temperature is below -2^{o}C. When air temperature is between 2^{o}C and -2^{o}C, precipitation would be a mixture of rain and snow (Simunek et al., 2011). Snowfall would accumulate into a snow layer on top of soil surface. When temperature rises above 0^{o}C, the accumulated snow would melt proportionally to air temperature (Sejna et al., 2011). All the snow related settings in this model were HYDRUS (2D/3D) defaults as they were not available for customization.

3.3.8 Initial pressure head

The initial pressure head was a key setting which could dictate the water balance for as much as the first three to six months of simulation. For this model, calibration started in June 2008, which was also the start of the field experiment. Since no previous data existed at this point, initial pressure head became a calibration parameter for the water flow calibration period. The pressure head was set as a linear gradient from -100 cm to -250 cm in plot 5, and from -60 cm to -210 cm in plot 9. The justification of setting different pressure head for the two duplicate plots was, even though plots 5 and 9 shared identical weather and very similar soil characteristics, their measured flow volumes in tile drainage differed significantly in July 2008, one month after the start of the experiment/simulation (see Figure 4.1). This can only be explained by a difference in soil water

storage in these two plots at the beginning of the field experiment, thus justifying the use of different initial pressure head settings for the two plots in simulation.

For the water flow validation period from 2010 to 2011, the initial pressure head was established in each plot by performing a pre-simulation which spanned five months before the start of the validation period. The results of the pre-simulation were then adapted as the initial pressure head of the validation period. The numeric values of pressure head at the soil surface and bottom are shown in Table 3.6.

Table 3.6 Initial pressure head simulation settings for calibration and validation.

Depth	Initial pressure head (cm) during calibration		Initial pressure head (cm) during validation as established by pre-simulation *	
	Plot 5	Plot 9	Plot 5	Plot 9
Soil surface (0 m)	-100	-60	-80 in edge section; -76 in center section	-80 in edge section; -76 in center section
Soil profile bottom (1.5 m)	-250	-210	74 in edge section; 78 in center section	74 in edge section; 78 in center section

* These values were approximated by visual estimations of the simulated pressure head distribution

3.3.9 Initial soil phosphorus concentration

The initial P concentration in soil can have a large impact on P simulation. At the start of the P calibration period, the initial soil P concentration was setup in three layers of varying concentrations. At the top soil horizon, from soil surface down to 0.15 m depth, P concentration was set to 0.03073 mg P / cm^3 soil in both plots 5 and 9. This value was derived directly from soil Olsen P measurements performed on site during spring 2008, which found the surface soil to contain 22.77 mg P /kg soil.

The second horizon was setup as a transition zone where P concentration linearly declined from 0.03073 mg P / cm^3 soil at 0.15 m depth, to 0.0000266 mg P / cm^3 soil at 1.00 m depth. The depth of the transition zone has been optimized by model calibration.

The deepest horizon below 1.00 m depth was assigned a uniform concentration of 0.0000266

mg P /cm^3 soil to represent the natural P concentration in soil, which is approximately 2 μM according to Raghothama (2005).

This initial soil P profile has been used for both plots 5 and 9 with only one exception. Recall that the centre tile drain was recently installed during fall 2007, and the soil directly above this tile drain was disturbed. It can be assumed that at least some top soil, with higher P concentration, fell downward during this disturbance. The model attempted to account for this disturbance by using surface soil P concentration of 0.03073 mg P / cm^3 near tile drain depth, and using the P concentration near the tile drain (0.0000266 mg P /cm^3) at the soil surface. The switching of P concentrations was done directly above the affected tile drain. In plot 5, two blocks of soil (100 cm^2 each in cross-section area) were switched for P concentrations; and in plot 9, two blocks of soil (200 cm^2 each in cross-section area) were switched for P concentrations. The area of soil being switched was decided by optimization in calibration. The difference in settings between plots 5 and 9 was probably due to very different soil moisture levels being present in the two plots at that time. The most direct effect of this P concentration switching was that, it increased P loss through the centre tile drain in the early few months of the simulation. Only P concentrations were changed in this process and not the soil hydraulic properties.

3.3.10 Phosphorus fertilization

Fertilization of the experimental field occurred from June 4th to 17th, 2008, at the rate of 100 kg P_2O_5/ha. This was equivalent to 43.6 kg of P/ha, or approximately 4.36 kg P per plot. HYDRUS (2D/3D) cannot process solid fertilizer as input, so an alternative approach was used similar to fertigation method. The inorganic P fertilizer Triple Superphosphate [$Ca(H_2PO_4)_2$•H2O] is a highly water soluble compound (International Plant Nutrition Institute, n.d.). In this model it was assumed to dissolve in rainwater during four days of rain which totaled 30.2 mm, from June 4th to 10th, 2008, at a constant concentration of 0.142 mg P/cm^3 rainwater. In the simulation, the mass of P being added into the soil profile was 4.29 kg P per plot, confirmed by simulation

outputs that tracked P mass transfer across the soil surface boundary.

3.3.11 Boundary conditions

Boundary conditions were an important part of the simulation. They did not constitute numeric inputs but decided how the other inputs were being calculated by HYDRUS (2D/3D). The 2D soil profile in this model has four external boundaries which are the soil surface, left side, right side, and bottom of the profile; plus an internal boundary lining the hollow circular opening of the tile drain. Each of the five boundaries needed to be specified a boundary setting for water flow, solute transport, and heat transport.

For water flow, the soil surface used an atmospheric boundary which can process daily atmospheric inputs of temperature, precipitation, evaporation and crop transpiration. The left and right sides of the soil profile had no flux (impermeable) boundary. These were located at midpoints between two adjacent tile drains so it was assumed that water did not flow horizontally across these boundaries. Finally the bottom of the soil profile at 1.5 m depth also used the no flux boundary. This was not an ideal setting because water does move across this depth in the field, but in HYDRUS (2D/3D) the no flux boundary was the only suitable option among all available choices. There is a distance of 0.65 m between the tile drain depth and the lower impermeable boundary. This is expected to not interfere with water flow near the tile drains, as this distance is greater than 0.45 m, the equivalent depth of impermeable layer below drains (Skaggs, 1980).

For solute transport, three boundary settings were available: no flux, first type, and third type. The first type is a concentration type boundary, also called Dirichlet, which assumes that concentration at soil surface is immediately equivalent to fertilizer input concentration. This setting frequently overestimates the incoming fertilizer amounts, and it is prone to serious error by allowing a fertilizer concentration of zero to spread to existing P concentration in soil profile. The third type is a flux type boundary, also called Cauchy or mixed, which is more realistic for considering water mixing time, i.e. the soil surface concentration would take time to gradually rise

to the specified fertilizer concentration. The third type boundary was chosen for P transport at the soil surface and tile drains, while all other boundaries were assumed to have zero flux of P.

The heat transport also has these three boundary settings: no flux, first type, and third type. The definitions of first and third type boundaries are similar to that of solute transport: the first type boundary would set the soil surface temperature to be instantaneously equivalent to air temperature, while the third type would require much more time for the heat transfer. In the case of heat transport, it was necessary to use the first type boundary at the soil surface, in order to transfer air temperature fast enough to achieve the correct snow accumulation. Tile drains present a different scenario, as they are not exposed to atmospheric air temperature. The tile drains could not use the zero flux heat boundary because a water flow boundary exists at the same location, preventing the usage of zero flux heat boundary. Therefore the third type heat boundary was used at the tile drains, in order to transfer heat as slowly as possible here to avoid distorting the heat distribution of the entire soil profile. A summary of boundary conditions is shown in Table 3.7.

Table 3.7 Summary of boundary conditions for water flow, solute, and heat transport.

Location	Water flow boundary	Solute transport boundary	Heat transport boundary
Soil surface	Atmospheric	Third type	First type
Left and right side of soil profile (halfway between 2 tile drains)	No flux	No flux	No flux
Bottom of soil profile at 1.5 m depth	No flux	No flux	No flux
Tile drain at 0.85 m depth	Seepage face at +21 cm pressure head	Third type	Third type

3.3.12 Phosphorus transport

The solution P moved around the soil profile mainly by soil water movements. Longitudinal dispersivity of soil was calibrated to be 20 cm. Transverse dispersivity of soil was 1 cm. The diffusion coefficient of orthophosphate ions in water was found to be 0.44 cm^2/day, obtained as average of values listed in Hatfield et al. (1966). Adsorbed P in soil was assumed to be immobile

unless desorption occurs.

3.3.13 Phosphorus adsorption

HYDRUS (2D/3D) has a generalized adsorption equation, which may be converted to Freundlich, Langmuir, or linear adsorption isotherms depending on empirical coefficients. This modeling study used linear adsorption isotherm, achieved when coefficients $\beta_k = 1$ and $\eta_k = 0$ in Equation 3.14. The adsorption coefficient K_d for P was calibrated to be 6.0.

$$s_k = \frac{K_d c_k^{\beta_k}}{1 + \eta_k c_k^{\beta_k}} = \frac{K_d c_k}{1} \tag{3.14}$$

where
s_k = adsorbed P (mg P/cm^3)
K_d = general adsorption coefficient
c_k = concentration of P in solution (mg P/cm^3)

The model used 1-site adsorption, which assumes that all adsorption sites have instantaneous rate of sorption. This is specified by parameter fract=1.0, which indicates that all adsorption sites (a fraction of 1.0) have instantaneous adsorption. When 0<fract<1.0, HYDRUS (2D/3D) would switch to 2-site adsorption setting with two types of adsorption sites, type one with instantaneous adsorption and type two with a user-specified kinetic adsorption rate.

3.3.14 Crop phosphorus uptake

In HYDRUS (2D/3D), the root distribution of crops determines the relative intensity of nutrient uptake at various depths. For this model, corn and soybean roots were setup to uptake nutrients and water mainly within the top 0.30 m of soil, where the roots are expected to be most dense and active. The remaining root uptake was setup to occur between 0.30-0.60 m depths, at gradually diminishing root intensities toward the deeper soil.

Crop uptake of P was calculated as a sum of passive root uptake and active root uptake, with the active root uptake being the dominant mechanism. The passive root uptake was calculated in

HYDRUS (2D/3D) by multiplying the amount of root water uptake with the concentration of P in soil solution at the root zone. The root water uptake was determined from the crop transpiration input, based on Feddes equation. The concentration of P in soil solution would be derived from real-time P simulations in the model. Since the concentrations of P in plant available form is usually very low in soil solution, the crop is assumed to uptake as much P as available by passive means. This is permitted by specifying a value of passive uptake threshold (cRoot) at a concentration of 0.1 mg / cm^3 water, well above P concentration in soil solution.

The active root uptake mechanism accounted for most of the P uptake by the crops. The rate of this uptake was defined by Michaelis-Mention equation with constant K_m of 0.1. Active root uptake required daily values of uptake concentration threshold (cRootAct), which was a calibrated parameter in the model, in order to achieve the correct crop P uptake as found in literature. Table 3.8 lists the values of active root uptake setting and the simulated amount of crop P uptake.

Table 3.8 Active root uptake threshold and simulated root P uptake by crops.

Crop, year	Date	Days after planting	Active uptake cRootAct (mg/cm^2/day)		Crop P uptake[1] (kg P /ha)	
			Plot 5	Plot 9	Plot 5	Plot 9
Corn, 2008	June 18th–July 18th	1-31	2	3	2.15	2.20
	July 19th–Aug 3rd	32-47	19	20	3.53	3.55
	Aug 4th–31st	48-75	33	34	8.45	8.44
	Sept 1st–16th	76-91	23	23	2.67	2.61
	Sept 17th–Nov 5th	92-141	0	0	0.61	0.59
	Sum	1-141	-	-	17.40	17.39
Soybean, 2009	May 22nd–June 10th	1-20	3	3	0.67	0.66
	June 11th–July 20th	21-60	28	28	7.76	7.72
	July 21st–Sept 18th	61-120	46	46	14.97	14.98
	Sept 19th–Oct 20th	121-152	0	0	0.25	0.25
	Sum	1-152	-	-	23.64	23.62

Note: The passive uptake threshold was 0.1 mg/cm^3 for the entire crop seasons.

[1] This is the sum of active and passive uptake.

Barber and Mackay (1986) reported corn uptake of P from 0 to 91 days of plant age for two

corn genotypes which received 227 kg/ha nitrogen application, similar to the N fertilizer rate used in this experiment. They found that, on average, the cumulative amount of P uptake by corn was 2.15 kg/ha at 31 days, 5.7 kg/ha at 47 days, 14.2 kg/ha at 75 days, and 16.8 kg/ha at 91 days. The model calibrated cRootAct parameter to achieve P uptake rates similar to the reported values during the first 91 days of corn crop. The model then assumed that, after 91 days, active uptake of P no longer occurred but passive uptake continued until crop harvest.

Panneerselvam et al. (2000) reported soybean uptake of P from planting to harvest during 1994 and 1995 June to September (kharif) seasons, with various herbicide/weeding options (W1, W2, and W3). On average, the cumulative P uptake for the aforementioned W1 to W3 options was 0.64 kg/ha at 20 days of soybean plant age, 8.4 kg/ha at 60 days, and 23.7 kg/ha at harvest time. The model assumed that all the active uptake of P occurred within 120 days of planting but passive root uptake continued until soybean crop harvest.

3.3.15 Special settings during model validation

This section addresses some special settings that have been applied only to the model validation periods.

Validation of water flow utilized identical settings as the calibration period, except for the initial conditions and weather related inputs. A pre-simulation was performed from Jan 1st 2010 to June 10th, 2010, and its results of pressure head and temperature were imported directly as the initial conditions of validation period. The weather inputs, new for the validation period, included daily precipitation, potential evaporation, potential transpiration, daily average temperature, and average temperature amplitude. The corn and soybean crop seasons also differed slightly between validation and calibration periods.

The validation period of P occurred consecutively after the calibration period, and these shared identical settings except that corn crop season occurred solely in calibration, whereas soybean crop season occurred solely in validation. The LAI, crop transpiration, and P uptake

values would differ between calibration and validation periods due to different crop types. For the P validation period, initial conditions such as pressure head, temperature, and soil P concentration did not need to be re-established as validation occurred consecutively after calibration.

3.3.16 Statistics

Nash-Sutcliffe modeling efficiency (NSE) in Equation 3.15 (Nash and Sutcliffe, 1970) has been used to evaluate the quality of the model simulation against observed data. NSE values may range between negative infinity to 1.0, with NSE=1.0 denoting perfect agreement of simulated and observed data. NSE value between 0 and 1.0 are considered acceptable (Moriasi et al., 2007).

$$\mathrm{NSE} = 1 - \frac{\sum_{i=1}^{n}(O_i - S_i)^2}{\sum_{i=1}^{n}(O_i - \bar{O})^2} \tag{3.15}$$

where
n = total number of observations (-)
O_i = observed data
S_i = simulated data
$\bar{O}$ = mean of observed data

The R^2 coefficient of determination (Krause et al., 2005) was used to evaluate the colinearity between observed and simulated data. First a linear regression (Equation 3.16) was fitted to the data in an attempt to predict simulated value based on observed value. The coefficient of determination, R^2, was then calculated using Equation 3.17 based on the linear regression. A perfect agreement between simulation and observation would have slope=1.0, intercept=0, and R^2=1.0.

$$y = mx + b \tag{3.16}$$

where
y = prediction of simulated data
m = slope of linear regression
x = observed field data
b = Y-intercept of linear regression

$$R^2 = \left(\frac{\sum_{i=1}^{n}(O_i - \bar{O})(S_i - \bar{S})}{\sqrt{\sum_{i=1}^{n}(O_i - \bar{O})^2}\sqrt{\sum_{i=1}^{n}(S_i - \bar{S})^2}} \right)^2 \quad (3.17)$$

where
n = total number of observations (-)
O_i = observed data
$\bar{O}$ = mean of observed data
S_i = simulated data
$\bar{S}$ = mean of simulated data

3.3.17 Sensitivity analyses

Sensitivity analyses examined ten input parameters that were expected to have the greatest influences on simulation results. Four of the parameters affect water flow patterns, and the other six parameters affect P simulation. For each parameter, one or two alternative values have been tested to assess model sensitivity. These parameters and their respective values are listed in Tables 3.9 and 3.10. A few of the values tested are unrealistic and only aim to demonstrate model sensitivity.

The four sensitivity parameters affecting water flow have been tested using plot 9 water flow simulation in calibration period. The parameters are: saturated hydraulic conductivity (K_s) of top soil layer, the use of multipliers for PET, the removal of crop canopy interception from precipitation in growing seasons, and the consideration of heat and snow module. These parameters would also affect P loss patterns indirectly due to changes in water flow.

The remaining six sensitivity parameters affect P chemistry directly, and these have been tested using the plot 9 P simulation, with both calibration and validation periods combined, in order to illustrate changes over a longer period of time. The parameters are: P adsorption coefficient (K_d), 1-site or 2-site adsorption which differ in the rate of adsorption (instantaneous or kinetic rates), longitudinal dispersivity of soil, diffusion rate of P in aqueous solution, fertilization rate of P, and the initial soil P concentration.

Table 3.9 Sensitivity analyses of parameters affecting water flow.

Parameter	Value in original simulation	Values for sensitivity analyses
Saturated hydraulic conductivity (K_s) of top soil layer	7.41 cm/day	4.41 cm/day; 10.41 cm/day
PET multiplier	Multipliers were used to reduce PET (see Table 3.4)	No multiplier
Crop canopy interception of precipitation	Yes (less precipitation reaches soil during growing season, see section 3.3.5)	No (all precipitation reaches soil)
Heat and snow module	Yes (see section 3.3.7)	No

Table 3.10 Sensitivity analyses of parameters affecting P simulation.

Parameter	Value in original simulation	Values for sensitivity analyses
P adsorption coefficient (K_d)	6.0	4.0; 8.0
1-site or 2-site adsorption model	1-site adsorption, 100% instantaneous adsorption sites	2-site adsorption, 50% instantaneous adsorption sites, 50% kinetic adsorption sites with 0.01 /day rate
Longitudinal dispersivity of soil	20 cm	5 cm; 35 cm
Diffusion rate of P in aqueous solution	0.44 cm^2/day	4.4 cm^2/day
Fertilization rate of P	100 kg P_2O_5/ha	0 kg P_2O_5/ha; 200 kg P_2O_5/ha
Initial soil P concentration	see section 3.3.9	All initial P concentrations multiplied by factor 50%; or multiplied by 150%

Chapter 4 Results and Discussion

4.1 Water Flow Calibration

The calibration of water flow was performed for subsurface tile flow and surface runoff of experimental plots 5 and 9, from Jun 4th, 2008 to Oct 23rd, 2009. Figure 4.1(a) shows precipitation and temperature of the calibration period. Figures 4.1(b) and 4.1(c) show results of the calibration in cumulative daily tile flow and cumulative daily surface runoff.

Measured tile flow and surface runoff exhibited little flow volume during summer and fall seasons, with the exception of occasional flow events which likely involved macropore flow. The majority of annual flow volume occurred during winter and spring seasons, when low evapotranspiration and abundant winter precipitation provide enough water for drainage. Overall tile drainage consisted of 71-77% of total annual drainage volume whereas surface runoff consisted of the remaining 23-29%.

Plots 5 and 9 were duplicate plots that shared identical precipitation, evaporation, temperature, and tile drainage setup; they only differed slightly in soil characteristics. It is therefore interesting to observe drastically different water flow measurements between these plots. For example, from July to November 2008, Plot 9 had accumulated 40,634 L and 64,600 L of water flow, respectively, in tile drainage and surface runoff; while plot 5 only accumulated 13,402 L and 26,446 L, respectively. The differences suggest that perhaps in the field, these two plots had started the experiment with very different levels of soil water storage. In order to reflect this in the simulation, the model utilized different initial conditions of pressure head for plots 5 and 9.

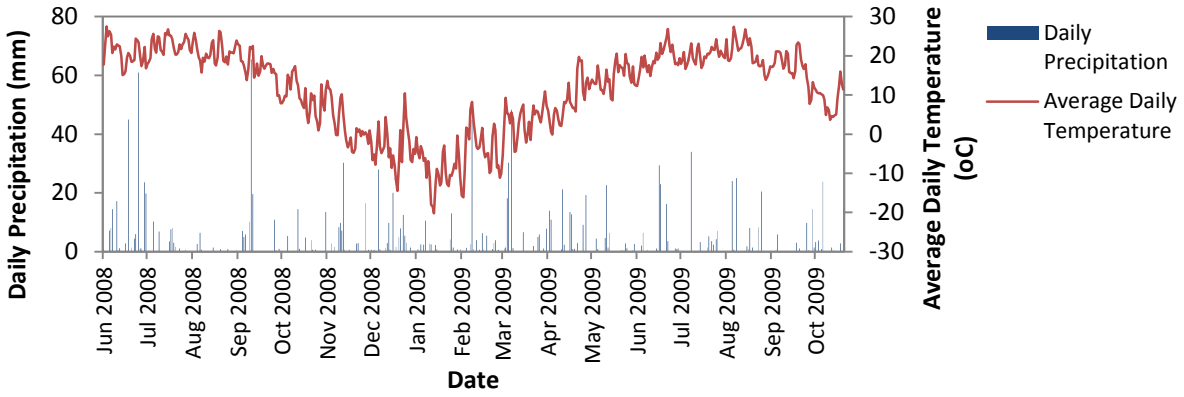

Figure 4.1(a) Daily precipitation and temperature during model calibration period.

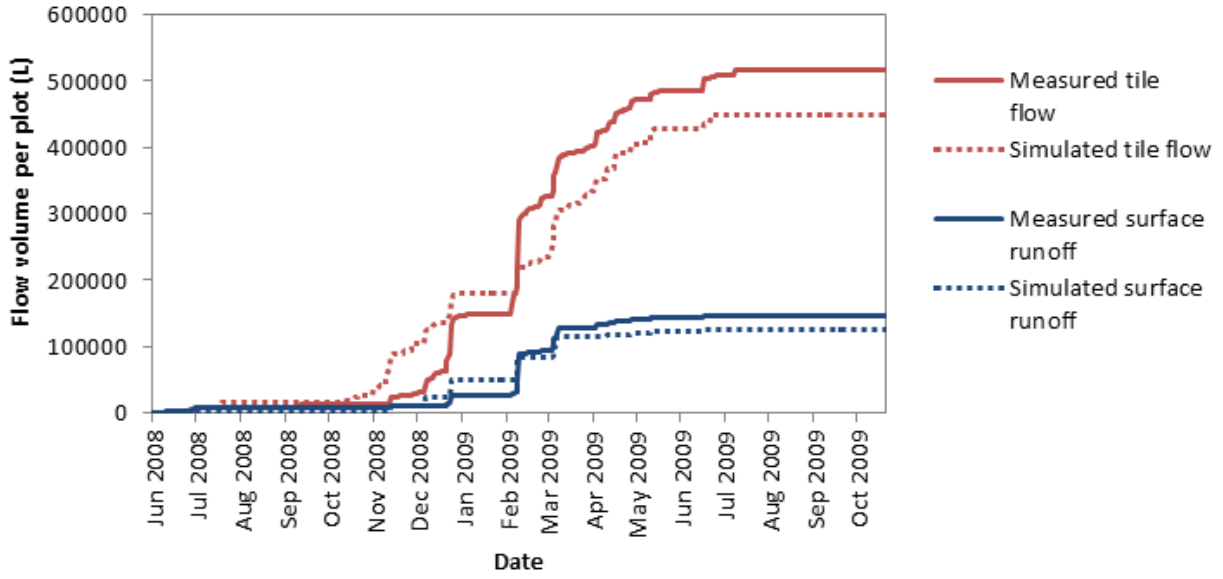

Figure 4.1(b) Water flow calibration for plot 5 from June 4th, 2008 to Oct 23rd, 2009.

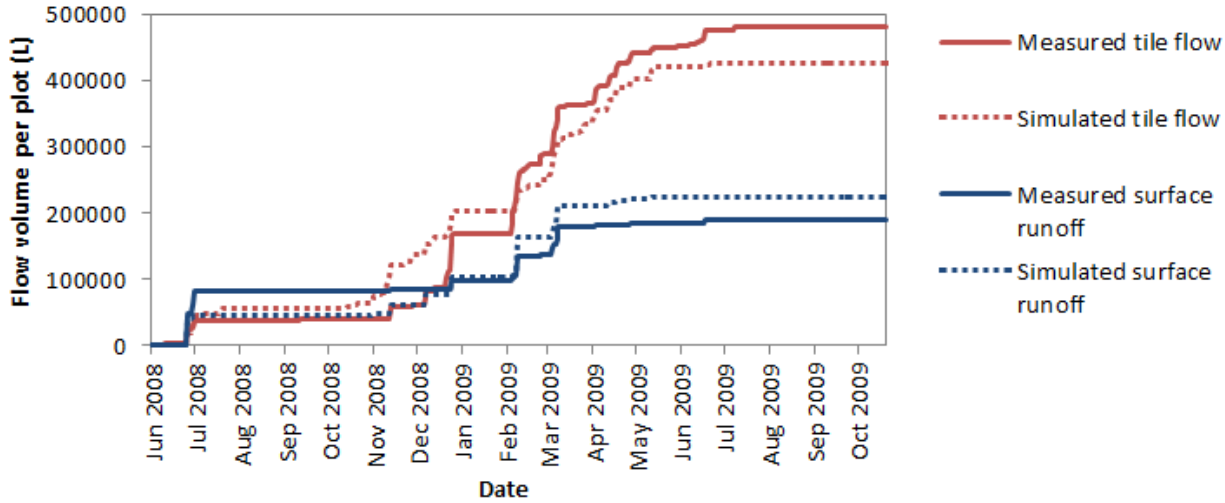

Figure 4.1(c) Water flow calibration for plot 9 from June 4th, 2008 to Oct 23rd, 2009.

The statistics of water flow calibration are shown in Table 4.1. The R^2 coefficient of determination was calculated based on daily data, whereas the Nash-Sutcliffe modeling efficiency (NSE) was calculated based on daily as well as weekly, monthly, and cumulative daily data. Daily statistics in the calibration period showed poor to medium correlation between simulation and measurements, as daily NSE statistics ranged from -0.087 to 0.524, and daily R^2 ranged from 0.180 to 0.575. Weekly NSE statistics demonstrated much better correlation from 0.436 to 0.676. Monthly NSE statistics ranged from 0.487 to 0.655, similar to weekly values. The large difference between daily and weekly statistics suggests frequent occurrence of time lags between measured and simulated water flows. Overall the model predicted weekly water flow at an acceptable level.

Table 4.1 Statistics of water flow calibration for plots 5 and 9.

Statistics	Plot 5 calibration		Plot 9 calibration	
	Tile flow	Surface runoff	Tile flow	Surface runoff
R^2 daily	0.264	0.180	0.522	0.575
NSE daily	0.250	-0.087	0.524	0.352
NSE weekly	0.436	0.676	0.598	0.445
NSE monthly	0.487	0.655	0.592	0.543
NSE cumulative daily	0.952	0.947	0.963	0.736

The most significant errors in tile drainage simulation occurred between October 2008 and February 2009, and these are reported in detail in Table 4.2. During a one-month period from Oct 15th to Nov 14th, 2008, the model overestimated tile flow in both plots 5 and 9. Next, during a seven-day snow-melting event from Dec 24th to 30th, 2008, the model significantly underestimated tile drainage by 46-52% in the two plots. And finally, during another seven-day snow melting event from Feb 7th to 13th, 2009, the model again significantly underestimated tile drainage, this time by 66-74%. The overall effect of these errors was that, for the entire calibration period, the cumulative tile drainage in the simulation was 13% lower than measurements in plot 5, and 12% lower than measurements in plot 9.

Simulation errors in surface runoff occurred less frequently than that of tile drainage, mainly because surface runoff itself occurred less often than tile drainage. It should be noted that, when the model simulates water flow in daily intervals, precipitation is redistributed over one day, which encourages infiltration and supresses surface runoff in the simulation. This is a flaw of the model. Simulating water flow in hourly interval may give more accurate infiltration and surface runoff, but may also lead to convergence issues due to large amount of data. Errors in surface runoff simulation are shown in Table 4.3. From Jun 28th to Jul 3rd, 2008, the model underestimated surface runoff by 100% and 42%, respectively, in plots 5 and 9. Then, during Feb 7th to 13th, 2009, the model underestimated surface runoff by 46% in plot 5 while overestimated that by 57% in plot 9. The net result of these errors was, for the entire calibration period, the cumulative surface runoff in the simulation was 15% less than measurements in plot 5; and 18% more than measurements in plot 9.

Table 4.2 Simulation errors of subsurface tile drainage during model calibration period.

Time period	Plot 5 tile drainage (L)			Plot 9 tile drainage (L)		
	Measured	Simulated	% Difference*	Measured	Simulated	% Difference*
Oct 15th–Nov 14th, 2008	0	51371	n/a	0	47122	n/a
Dec 24th–30th, 2008	81171	44187	-46%	81430	38786	-52%
Feb 7th–13th, 2009	153276	40235	-74%	97670	33479	-66%
Entire calibration period Jun 4th, 2008–Oct 23rd, 2009	515434	448590	-13%	482413	426763	-12%

* % Difference = (Simulated – Measured) / Measured x 100%.

Table 4.3 Simulation errors of surface runoff during model calibration period.

Time period	Plot 5 surface runoff (L)			Plot 9 surface runoff (L)		
	Measured	Simulated	% Difference*	Measured	Simulated	% Difference*
Jun 28th–Jul 3rd, 2008	7045	0	-100%	80975	46850	-42%
Feb 7th–13th, 2009	63064	34362	-46%	38994	61264	57%
Entire calibration period Jun 4th, 2008–Oct 23rd, 2009	146874	125250	-15%	190585	225033	18%

* % Difference = (Simulated – Measured) / Measured x 100%.

There are several explanations for these discrepancies between model simulation and measured field data. The first explanation concerns the function of heat transport and snow accumulation in HYDRUS (2D/3D). In an outdoor environment, snow accumulation and melting are mainly determined by air temperature, but other factors can be important too, such as wind transport and deposition of snow, soil surface temperature (which may be different from air temperature), wetness of soil surface, density of snow, solar irradiation, sublimation of snow, etc. HYDRUS (2D/3D) calculates snow melt solely based on air temperature, and assumes soil surface temperature to be equal to air temperature. This simpler representation of snow may be a source of simulation error. In addition, soil water storage is also affected by conditions of freezing soil temperature; it is possible that this model did not simulate freezing soil conditions as accurately as desired.

Second, the version of model used in this study could not account for macropore flows which can lead to much higher effective saturated hydraulic conductivity (K_s) than matrix flow. The local clay loam soil is known to have macropore formation in the summer season, which means it is difficult for the model to accurately describe water balance and flows during this time.

Third, the model could not account for soil disturbance that occurred during fall 2007 when a new tile drain was installed in the centre of every experimental plot. This event occurred less than one year before the start of the experiment so it is expected that the bulk density and K_s of the disturbed soil have not yet returned to normal at the time of the simulation.

Finally, it should be noted that all the data used for model calibration were produced in the first 1.5 years of the experiment. The soil did not have enough time to stabilize under the new experimental setting, and this can be a major source of inaccuracy for modeling. The quality of data can be observed by comparing measurements of duplicate plots. Ideally duplicate plots such as plots 5 and 9 should produce similar measurements, but during calibration period, they frequently produced very different measurements of tile drainage and surface runoff. Such trend was also observed in other pairs of duplicate plots during 2008 and 2009. The gaps between

duplicate plots became significantly smaller two years after the start of the experiment, during 2010 and 2011. It is therefore reasonable to believe that measured data will improve in quality as the field experiment progresses, and be more suitable for modeling purposes. One case of suspected measurement issue in calibration period occurred during Feb 7th to 13th, 2009, when plot 5 measured 153,276 L of tile drainage, significantly more than the 97,670 L measured in duplicate plot 9. This could have been caused by leakage of snowmelt water from an adjacent plot into plot 5 in the first year of the simulation.

4.2 Water Flow Validation

The model was validated for tile drainage and surface runoff in plots 5 and 9, using data from Jun 11th, 2010 to Aug 5th, 2011. Figure 4.2(a) shows precipitation and temperature of the validation period. Figures 4.2(b) and 4.2(c) display results of model validation in cumulative daily tile flow and cumulative daily surface runoff.

The observed flow pattern during validation was similar to that of the calibration period. Tile flow and surface runoff mainly occurred during winter and spring, and much less during summer and fall. The high flow event in May 2011 was possibly a result of macropore flow.

Model validation produced better statistics than calibration, as shown in Table 4.4. Weekly NSE for validation ranged from 0.513 to 0.738. The fact that validation outperformed calibration was most likely due to the fact that validation period used data of better quality. The effect of soil disturbance would have diminished in the third year of the field experiment, leading to more consistent flow measurements. The daily statistics of NSE (0.165 to 0.520) and R^2 (0.160 to 0.530) in validation also performed better than in the calibration period, although daily statistics still showed poorer correlation compared with weekly statistics, due to time lag between observed and simulated water flow.

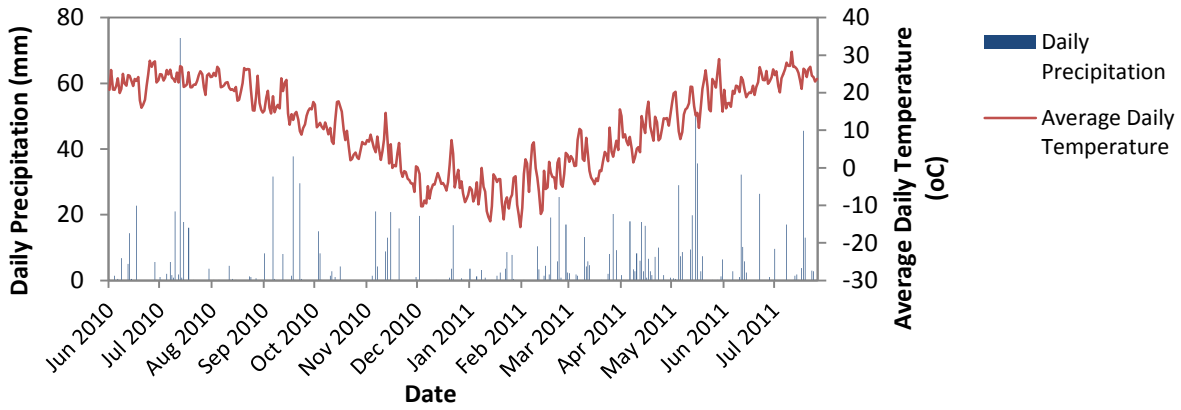

Figure 4.2(a) Daily precipitation and temperature during model validation period.

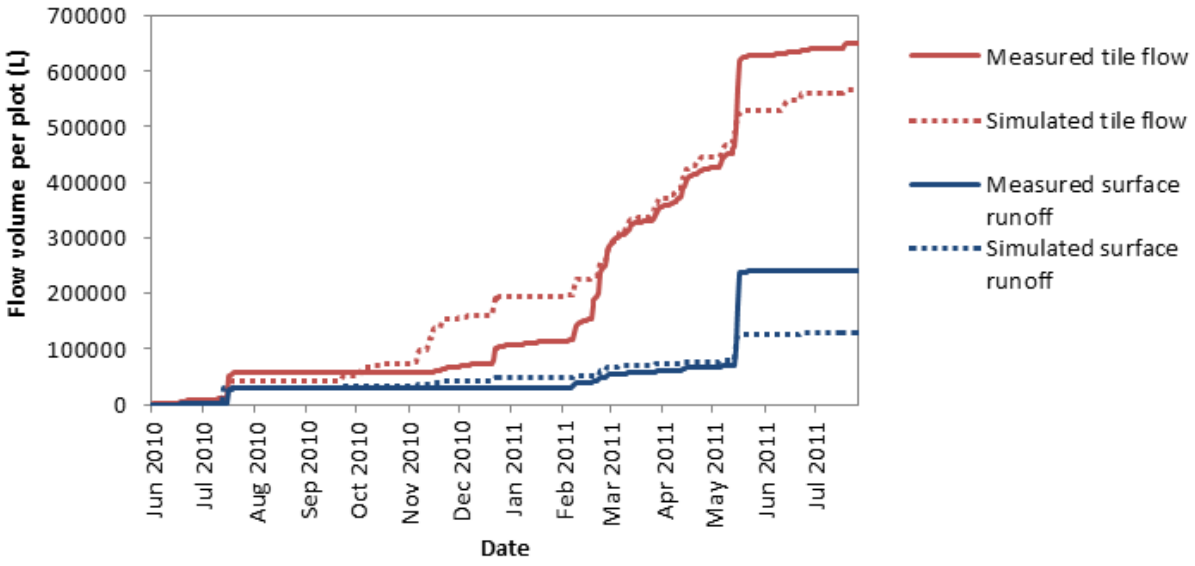

Figure 4.2(b) Water flow validation for plot 5 from June 11th, 2010 to Aug 5th, 2011.

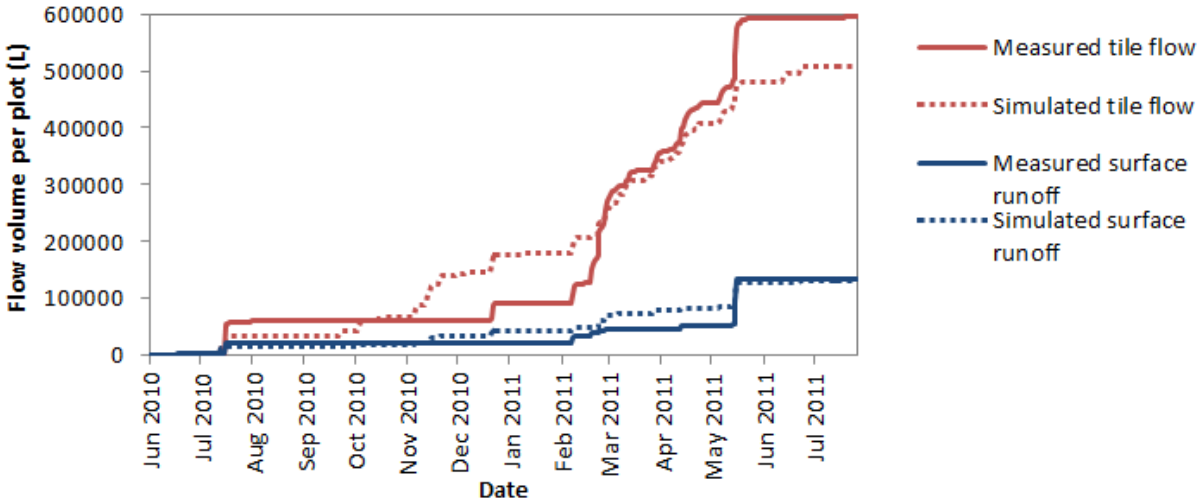

Figure 4.2(c) Water flow validation for plot 9 from June 11th, 2010 to Aug 5th, 2011.

Table 4.4 Statistics of water flow validation for plots 5 and 9.

Statistics	Plot 5 validation		Plot 9 validation	
	Tile flow	Surface runoff	Tile flow	Surface runoff
R^2 daily	0.294	0.160	0.355	0.530
NSE* daily	0.290	0.165	0.351	0.520
NSE weekly	0.570	0.513	0.587	0.738
NSE monthly	0.595	0.419	0.615	0.620
NSE cumulative daily	0.943	0.679	0.929	0.882

The most significant simulation errors during validation are reported in Tables 4.5 and 4.6, respectively, for tile drainage and surface runoff. The model overestimated tile drainage from Nov 14th to 26th, 2010, then underestimated tile drainage by 67-74% from Feb 23rd to Mar 5th, 2011. This pattern, which occurred from November to February, was similar to that of calibration period, which suggests that it is a part of the model that still needs improvement, possibly in the snow related parameters or frozen soil conditions. Another simulation error occurred during May 2011, where the model underestimated tile drainage and surface runoff by 63% and 55%, respectively. This was possibly due to the presence of macropores in the field which were not simulated by the model. Overall, model validation showed good correlation with measured data, but underestimated tile drainage in plots 5 and 9, respectively, by 13% and 15%; and underestimated surface runoff in plots 5 and 9, respectively, by 46% and 2.7%.

Table 4.5 Simulation errors of subsurface tile drainage during model validation period.

Time period	Plot 5 tile drainage (L)			Plot 9 tile drainage (L)		
	Measured	Simulated	% Difference*	Measured	Simulated	% Difference*
Nov 14th–26th, 2010	2002	63080	3051%	0	57307	n/a
Feb 23rd–Mar 5th, 2011	87893	28746	-67%	90201	23782	-74%
May 22th–30th, 2011	173901	64134	-63%	117558	53063	-55%
Entire validation period Jun 11th, 2010–Aug 5th, 2011	649462	566156	-13%	594877	507773	-15%

* % Difference = (Simulated – Measured) / Measured x 100%.

Table 4.6 Simulation errors of surface runoff during model validation period.

Time period	Plot 5 surface runoff (L)			Plot 9 surface runoff (L)		
	Measured	Simulated	% Difference*	Measured	Simulated	% Difference*
May 22nd–30th, 2011	169187	47223	-72%	81557	41513	-49%
Entire validation period Jun 11th, 2010–Aug 5th, 2011	240428	129831	-46%	135179	131508	-2.7%

* % Difference = (Simulated – Measured) / Measured x 100%.

4.3 Phosphorus Calibration and Validation

Model calibration of P loss and transport used 239 days of data from Jun 17th, 2008 to Feb 11th, 2009, which consisted of three sampling periods 122, 123 and 124. Model validation used 254 days of data from Feb 11th to Oct 23rd, 2009, which consisted of four sampling periods 125, 126, 127 and 128. Data was only available for these seven sampling periods, and each period only provided one laboratory-measured value of dissolved reactive P (DRP) that could be compared with model simulations of solution P (orthophosphates). The model had simulated the P loss in daily time unit, but had to convert results into sampling periods for comparison with measurements. The unit of simulation was mg/plot and here it has been converted to kg/ha for convenience (each experimental plot has an area of approximately 0.1 ha).

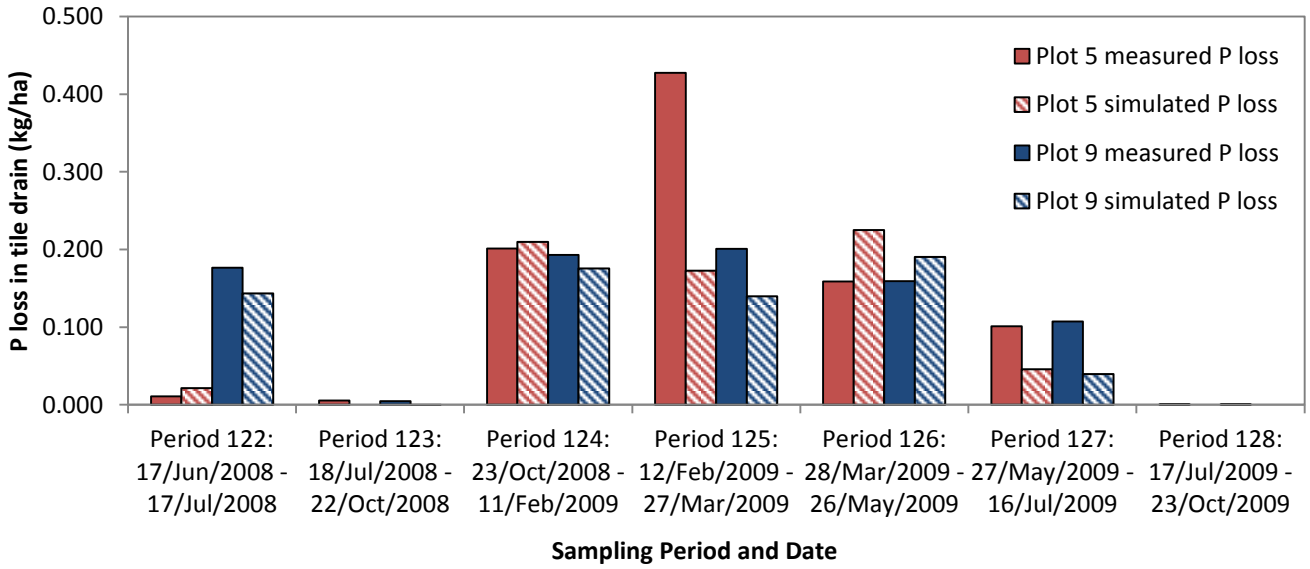

Figure 4.3 P loss in tile drainage, simulated from June 17th, 2008 to Feb 11th, 2009. Model calibration consisted of periods 122 to 124, model validation consisted of periods 125 to 128.

Most of the measured P loss occurred during winter and spring seasons as a result of high flow volumes in tile drainage. P loss during summer and fall was relatively low because of lower flow volumes and crop uptake.

P loss in tile drainage was modeled very well during calibration period, with plot 5 calibration demonstrating NSE of 0.974 and R^2 of 0.993; and plot 9 calibration demonstrating NSE of 0.936 and R^2 of 0.991. Validation statistics are slightly lower than calibration statistics, with NSE of 0.769, R^2 of 0.992 for plot 5, and NSE of 0.587, R^2 of 0.720 for plot 9 (see Table 4.7). Figure 4.3 shows that validation for plot 5 significantly underestimated tile drainage P loss by 60% during sampling period 125; but curiously plot 5 still produced better validation statistics than plot 9. It should be noted that, due to the small sampling size (3 measurements during calibration, and 4 measurements during validation), the statistics were not a truly reliable means of evaluating model quality. More data is required to evaluate the model, either by using more sampling periods of data, or by using more frequent field measurements such as daily or weekly P loss.

Table 4.7 Statistics of phosphorus calibration and validation for plots 5 and 9.

	Calibration		Validation	
	plot 5	plot 9	plot 5	plot 9
NSE for sampling periods	0.974	0.936	0.768	0.587
R^2 for sampling periods	0.993	0.991	0.992	0.720

Tables 4.8 and 4.9 report the simulation errors of tile drainage P loss and flow volumes in each sampling period. Most of the errors in P loss simulation can be attributed at least partly to errors in water flow simulation. For example, in sampling period 125 (Feb 12th to Mar 27th, 2009), the model underestimated P loss from plot 5 by 60% mainly because the tile drainage volume was underestimated by 43%. Here the water flow error accounted for most of the error in P loss simulation. With this situation in mind, it is speculated that HYDRUS (2D/3D) was able to simulate P transport and loss quite well, and model performance can be further improved by optimizing water flow simulation.

Table 4.8 Simulation errors in plot 5 P loss and tile drainage flow by sampling periods.

	Sampling period	Plot 5 P loss in tile drainage (kg/ha)			Plot 5 Tile drainage (L)		
	(see footnote)	Measured	Simulated	% Error	Measured	Simulated	% Error
Calibration	122	0.0108	0.0216	100%	8220	8917	8%
	123	0.0055	0.0000	-100%	4093	13840	238%
	124	0.2011	0.2099	4%	204348	194342	-5%
	Sub-total	0.2174	0.2315	7%	216661	217099	0%
Validation	125	0.4276	0.1729	-60%	175908	99956	-43%
	126	0.1587	0.2252	42%	90864	110863	22%
	127	0.1011	0.0460	-54%	30829	20674	-33%
	128	0.0001	0.0000	-100%	83	0	-100%
	Sub-total	0.6875	0.4441	-35%	297685	231492	-22%
All	Total	0.9049	0.6757	-25%	514345	448590	-13%

Sampling period 122: 17/Jun/2008 - 17/Jul/2008,
Sampling period 123: 18/Jul/2008 - 22/Oct/2008
Sampling period 124: 23/Oct/2008 - 11/Feb/2009
Sampling period 125: 12/Feb/2009 - 27/Mar/2009
Sampling period 126: 28/Mar/2009 - 26/May/2009
Sampling period 127: 27/May/2009 - 16/Jul/2009
Sampling period 128: 17/Jul/2009 - 23/Oct/2009

Table 4.9 Simulation errors in plot 9 P loss and tile drainage flow by sampling periods.

	Sampling period	Plot 9 P loss in tile drainage (kg/ha)			Plot 9 Tile drainage (L)		
	(see footnote)	Measured	Simulated	% Error	Measured	Simulated	% Error
Calibration	122	0.1765	0.1435	-19%	34395	48550	41%
	123	0.0047	0.0006	-88%	3772	12590	234%
	124	0.1932	0.1758	-9%	207966	171039	-18%
	Sub-total	0.3743	0.3199	-15%	246133	232179	-6%
Validation	125	0.2008	0.1397	-30%	113656	90867	-20%
	126	0.1594	0.1907	20%	86997	98161	13%
	127	0.1075	0.0395	-63%	33073	5556	-83%
	128	0.0001	0.0000	-100%	88	0	-100%
	Sub-total	0.4677	0.3700	-21%	233813	194583	-17%
All	Total	0.8421	0.6898	-18%	479946	426763	-11%

Sampling period 122: 17/Jun/2008 - 17/Jul/2008
Sampling period 123: 18/Jul/2008 - 22/Oct/2008
Sampling period 124: 23/Oct/2008 - 11/Feb/2009
Sampling period 125: 12/Feb/2009 - 27/Mar/2009
Sampling period 126: 28/Mar/2009 - 26/May/2009
Sampling period 127: 27/May/2009 - 16/Jul/2009
Sampling period 128: 17/Jul/2009 - 23/Oct/2009

In Tables 4.8 and 4.9, there were periods when % error of P loss was extreme, such as 100% and -100% in sampling periods 122, 123, and 128. These should not cause concern because the absolute amounts of P loss were small, and the errors occurred mainly because very small events of precipitation were not being simulated properly.

4.4 Sensitivity Analyses I: Water Flow

Sensitivity analyses tested input parameters that were expected to have significant impact on simulation results. Four parameters have been tested for their influence on water flow patterns. To test these, the water flow simulation from plot 9 calibration period was used as a basis of comparison. These parameters would also affect solute simulation indirectly due to changes in water flow simulation.

The first parameter tested was the saturated hydraulic conductivity (K_s) of surface soil layer. The original value used in the model was 7.41 cm/day. When K_s was reduced to 4.41 cm/day, tile drainage over a period of 507 days was reduced by 4.1%, and surface runoff was increased by 9.4%, as expected. When K_s was increased to 10.41 cm/day, tile drainage was reduced by 5.0% and surface runoff was reduced by 1.9%. Normally an increase in K_s is expected to cause increased tile flow, but in this particular case, the opposite occurred, probably because only the K_s of the surface soil was modified but tile drainage was still limited by K_s of the lower soil depths. Results are shown in Figures 4.4(a) and (b).

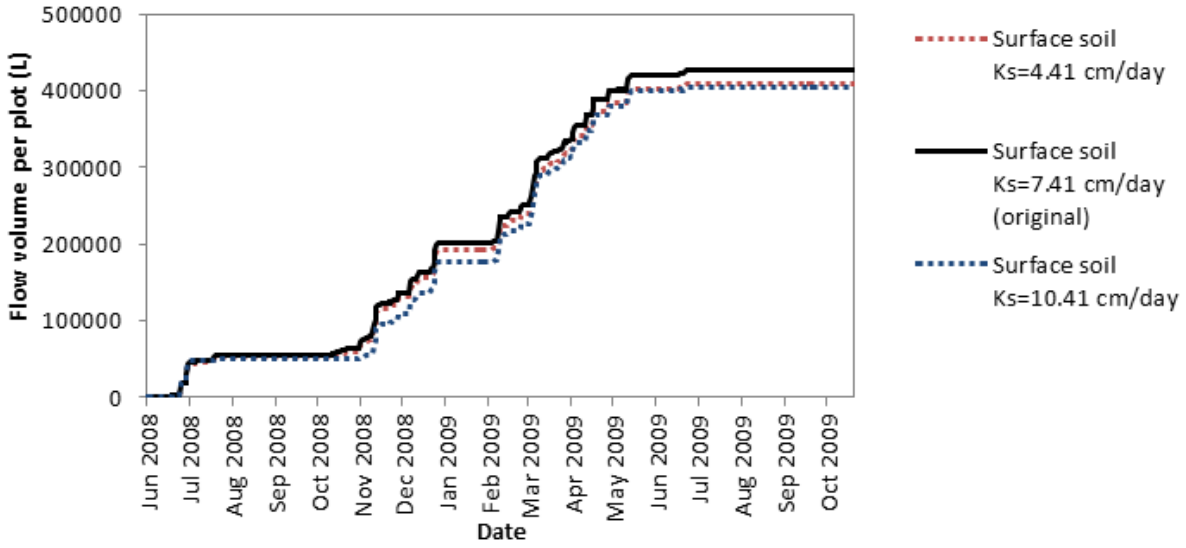

Figure 4.4(a) Tile drainage simulation in plot 9 as affected by saturated hydraulic conductivity (K_s) in surface soil layer.

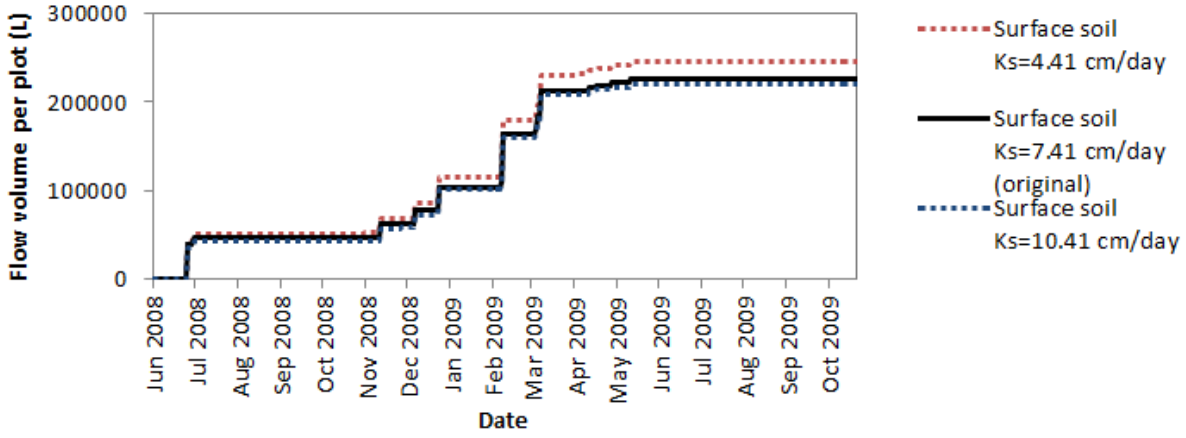

Figure 4.4(b) Surface runoff simulation in plot 9 as affected by saturated hydraulic conductivity (K_s) in surface soil layer.

The second parameter analyzed was the multiplier of potential evapotranspiration (PET). As discussed previously, PET multipliers were necessary to reduce PET to realistic values in order to maintain a proper water balance in the soil. Without multiplier, the PET completely dried the soil profile in the simulation and significantly reduced both tile drainage and surface runoff by 80.4% and 85.5%, respectively, far below field measurement and original simulation levels. It should be noted that even though HYDRUS (2D/3D) calculates actual ET based on PET inputs and soil

moisture in real-time, in this particular case, the model could not derive the correct actual ET if PET was not first reduced by multipliers. The comparison is shown in Figure 4.5.

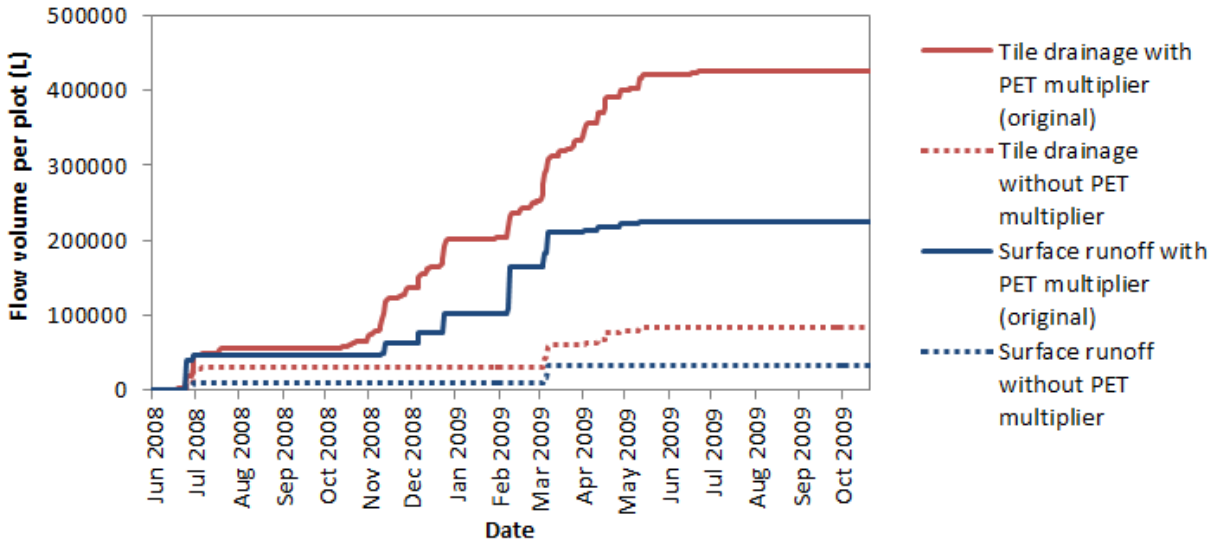

Figure 4.5 Water flow simulation in plot 9 as affected by PET multiplier.

The third parameter was the crop canopy interception of precipitation. If interception did not occur, all measured precipitation would have reached the soil profile. Figure 4.6 shows that, without interception, there would be more water entering the soil profile; tile drainage would increase by 26.6% while surface runoff would increase by 6.2%. A point of interest is, in the simulation, the removal of crop interception caused greater effect in tile drainage rather than in surface runoff, but in reality the greater effect might be observed in surface runoff instead. The explanation here is that the model performed simulations on a daily time scale. Normally when an intense precipitation event occurs, more water should be lost via runoff. But simulation on a daily time scale forces the precipitation to be redistributed over the entire day, which encourages soil infiltration instead of surface runoff. To avoid this problem, the model could perform simulations on hourly time scale, but at a cost of significantly longer run times and possible issues of calculation convergence due to large amounts of data.

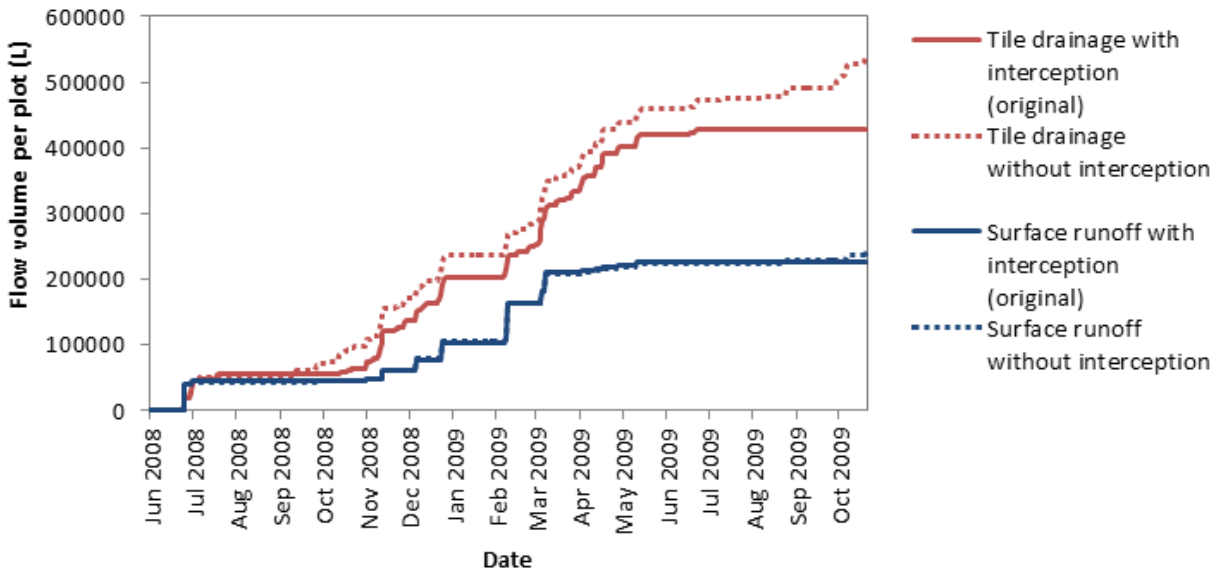

Figure 4.6 Water flow simulation in plot 9 as affected by crop canopy interception.

The final parameter in this section is the utilization of heat transport module and its snow accumulation/melting function. In cold climates such as Canada, snow plays a very significant role in water balance from winter to spring. Snowfall delays the time at which precipitation enters soil profile, and the melting of the snow layer tends to create large volumes of surface runoff water in early spring or warm days during winter. Figure 4.7 shows that, when temperature was not considered in the simulation, tile drainage was increased by 35.0% from the original simulation, and surface runoff was decreased by 25.2%. These changes were just as expected and they highlight the importance of heat and snow functions in the model.

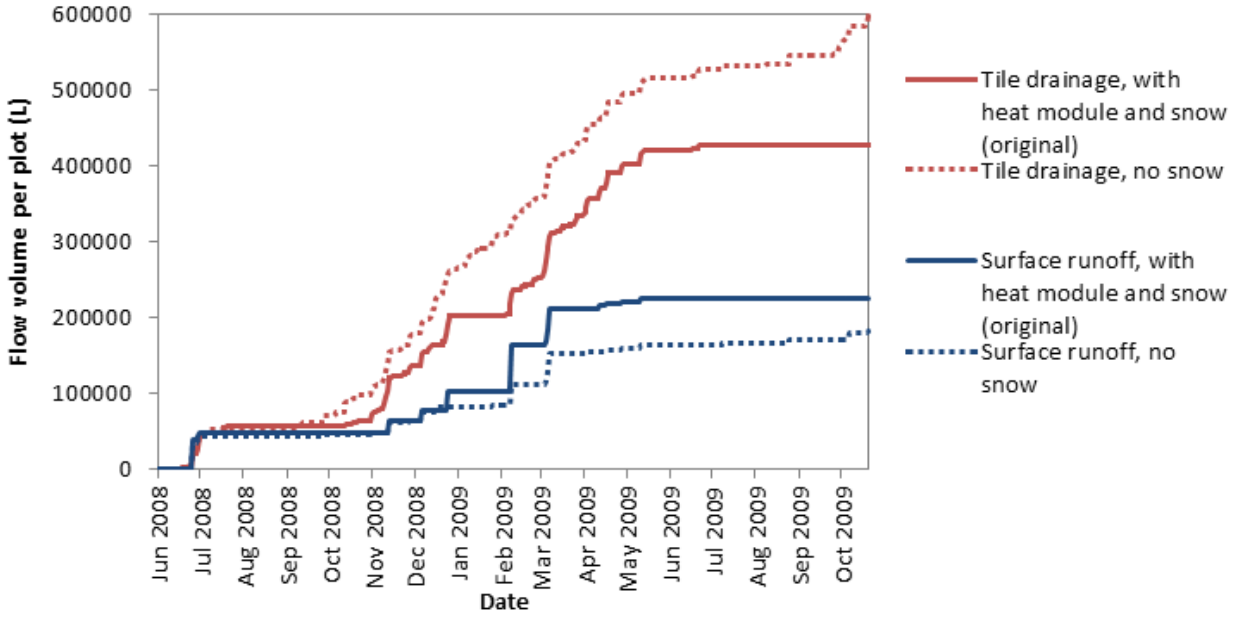

Figure 4.7 Water flow simulation in plot 9 as affected by heat transport and snow accumulation functions.

4.5 Sensitivity Analyses II: P loss

This section investigates six more input parameters which directly affect solute dynamics. P simulation results from plot 9 were used as a basis of comparison. The simulation spans a total of 493 days divided into seven sampling periods, which includes both calibration and validation periods.

The first parameter tested was the linear adsorption coefficient (K_d) of P in soil. The original simulation used K_d=6.0, whereas sensitivity analyses tested alternative values of K_d=4.0 and K_d=8.0. Results in Figure 4.8 show that, when K_d=4.0, less P was being adsorbed onto soil particles, resulting in a significant increase of 103.1% in tile drainage P loss. When K_d=8.0, more P was being adsorbed onto soil particles and rendered immobile, leading to a 67.1% reduction of P loss. It can be concluded that K_d has a significant effect on P balance and tile drainage P loss.

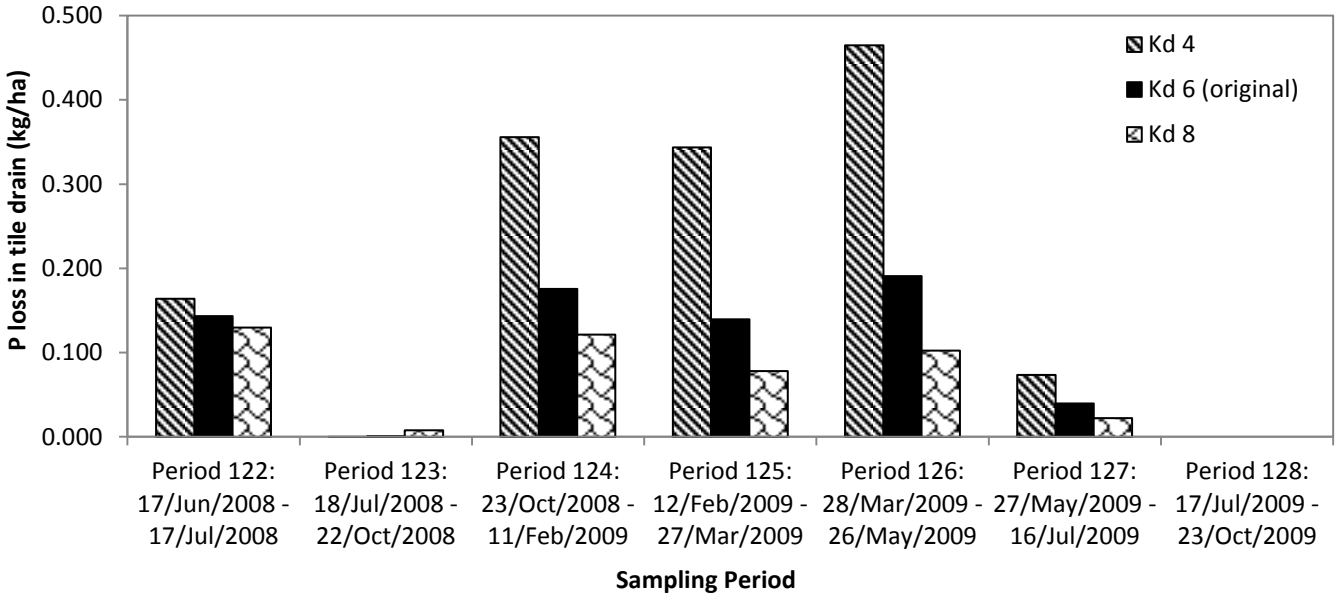

Figure 4.8 Simulated tile drainage P loss in plot 9 as affected by adsorption coefficient K_d in all soil layers.

The second parameter tested the difference between 1-site and 2-site adsorption modes. The original simulation used 1-site adsorption, which assumes that instantaneous adsorption rate occurs at all adsorption sites. The alternative is 2-site adsorption, which assumes that some adsorption sites are "kinetic", where P sorption occurs at a slower rate. The sensitivity analysis here tested a scenario of 2-site adsorption with 50% kinetic adsorption sites which function at an adsorption rate of 0.01 per day. Results in Figure 4.9 show 29.1% more P loss by 2-site adsorption than 1-site adsorption. This was the expected result because 2-site adsorption requires more time for the adsorption process, therefore more of solution P would be mobile in soil solution, prone to loss via tile drainage. The reverse trend that occurred in the first sampling period 122 was due to a special setup in initial soil P concentration (see Methods section 3.3.9).

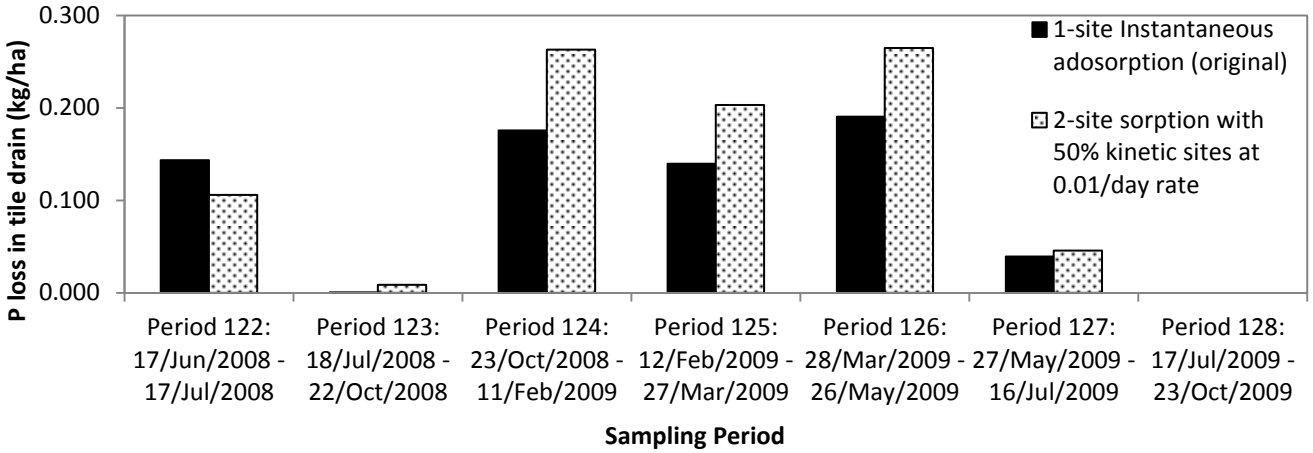

Figure 4.9 Simulated tile drainage P loss in plot 9 as affected by 1-site or 2-site adsorption.

The third parameter was longitudinal dispersivity, a soil specific parameter that affects the rate of P movement in the soil profile. The original simulation used a calibrated dispersivity value of 20 cm. The sensitivity analysis here tested alternative values of 5 cm and 35 cm. Results in Figure 4.10 demonstrate that, when dispersivity was reduced to 5 cm, P loss was reduced by 29.0%; when dispersivity was increased to 35 cm, P loss was increased by 112.7%. These were expected trends, as increased dispersivity leads to greater P mobility in the soil profile, resulting in greater P loss in tile drainage; and vice versa. The reversal of trends in the initial sampling period 122 was again caused by the special case of initial P concentration.

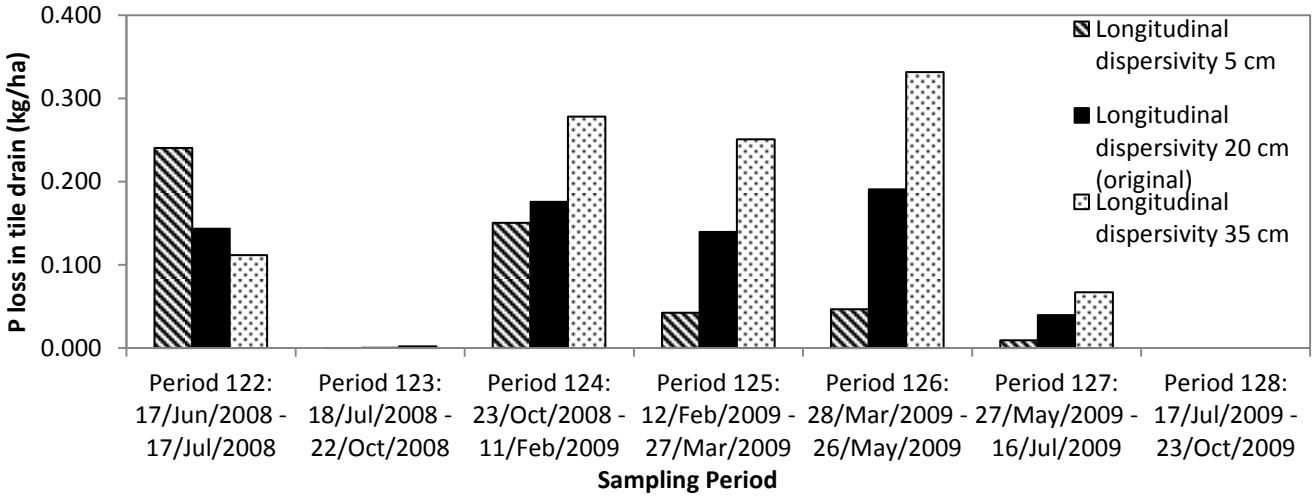

Figure 4.10 Simulated tile drainage P loss in plot 9 as affected by longitudinal dispersivity of all soil layers.

The fourth parameter was the diffusion rate of P, a solute-specific parameter that affects the rate of P movement in the soil solution. The original simulation used a diffusion rate of 0.44 cm^2/day found in Hatfield et al. (1966). The sensitivity analysis here tested an alternative value of 4.4 cm^2/day. Figure 4.11 shows that P loss in tile drainage was only increased by 10.9% when diffusion rate had increased 10-fold. The conclusion is therefore the diffusion of P in the model accounts for a very small proportion of P movement in soil especially in comparison with the longitudinal dispersivity.

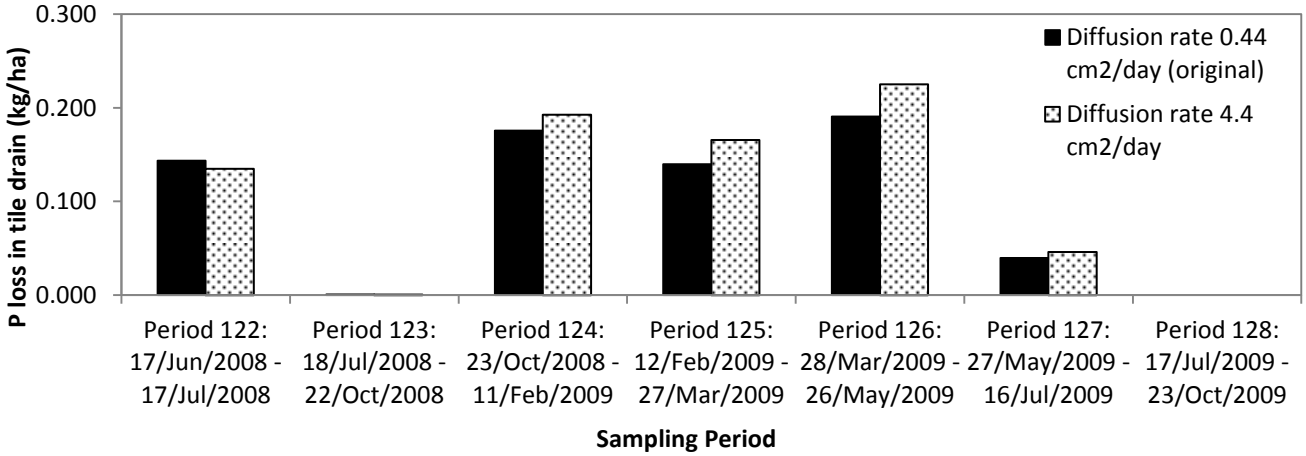

Figure 4.11 Simulated tile drainage P loss in plot 9 as affected by aqueous diffusion rate of P.

The fifth parameter was the fertilization rate of P, which occurred once every two years in this field experiment. In the field experiment as well as in the original simulation, fertilization rate was 100 kg P_2O_5/ha. The sensitivity analysis here explored alternative rates of 0 kg P_2O_5/ha and 200 kg P_2O_5/ha. The zero fertilization rate actually mirrored the P "draw down" treatment in the field experiment, although simulation conditions were not adjusted to those specific experimental plots. Results in Figure 4.12 show that, there was very little difference in P loss between these three fertilization rates over 493 days of simulation, as long as the initial soil P concentration remained the same. The 0 kg P_2O_5/ha fertilization rate caused 2.4% less P loss, while the 200 kg P_2O_5/ha fertilization rate caused 5.0% more P loss. The lack of differences between these results may come as a surprise, but it should be noted that in a typical long-term agricultural soil, most of the soil P

would have been accumulated over decades of previous fertilization, and the amount of P fertilized every year (or every two years) is usually only a small fraction of the total soil P. Another note is, this sensitivity analysis explored only 493 days of the P dynamics, less than one cycle of P fertilization in the field experiment. Should the simulation period be longer, then over time, these rates of fertilization would certainly differentiate into greater differences in soil P content and tile drainage P loss.

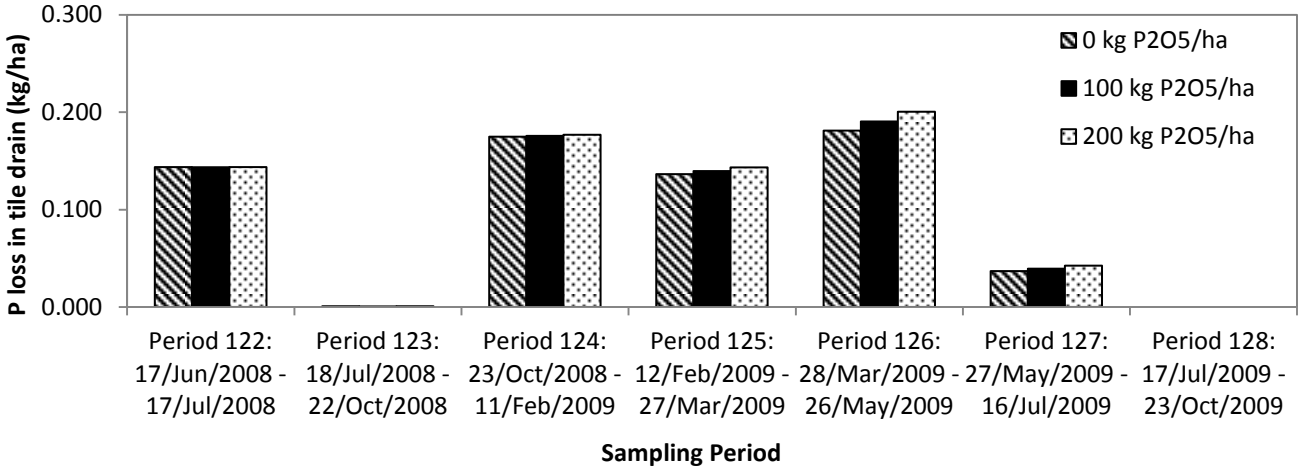

Figure 4.12 Simulated tile drainage P loss in plot 9 as affected by various fertilization rates.

The last parameter tested was the initial P concentration in soil at the beginning of the simulation. The original simulation used a gradient of soil P concentration, which had the highest concentration of 0.03073 mg P/cm^3 at the soil surface, and the lowest concentration of 0.0000266 mg P/cm^3 below 1.00 m of soil depth. This sensitivity analysis tested alternative values of the initial soil concentration by multiplying all concentrations by 50% and 150%, respectively. Results in Figure 4.13 show that, when initial soil P was reduced to 50% of original value, P loss was reduced by 48.9%; and when initial soil P was increased to 150% of original value, P loss was increased by 48.5%. These results indicate that initial soil P has a significant and very direct impact on the amount of P loss via tile drainage for this 493-day simulation. Due to its importance, this parameter should ideally be setup according to field measurements whenever possible, or

calibrated with great caution if field measurements are lacking.

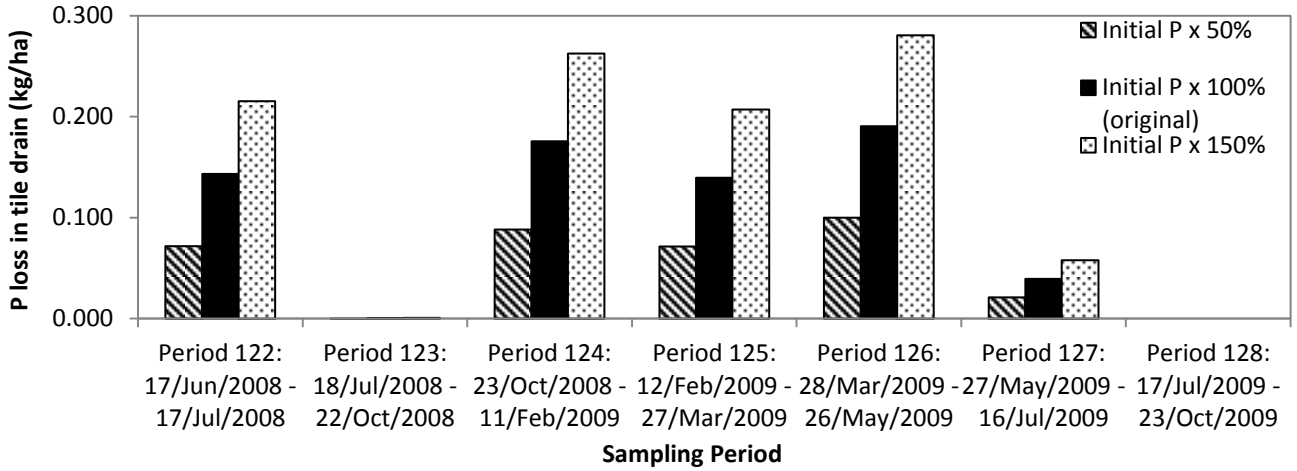

Figure 4.13 Simulated tile drainage P loss in plot 9 as affected varying concentrations of initial soil P at the start of the experiment.

4.6 Difficulties and Limitations of HYDRUS (2D/3D) modeling

This section discusses the difficulties encountered during this modeling study and some inherent limitations of the HYDRUS (2D/3D) software. The main areas discussed here will be: soil domain, finite element mesh, macropores, snow accumulation, sub-irrigation, fertilizer type, multiple solutes, active root solute uptake, particulate P and surface runoff P.

Soil domain

For this simulation, the soil profile has dimensions of 15.2 m by 1.5 m (width x depth). However calculations cannot converge with such dimensions, possibly due to insufficient computer memory or the width to depth ratio of 10.1 was too great for the nodal calculations to converge. This problem was solved by dividing the soil profile into three sections (left, centre, right) based on locations of its three tile drains. The sections were simulated separately, and their outputs were combined afterwards to provide results of the entire field. The use of three separate sections assumed that water flowed only to the nearest tile drain and did not move across to the

adjacent section. However this assumption automatically becomes a source of error when the simulated field sections become even slightly different in terms of water table height, temperature, and P concentrations.

Finite element mesh

HYDRUS (2D/3D) calculates results based on nodes that form a finite element mesh (FE-mesh). Any error in mesh size or distribution due to improper design may easily cause convergence errors in the subsequent simulations. When the FE-mesh is too dense, or have very elongated triangles, or when there is a sharp transition from large grid size to small grid size within a small area, convergence errors can be quite common. These issues may be solved by using an adequate grid size, adjusting nodal distribution in horizontal/vertical directions, or by drawing user defined lines and shapes as guidance for FE-mesh creation. The mesh creation process may require many attempts before a simulation can be successfully calculated. There is also a general belief that nodes should be placed more densely at the soil surface (the atmospheric boundary) where pressure head changes quickly over time. This is the recommended practice but it should not be blindly followed. For example, in Hydrus-1D model, the density of nodes at soil surface versus bottom of soil profile can be as much as 50:1 ratio without any convergence problems; whereas in HYDRUS (2D/3D) model, having even slightly dense nodes might cause convergence errors or significantly slow down simulations without improving the accuracy/precision of results. For this modeling study, nodes could not be made to be dense at the soil surface, so instead they were distributed evenly between soil surfaces to bottom, with constant distance intervals of approximately 5 cm. In contrast to the sparse mesh size at soil surface, the model was able to use a very dense FE-mesh in the area surrounding the tile drain.

Macropores

Macropores, or soil cracking, is a common phenomenon in soils with rich clay content during

dry seasons. These have been frequently observed at the AAFC experimental field in summer months. Water flowing through macropores can quickly reach the tile drains, and it has a significant impact on both tile drainage and surface runoff. HYDRUS (2D/3D) offers two main options to address macropore flow. One can use the mobile-immobile water flow equation which assumes that water and solutes only move in macropores but not in soil matrix; this is clearly inaccurate by ignoring matrix flow. Alternatively, there is an add-on module called "Dual Permeability" which allows water and solutes to move concurrently in soil matrix and in macropores. However this module reduces model stability and is only recommended for small scale simulations, which may pose additional calibration difficulties for large field-scale simulations.

Snow

HYDRUS (2D/3D) has a built-in snow accumulation/melting function that follows a set of temperature-based rules to determine snow dynamics. This function appears to perform decently because the model has predicted water flow moderately well on weekly scale. However the accuracy of the snow simulation is very difficult to verify with field observations. The snow related settings are also not available for user calibration. Other factors that affect snow, such as solar irradiation, wind deposition and transport of snow, etc. are not being considered by HYDRUS (2D/3D).

Sub-irrigation

In the field experiment, half of the test plots were under the treatment of controlled drainage with sub-irrigation. HYDRUS (2D/3D) can simulate either controlled drainage or sub-irrigation, but not both functions simultaneously due to conflicting settings of boundary conditions. This limitation means HYDRUS (2D/3D) is unable to simulate half of the field results from this AAFC experiment.

Fertilizer type

Currently HYDRUS (2D/3D) cannot process fertilization in any solid or organic form, whether it is solid inorganic fertilizer, solid manure, or liquid manure. In this field experiment, the inorganic fertilizer was very soluble in water, and the model was able to use a fertigation method to simulate the fertilizer—by assuming that it dissolved in rainwater. This is clearly not the best practice but no other practical options exist. It could not have been applied to an inorganic fertilizer that is less water soluble. In addition, organic fertilizers are completely beyond capabilities of HYDRUS (2D/3D) at this moment due to their complex chemistry and biological processes. Finally the fertilization methods such as broadcast or banded application are not being considered by HYDRUS (2D/3D).

Active root solute uptake

For nutrients that are naturally scarce in soil, such as P, plants often need to use the active root uptake mechanism to uptake the required mass of nutrient. This model chose to use active root uptake of P but not multiple solutes, as the two functions are not compatible.

Multiple solutes

HYDRUS (2D/3D) is capable of simulating multiple solutes, and these solutes can be linked by unidirectional decay reactions with either 0^{th} order or 1^{st} order decay. The process can be illustrated by: solute A decays to B, B decays to C, C decays to D, etc. but not in reverse. This restricted form of decay chain means the solute module is only applicable to solutes with a single chemical form, or solutes that have a simple unidirectional decay reaction. It presents a serious difficulty for P simulation, since much of the P chemical processes occur as bi-directional transformations or equilibriums. For this study, the model had assumed a single solute approach in order to simulate P in HYDRUS (2D/3D), at a cost of completely disregarding organic P which plays a large role in the P cycle.

Particulate P and surface runoff P

The loss of dissolved P was predicted relatively well by HYDRUS (2D/3D), however dissolved P does not constitute all the P loss. Previous field studies have demonstrated the importance of particulate P, which is sometimes the dominant speciation of P lost from the field (Tan and Zhang, 2011; Ulen and Persson, 1999; Uusitalo et al., 2001). The contribution of surface runoff P loss can also be significant depending on drainage installation and slope factors (Gaynor and Findlay, 1995; Heathwaite and Dils, 2000; Melland et al., 2008; Tan and Zhang, 2011). Unfortunately HYDRUS (2D/3D) could not address those forms of P loss. It is hoped that future software versions of the HYDRUS (2D/3D) model will eventually include these important functions.

Chapter 5 Summary and Conclusions

5.1 Summary and Conclusions

The main purpose of this modeling study was to model phosphorus fate and transport in two tile-drained, 0.1 ha field plots with clay loam soil in southern Ontario. These plots had controlled tile drainage and a corn-soybean crop rotation. The surface and subsurface water flows in test plots were monitored and samples collected continuously year round using an auto-sampling system. The model used HYDRUS (2D/3D) software to simulate tile drainage flow, surface runoff flow, and the loss of dissolved reactive phosphorus (DRP) in tile drainage.

For water flow simulation, the model considered precipitation, snow accumulation and melting, evaporation, crop transpiration, surface runoff, subsurface tile drainage flow, and crop water uptake. Water flow simulation was calibrated using observed data from June 4th, 2008 to Oct 23rd, 2009, and validated using data from June 11th, 2010 to Aug 5th, 2011.

For P simulation, the model considered P fertilization, initial P concentration in soil profile before the experiment, P transport in soil by dispersivity and diffusion, P adsorption, crop uptake of P by passive and active means, and loss of DRP in tile drainage. P simulation was calibrated using observed data from June 17th, 2008 to Feb 11th, 2009, and validated using data from Feb 11th, 2009 to Oct 23rd, 2009.

The following conclusions can be drawn from this study:

1. Overall the model estimated water flow relatively well on a weekly scale during water flow validation, achieving Nash-Sutcliffe modeling efficiency (NSE) of 0.570 and 0.587 for tile drainage in two duplicate plots; and NSE of 0.513 and 0.738 for surface runoff in the same plots. The major errors in simulation mainly occurred from November to February, which suggests the model would benefit from further optimization of snow dynamics. Some of the simulation errors may also be attributed to soil cracking in the summer which consequently enhanced macropore flow. The model estimated water flow poorly on daily

time scale, suggesting frequent occurrence of time lags between simulated and measured water flow.

2. The model was able to simulate tile drainage loss of dissolved P relatively well, achieving NSE of 0.768 and 0.587 in the validation period, respectively, for the two plots. Most of the errors in P loss simulation can be attributed at least partly to errors in water flow simulation during the corresponding time period.

5.2 Recommendations for Future Studies

The model being developed for this study serves as a starting point for the simulation of P loss in tile drainage in agricultural field conditions. Improvements can be made to the current model in the following ways.

1. The model can be improved for its simulation from fall to winter season, which currently has the greatest simulation errors. The recommended area of optimization is snowfall accumulation and melting, and frozen soil conditions.
2. The current model only simulated water flow until August 2011 and only simulated P transport until October 2009. Data was limited due to various reasons such as malfunctioning equipment, occasional pipes leakages, and a backlog of laboratory analyses. As additional data becomes available in the future, they should be used to further evaluate this model to establish its validity for the AAFC field experiment.
3. The current model had divided the field into two "edge" and one "centre" sections and simulated them separately due to convergence issues. It is recommended that the entire field be simulated together in one simulation. This can be achieved perhaps by using fewer nodes in the FE-mesh or a better FE-mesh design.
4. The AAFC field experiment consists of sixteen test plots. The current model only simulated two duplicate plots #5 and #9 which have controlled drainage and inorganic P fertilizer. There are fourteen other experimental plots in this field experiment and it would be an

excellent opportunity to perform comparison modeling to test the effects of different fertilizers and drainage settings in modeling. Four of these plots have the "draw down" (no P fertilization) treatment; two of which (without sub-irrigation) can be simulated using the current model but requires field data of later years in order to make meaningful observations over time. The rest of the plots have sub-irrigation and/or manure fertilizer treatments which are currently beyond the capabilities of HYDRUS (2D/3D). They require a model which is able to process manure fertilizer but also able to simulate controlled tile drainage simultaneously with sub-irrigation.

5. More work is needed to test the capabilities of the model beyond the AAFC field experiment, by using field data from different climates, soil types, crops, and drainage settings. It may also be useful to verify the model with laboratory controlled tests or outdoor soil column tests in order to examine its performance in more specific areas.

For model developers, there are a number of features that would greatly enhance the modeling of P in soil and water. An ideal model that encompasses all the needs should have a strong water flow component which is capable of simulating macropore flow and matrix flow, tile drainage with and without water table control, and sub-irrigation. It should have a plant growth component such as that of DSSAT model (Jones et al., 2003) which considers crop type, growth stage, leaf area index, yield, and nutrient demand determined by crop type, seeding density, and growth stage. There needs to be a good chemistry component that allows for multiple solute pools, connected by chemical processes that can be user-defined based on pH, soil moisture, temperature, soil fertility, etc. A microbial module may help administer the biological degradation processes for P as well as for nitrogen and other chemicals. Furthermore, incorporating agricultural processes such as fertilization (manure or inorganic), tillage, pesticides, and harvest would increase the accuracy of the entire model by making it more realistic. It would also be meaningful to incorporate nitrogen and carbon components into a P model as these factors are closely related to

each other through soil fertility (Havlin et al., 2005). Finally, a model that can compute the losses of both dissolved and particulate P, in subsurface drainage as well as in surface runoff, would be a comprehensive tool to evaluate total P loss from the field.

All of the model functions described here can already be found in existing models, although each existing model usually only hosts some of these functions and lacks in other areas. The recommendation for future developers is thus to combine existing models into hybrids to offer greater model capabilities and to simulate field conditions as close to reality as possible. A good computer model will be an invaluable prediction tool for future trends in agricultural pollution, be a guideline for best management practices, and be more convincing to policy makers for agricultural and environmental policies and regulations.

References

Abou Nohra, J. S., C. A. Madramootoo, and W. H. Hendershot. 2007. Modelling phosphate adsorption to the soil: Application of the non-ideal competitive adsorption model. *Environ. Pollut.* 149(1):1-9.

Anonymous. 1972. Great Lakes water quality agreement. North America: International Joint Commission: Canada and United States.

Art, H. W. 1993. Eutrophication. In *A Dictionary of Ecology and Environmental Science*, 196. New York, NY: Henry Holt and Company.

Barber, S. A., and A. D. Mackay. 1986. Root-growth and phosphorus and potassium uptake by 2 corn genotypes in the field. *Fertil. Res.* 10(3):217-230.

Baver, L. D. 1938. Ewald Wollny - a pioneer in soil and water conservation research. *Soil Sci. Soc. Proc.* 3:300-333.

Beauchemin, S., R. R. Simard, and D. Cluis. 1998. Forms and concentration of phosphorus in drainage water of twenty-seven tile-drained soils. *J. Environ. Qual.* 27:721-728.

Beegle, D. 2005. Assessing soil phosphorus for crop production by soil testing. In *Phosphorus: Agriculture and the Environment*, 145-180. J. T. Sims, and A. N. Sharpley, eds. Madison, WI: American Society of Agronomy, Inc.; Crop Science Society of America, Inc.; Soil Science Society of America, Inc.

Ben-Gal, A., and L. M. Dudley. 2003. Phosphorus availability under continuous point source irrigation. *Soil Sci. Soc. Am. J.* 67:1449-1456.

Benbi, D. K., and J. Richter. 2002. A critical review of some approaches to modelling nitrogen mineralization. *Biol. Fertil. Soils* 35(3):168-183.

Bender, M. R., and C. W. Wood. 2000. Total phosphorous in soil. In *Methods of Phosphorus Analysis for Soils, Sediments, Residuals, and Waters*, 45-49. G. M. Pierzynski, ed. Raleigh, NC: North Carolina State University.

Bengtson, R. L., C. E. Carter, H. F. Morris, and S. A. Bartkiewicz. 1988. The influence of subsurface drainage practices on nitrogen and phosphorus losses in a warm, humid climate. *Trans. ASABE* 31(3):729-733.

Bolan, N. S. 1991. A critical review on the role of mycorrhizal fungi in the uptake of phosphorus by plants. *Plant Soil* 134(2):189-207.

Bray, R. H., and L. t. Kurtz. 1945. Determination of total, organic, and available forms of phosphorus in soils. *Soil Sci.* 59:39-45.

Canada Gazette. 2009. Archived - regulations amending the phosphorus concentration regulations. Canada Gazette. Available at: http://gazette.gc.ca/rp-pr/p2/2009/2009-06-24/html/sor-dors178-eng.html.

Carsel, R. F., L. A. Mulkey, M. N. Lorber, and L. B. Baskin. 1985. The pesticide root zone model (PRZM): A procedure for evaluating pesticide leaching threats to groundwater. *Ecol.*

Model. 30(1–2):49-69.

Condron, L. M., B. L. Turner, and B. J. Cade-Menun. 2005. Chemistry and dynamics of soil organic phosphorus. In *Phosphorus: Agriculture and the Environment*, 87-122. J. T. Sims, and A. N. Sharpley, eds. Madison, WI: American Society of Agronomy, Inc.; Crop Science Society of America, Inc.; Soil Science Society of America, Inc.

Dawson, R. M. 1998. The toxicology of microcystins. *Toxicon* 36(7):953-962.

Djodjic, F., B. Ulen, and L. Bergstrom. 2000. Temporal and spatial variations of phosphorus losses and drainage in a structured clay soil. *Water Res.* 34(5):1687-1695.

Eastman, M., A. Gollamudi, N. Stampfli, C. A. Madramootoo, and A. Sarangi. 2010. Comparative evaluation of phosphorus losses from subsurface and naturally drained agricultural fields in the Pike River watershed of Quebec, Canada. *Agric. Water Mgmt.* 97:596-604.

Elmi, A., J. S. Abou Nohra, C. A. Madramootoo, and W. Hendershot. 2012. Estimating phosphorus leachability in reconstructed soil columns using HYDRUS-1D model. *Environ. Earth Sci.* 65:1751-1758.

Environment Canada. 2008. Daily data for Harrow CDA AUTO Ontario. Canada: Environment Canada. Available at: http://climate.weather.gc.ca/climateData/dailydata_e.html?timeframe=2&Prov=&StationID=30266&dlyRange=2000-07-25|2013-07-29&Year=2008&Month=6&Day=29.

Environment Canada. 2012. Phosphorus levels in the Great Lakes data: Status and trends of phosphorus levels in the open waters of the Canadian Great Lakes, 1970 to 2010. Environment Canada. Available at: http://www.ec.gc.ca/indicateurs-indicators/default.asp?lang=en&n=3DBD02C3-1.

Freeze, R. A., and J. A. Cherry. 1979. *Groundwater*. Prentice Hall, Englewood Cliffs, NJ.

Gaynor, J. D., and W. I. Findlay. 1995. Soil and phosphorus loss from conservation and conventional tillage in corn production. *J. Environ. Qual.* 24:734-741.

Gelbrecht, J., H. Lengsfeld, R. Pothig, and D. Opitz. 2005. Temporal and spatial variation of phosphorus input, retention and loss in a small catchment of NE Germany. *J. Hydrol.* 304:151-165.

Goldberg, S., and G. Sposito. 1984a. A chemical model of phosphate adsorption by soils: I. Reference oxide minerals. *Soil Sci. Soc. Am. J.* 48:772-778.

Goldberg, S., and G. Sposito. 1984b. A chemical model of phosphate adsorption by soils: II. Noncalcareous soils. *Soil Sci. Soc. Am. J.* 48:779-783.

Goldberg, S., and G. Sposito. 1985. On the mechanism of specific phosphate adsorption by hydroxylated mineral surfaces: A review. *Comm. Soil Sci. Plant Anal.* 16(8):801-821.

Goulet, M., J. Gallichand, M. Duchemin, and M. Giroux. 2006. Measured and computed phosphorus losses by runoff and subsurface drainage in Eastern Canada. *Appl. Eng. Agric.* 22(2):203-213.

Grant, R., A. Laubel, B. Kronvang, H. E. Andersen, L. M. Svendsen, and A. Fuglsang. 1996. Loss of dissolved and particulate phosphorus from arable catchments by subsurface drainage.

Water Res. 30(11):2633-2642.

Guildford, S. J., and R. E. Hecky. 2000. Total nitrogen, total phosphorus, and nutrient limitation in lakes and oceans: Is there a common relationship? *Limnol. Oceanogr.* 45(6):1213-1223.

Hatfield, J. D., O. W. Edwards, and R. L. Dunn. 1966. Diffusion coefficients of aqueous solutions of ammonium and potassium orthophosphates at 25 degrees. *J. Phys. Chem.* 70(8):2555-2561.

Havlin, J. L., J. D. Beaton, S. L. Tisdale, and W. L. Nelson. 2005. *Soil Fertility and Fertilizers: An Introduction to Nutrient Management*. 7 ed. Pearson Prentice Hall, Upper Saddle River, NJ.

Heathwaite, A. L., and R. N. Dils. 2000. Characterising phosphorus loss in surface and subsurface hydrological pathways. *Sci. Total Environ.* 251/252:523-538.

Heckrath, G., P. C. Brookes, P. R. Poulton, and K. W. T. Goulding. 1995. Phosphorus leaching from soils containing different phosphorus concentrations in the broadbalk experiment. *J. Environ. Qual.* 24(5):904-910.

Hutson, J. L. 2003. *Leaching estimation and chemistry model: A process-based model of water and solute movement, transformations, plant uptake and chemical reactions in the unsaturated zone. Model description and user's guide.* Ithaca, New York: Cornell University.

Hutson, J. L., and R. J. Wagenet. 1987. *LEACHM leaching estimation and chemistry model.* Ithaca, New York: Cornell University.

International Plant Nutrition Institute. n.d. Nutrient source specifics - triple superphosphate. Norcross, Ga.: International Plant Nutrition Institute. Available at: http://www.ipni.net/publication/nss.nsf/0/35039C5F78D8740C852579AF0076567A/$FILE/NSS-14%20Triple%20Superphosphate.pdf.

Jacques, D., and J. Simunek. 2005. *User manual of the multicomponent variably-saturated flow and transport model hp1, description, verification and examples.* Ver. 1.0. Mol, Belgium: SCK•CEN-BLG-998, Waste and Disposal, SCK•CEN.

Jones, C. A., C. V. Cole, A. N. Sharpley, and J. R. Williams. 1984. A simplified soil and plant phosphorus model: I. Documentation. *Soil Sci. Soc. Am. J.* 48:800-805.

Jones, J. W., G. Hoogenboom, C. H. Porter, K. J. Boote, W. D. Batchelor, L. A. Hunt, P. W. Wilkens, U. Singh, A. J. Gijsman, and J. T. Ritchie. 2003. The DSSAT cropping system model. *Eur. J. Agron.* 18(3–4):235-265.

Kirkham, D., and W. L. Powers. 1972. *Advanced Soil Physics*. John Wiley & Sons, New York, NY.

Koopal, L. K., W. H. Vanriemsdijk, J. C. M. Dewit, and M. F. Benedetti. 1994. Analytical isotherm equations for multicomponent adsorption to heterogeneous surfaces. *J. Colloid Interface Sci.* 166(1):51-60.

Krause, P., D. P. Boyle, and F. Base. 2005. Comparison of different efficiency criteria for hydrological model assessment. *Adv. Geosci.* 5:89-97.

Larsson, M. H., K. Persson, B. Ulen, A. Lindsjo, and N. J. Jarvis. 2007. A dual porosity model to quantify phosphorus losses from macroporous soils. *Ecol. Model.* 205:123-134.

Laubel, A., O. H. Jacobson, B. Kronvang, R. Grant, and H. E. Andersen. 1999. Subsurface drainage loss of particles and phosphorus from field plot experiments and a tile-drained catchment. *J. Environ. Qual.* 28:576-584.

Leikam, D. F., and F. P. Achorn. 2005. Phosphate fertilizers: Production, characteristics, and technologies. In *Phosphorus: Agriculture and the Environment*, 23-50. J. T. Sims, and A. N. Sharpley, eds. Madison, WI: American Society of Agronomy, Inc.; Crop Science Society of America, Inc.; Soil Science Society of America, Inc.

Loecke, T. D., M. Liebman, C. A. Cambardella, and T. L. Richard. 2004. Corn growth responses to composted and fresh solid swine manures. *Crop Sci.* 44:177-184.

Lull, H. W. 1964. Ecological and silvicultural aspects. In *Handbook of Applied Hydrology*. V. T. Chow, ed. New York, NY: McGraw-Hill.

Manzoni, S., and A. Porporato. 2009. Soil carbon and nitrogen mineralization: Theory and models across scales. *Soil Biol. Biochem.* 41(7):1355-1379.

McGechan, M. B., and D. R. Lewis. 2002. Sorption of phosphorus by soil, part 1: Principles, equations and models. *Biosys. Eng.* 82(1):1-24.

McKelvie, I. D. 2005. Separation, preconcentration and speciation of organic phosphorus in environmental samples. In *Organic Phosphorus in the Environment*, 1-20. B. L. Turner, E. Frossard, and D. S. Baldwin, eds. Cambridge, MA: CAB International.

Mehlich, A. 1984. Mehlich 3 soil test extractant: A modification of Mehlich 2 extractant. *Comm. Soil Sci. Plant Anal.* 15:1409-1416.

Melland, A. R., M. R. Mc Caskill, R. E. White, and D. F. Chapman. 2008. Loss of phosphorus and nitrogen in runoff and subsurface drainage from high and low input pastures grazed by sheep in southern Australia. *Aust. J. Soil Res.* 46:161-172.

Moriasi, D. N., J. G. Arnold, M. W. Van Liew, R. L. Bingner, R. D. Harmel, and T. L. Veith. 2007. Model evaluation guidelines for systematic quantification of accuracy in watershed simulations. *Trans. ASABE* 50(3):885-900.

Morrison, J., C. A. Madramootoo, and M. Chikhaoui. 2013. Modeling the influence of tile drainage flow and tile spacing on phosphorus losses from two agricultural fields in southern Quebec. *Water Qual. Res. J. Can.* 48(3).

Mualem, Y. 1976. A new model for predicting the hydraulic conductivity of unsaturated porous media. *Water Resour. Res.* 12(3):513-522.

Nash, J. E., and J. V. Sutcliffe. 1970. River flow forecasting through conceptual models: Part 1. A discussion of principles. *J. Hydrol.* 10(3):282-290.

Nofziger, D. L., and J. Wu. 2003. *Chemflo - 2000 interactive software for simulating water and chemical movement in unsaturated soils.* Ver. 2015.10.13. Stillwater, OK: Oklahoma State University.

Oberson, A., and E. J. Joner. 2005. Microbial turnover of phosphorus in soil. In *Organic*

Phosphorus in the Environment, 133-164. B. L. Turner, E. Frossard, and D. S. Baldwin, eds. Cambridge, MA: CAB International.

Oehmen, A., P. C. Lemos, G. Carvalho, Z. G. Yuan, J. Keller, L. L. Blackall, and M. A. M. Reis. 2007. Advances in enhanced biological phosphorus removal: From micro to macro scale. *Water Res.* 41(11):2271-2300.

Olsen, S. R., C. V. Cole, F. S. Watanabe, and L. A. Dean. 1954. Estimation of available phosphorus in soils by extraction with sodium bicarbonate. Washington, DC: U.S. Gov. Print. Office.

Panneerselvam, S., A. C. Lourduraj, and N. Balasubramanian. 2000. Soil available phosphorus and its uptake by soybean (Glycine max. (l.) Merrill) as influenced by organic manures, inorganic fertilizers and weed management practices. *Indian J. Agric. Res.* 34(1):9-16.

Pierzynski, G. M., R. W. McDowell, and J. T. Sims. 2005. Chemistry, cycling, and potential movement of inorganic phosphorus in soils. In *Phosphorus: Agriculture and the Environment*, 53-86. J. T. Sims, and A. N. Sharpley, eds. Madison, WI: American Society of Agronomy, Inc.; Crop Science Society of America, Inc.; Soil Science Society of America, Inc.

Pote, D. H., and T. C. Daniel. 2000a. Analyzing for dissolved reactive phosphorus in water samples In *Methods of Phosphorus Analysis for Soils, Sediments, Residuals, and Waters*, 91-93. G. M. Pierzynski, ed. Raleigh, NC: North Carolina State University.

Pote, D. H., and T. C. Daniel. 2000b. Analyzing for total phosphorus and total dissolved phosphorus in water samples. In *Methods of Phosphorus Analysis for Soils, Sediments, Residuals, and Waters*, 94-97. G. M. Pierzynski, ed. Raleigh, NC: North Carolina State University.

Raghothama, K. G. 2005. Phosphorus and plant nutrition: And overview. In *Phosphorus: Agriculture and the Environment*, 355-378. J. T. Sims, and A. N. Sharpley, eds. Madison, WI: American Society of Agronomy, Inc.; Crop Science Society of America, Inc.; Soil Science Society of America, Inc.

Raghothama, K. G., and A. S. Karthikeyan. 2005. Phosphate acquisition. *Plant Soil* 274(1-2):37-49.

Reynolds, W. D., and G. C. Topp. 2007. Soil water desorption and imbibition: Tension and pressure techniques. In *Soil Sampling Methods of Analysis*, 981-997. M. R. Carter, and G. E. G., eds. Boca Raton, FL: Canadian Society of Soil Science; Taylor and Francis, LLC.

Richardson, A. E., T. George, S., M. Hens, and R. J. Simpson. 2005. Utilization of soil organic phosphorus by higher plants. In *Organic Phosphorus in the Environment*, 165-184. B. L. Turner, E. Frossard, and D. S. Baldwin, eds. Cambridge, MA: CAB International.

Salazar, O., I. Wesstrom, M. A. Youssef, R. W. Skaggs, and A. Joel. 2009. Evaluation of the DRAINMOD-N II model for predicting nitrogen losses in a loamy sand under cultivation in south-east Sweden. *Agric. Water Mgmt.* 96(2):267-281.

Sedorovich, D. M., C. A. Rotz, P. A. Vadas, and R. D. Harmel. 2007. Simulating management

effects on phosphorus loss from farming systems. *Trans. ASABE* 50(4):1443-1453.

Sejna, M., J. Simunek, and M. T. van Genuchten. 2011. *HYDRUS user manual: Software package for simulating the two- and three-dimensional movement of water, heat and multiple solutes in variably-saturated media.* Ver. 2.x. Prague, Czech Republic: PC-Progress.

Setiyono, T. D., A. Weiss, J. E. Specht, K. G. Cassman, and A. Dobermann. 2008. Leaf area index simulation in soybean grown under near-optimal conditions. *Field Crop Res* 108(1):82-92.

Sharpley, A. N. 1995. Dependence of runoff phoshorus on extractable soil-phosphorus. *J. Environ. Qual.* 24(5):920-926.

Simunek, J., M. Sejna, H. Saito, M. Sakai, and M. T. Van Genuchten. 2009. The HYDRUS-1D software package for simulating the one-dimensional movement of water, heat, and multiple solutes in variably-saturated media: Version 4.08. University of California Riverside. Riverside, CA.

Simunek, J., M. T. van Genuchten, and M. Sejna. 2011. *HYDRUS technical manual: Software package for simulating the two- and three-dimensional movement of water, heat and multiple solutes in variably-saturated media.* Ver. 2.x. Prague, Czech Republic: PC-Progress.

Skaggs, R. W. 1980. DRAINMOD reference report: Methods for design and evaluation of drainage-water management systems for soils with high water tables. USDA Natural Resources Conservation Service, Wetlands Science Institute.

Skaggs, R. W. 2012. *DRAINMOD.* Ver. 6.1. NC: North Carolina State University.

Skaggs, R. W., C. Chescheir, M. Youssef, and B. Phillips. 2012. *DRAINMOD 6.1 help file.* Raleigh, NC: North Carolina State University.

Stewart, W. M., L. L. Hammond, and S. J. Van Kauwenbergh. 2005. Phosphorus as a natural resource. In *Phosphorus: Agriculture and the Environment*, 3-22. J. T. Sims, and A. N. Sharpley, eds. Madison, WI: American Society of Agronomy, Inc.; Crop Science Society of America, Inc.; Soil Science Society of America, Inc.

Surampalli, R. Y., S. K. Banerji, C. J. Pycha, and E. R. Lopez. 1995. Phosphorus removal in ponds. *Water Sci. Technol.* 31(12):331-339.

Tan, C. S., C. F. Drury, J. D. Gaynor, T. W. Welacky, and W. D. Reynolds. 2002. Effect of tillage and water table control on evapotranspiration, surface runoff, tile drainage and soil water content under maize on a clay loam soil. *Agric. Water Mgmt.* 54(3):173-188.

Tan, C. S., and R. E. C. Layne. 1981. Application of a simplified evapotranspiration model for predicting irrigation requirements of peach. *HortScience* 16(2):172-173.

Tan, C. S., and T. Q. Zhang. 2011. Surface runoff and sub-surface drainage phosphorus losses under regular free drainage and controlled drainage with sub-irrigation systems in southern Ontario. *Can. J. Soil Sci.* 91:349-359.

Tan, C. S., T. Q. Zhang, and T. W. Welacky. 2011. Comparison of organic fertilizer with solid and liquid manures vs. Inorganic fertilizer on water quality and crop production under free drainage and water table control systems. In *ASABE Annual International Meeting*.

Louisville, KY: American Society of Agricultural and Biological Engineers.

Tiemeyer, B., P. Kahle, and B. Lennartz. 2009. Phosphorus losses from an artificially drained rural lowland catchment in North-Eastern Germany. *Agric. Water Mgmt.* 96:677-690.

Tim, U. S., and S. Mostaghimi. 1989. Modeling phosphorus movement and distribution in the vadose zone. *Trans. ASABE* 32(2):655-661.

Turner, B. L., and P. M. Haygarth. 2000. Phosphorus forms and concentrations in leachate under four grassland soil types. *Soil Sci. Soc. Am. J.* 64:1090-1099.

Turtola, E., and A. Jaakkola. 1995. Loss of phosphorus by surface runoff and leaching from a heavy clay soil under barley and grass ley in finland. *Acta Agric. Scand., Sec. B - Soil Plant Sci.* 45:159-165.

Turtola, E., and A. Paajanen. 1995. Influence of improved subsurface drainage on phosphorus losses and nitrogen leaching from a heavy clay soil. *Agric. Water Mgmt.* 28:295-310.

U.S. Geological Survey. 2013a. Eutrophication. USA: U.S. Geological Survey. Available at: http://toxics.usgs.gov/definitions/eutrophication.html.

U.S. Geological Survey. 2013b. Phosphate rock statistics and information: Mineral commodities summaries, January 2013. USA: U.S. Geological Survey. Available at: http://minerals.usgs.gov/minerals/pubs/commodity/phosphate_rock/mcs-2013-phosp.pdf.

Ulen, B., and K. Persson. 1999. Field-scale phosphorus losses from a drained clay soil in Sweden. *Hydrol. Process.* 13:2801-2812.

USDA Agricultural Systems Research Unit. 2013. *Root zone water quality model 2 (RZWQM2).* Fort Collins, CO: USDA Agricultural Systems Research Unit.

Uusitalo, R., E. Turtola, T. Kauppila, and T. Lilja. 2001. Particulate phosphorus and sediment in surface runoff and drainflow from clayey soils. *J. Environ. Qual.* 30:589-595.

van der Salm, C., R. Dupas, R. Grant, G. Heckrath, B. V. Iversen, B. Kronvang, C. Levi, G. H. Rubaek, and O. F. Schoumans. 2011. Predicting phosphorus losses with the PLEASE model on a local scale in Denmark and the Netherlands. *J. Environ. Qual.* 40:1617-1626.

van Genuchten, M. T. 1980. A closed-form equation for predicting the hydraulic conductivity of unsaturated soils. *Soil Sci. Soc. Am. J.* 44:892-898.

van Genuchten, M. T., and R. J. Wagenet. 1989. Two-site/two-region models for pesticide transport and degradation: Theoretical development and analytical solutions. *Soil Sci. Soc. Am. J.* 53(5):1303-1310.

Vimoke, B. S., and G. S. Taylor. 1962. Simulating water flow in soil with an electric resistance network, report No. 41-65. U. S. A. R. S. Soil and Water Conserv. Res. Div., ed. Columbus, OH.

Wild, A., and L. H. P. Jones. 1988. Mineral nutrition of plant roots. In *Russell's Soil Conditions and Plant Growth*, 69-112. A. Wild, ed. Essex, UK: Longman.

Williams, J. W., R. C. Izaurralde, and E. M. Steglich. 2008. *Agricultural policy/environmental extender model theoretical documentation.* Ver. 0604. Temple, Texas: Blackland Research and Extension Center.